T.R.
GEBZE TECHNICAL UNIVERSITY
GRADUATE SCHOOL

AIR COOLING SYSTEM DESIGN OPTIMIZATIONS FOR RECIPROCATING TWO TURBOCHARGER DIESEL ENGINES OF HIGH ALTITUDE AIR VEHICLES

KEMAL BUGRA AVSAR

A THESIS OF MASTER OF SCIENCE
DEPARTMENT OF ENERGY TECHNOLOGIES
APPLIED PROPULSION SYSTEM DESIGN &ENGINEERING FOR AEROSPACE TECHNOLOGIES PROGRAM

ADVISOR: ASSIST.PROF.DR. FATIH USTA

JULY 2024

T.R.
GEBZE TECHNICAL UNIVERSITY
GRADUATE SCHOOL

AIR COOLING SYSTEM DESIGN OPTIMIZATIONS FOR RECIPROCATING TWO TURBOCHARGER DIESEL ENGINES OF HIGH ALTITUDE AIR VEHICLES

KEMAL BUGRA AVSAR

A THESIS OF MASTER OF SCIENCE
DEPARTMENT OF ENERGY TECHNOLOGIES
APPLIED PROPULSION SYSTEM DESIGN &ENGINEERING FOR AEROSPACE TECHNOLOGIES PROGRAM

ADVISOR: ASSIST.PROF.DR. FATIH USTA

JULY 2024

T.C.
GEBZE TEKNİK ÜNİVERSİTESİ
LİSANSÜSTÜ EĞİTİM ENSTİTÜSÜ

ÇİFT TURBO MOTORLU YÜKSEK İRTİFA HAVA ARAÇLARINDA HAVA SOĞUTMA SİSTEMİ TASARIM OPTİMİZASYONU

KEMAL BUĞRA AVŞAR

YÜKSEK LİSANS TEZİ
ENERJİ TEKNOLOJİLERİ ANABİLİM DALI
HAVACILIK VE UZAY TEKNOLOJİLERİNDE UYGULAMALI İTKİ SİSTEMİ TASARIM MÜHENDİSLİĞİ PROGRAMI

DANIŞMAN: DR. ÖĞR. ÜYESİ FATİH USTA

TEMMUZ 2024

MASTER of SCIENCE JURY APPROVAL FORM

A thesis submitted by Kemal Bugra, Avsar, defended on 10/07/2024 before the jury formed with the 08/07/2024 date and 2024/35 numbered decision of the GTU Graduate Administration Board, has been accepted as a MASTER of SCIENCE thesis in the Department of Energy Technologies, In Applied Propulsıon System Design & Engineering for Aerospace Technologies Program.

JURY

MEMBER
(THESIS ADVISOR) : ASSIST.PROF.DR. FATIH USTA

MEMBER : ASSIST.PROF.DR. KAAN YILDIZ

MEMBER : ASSIST.PROF.DR. ONUR SON

APPROVAL

Gebze Technical University Graduate Administration Board

…..…/…..…/..…… date and ……/…….. numbered decision.

SIGNATURE/SEAL

Babam'a …

ABSTRACT

This thesis study explores the design and optimization challenges of air cooling systems in two turbocharged piston engines for unmanned MALE (Medium Altitude Long Endurance) aircraft. Turbochargers increase the engine's inlet air pressure, consequently raising its temperature during compression. It is crucial to maintain the engine inlet air temperature at an optimal level, as elevated temperatures can lead to performance degradation and engine component damage, while excessive cooling can result in irregular combustion and the formation of undesirable chemicals in the combustion chamber. The air cooling system must effectively manage thermal loads, perform reliably across all mission profiles, and minimize weight and aerodynamic drag. Efficient and lightweight air cooling systems are essential to prevent both overheating and overcooling of the engine's inlet air. In aircraft utilizing a two turbocharger heavy fuel engine, two separate intercoolers are required to cool the compressed air from each turbocharger. These intercoolers must have sufficient capacity to handle the thermal loads during takeoff in the hottest ambient conditions, while also being compact enough to avoid overcooling at high altitudes. Additionally, an intercooler bypass system is necessary at higher altitudes to maintain the minimum required engine inlet air temperature. This study aims to validate the design and optimization of the dual intercooler and bypass systems through flight tests conducted at altitudes up to 30,000 feet.

Keywords: UAV, Aircooling, Piston Engine, Turbocharger, Intercooler

ÖZET

Bu tez çalışması, insansız MALE (Orta İrtifa Uzun Dayanım) hava araçlarında kullanılan iki turboşarjlı piston motoru için hava soğutma sistemlerinin tasarım ve optimizasyon zorluklarını incelemektedir. Turboşarjlar, motorun giriş hava basıncını artırarak, sıkıştırma sırasında hava sıcaklığının yükselmesine neden olur. Motor giriş hava sıcaklığının optimal seviyede tutulması kritik öneme sahiptir; zira yüksek sıcaklıklar performans kaybına ve motor bileşenlerinde hasara yol açabilirken, aşırı soğutma ise düzensiz yanmaya ve yanma odasında istenmeyen kimyasalların oluşumuna sebep olabilir. Hava soğutma sistemi, termal yükleri etkin bir şekilde yönetmeli, tüm görev profilleri boyunca güvenilir performans sergilemeli ve ağırlık ile aerodinamik sürtünmeyi en aza indirmelidir. Verimli ve hafif hava soğutma sistemleri, motor giriş hava sıcaklığının hem aşırı ısınmasını hem de aşırı soğutulmasını önlemek için hayati öneme sahiptir. İki turboşarjlı ağır yakıt motoru kullanan hava araçlarında, her bir turboşarjdan gelen sıkıştırılmış havayı soğutmak için iki ayrı intercooler gereklidir. Bu intercoolerlar, en sıcak çevre koşullarında kalkış sırasında termal yükleri karşılayacak kapasitede olmalı, aynı zamanda yüksek irtifalarda aşırı soğutmayı önlemek için yeterince kompakt olmalıdır. Ayrıca, yüksek irtifalarda motor giriş hava sıcaklığının minimum gereksinimlerini karşılamak için bir intercooler baypas sistemi gereklidir. Bu çalışma, 30.000 fit irtifaya kadar yapılan uçuş testleri ile çift intercooler ve baypas sistemlerinin tasarım ve optimizasyonunu doğrulamayı amaçlamaktadır.

Anahtar Kelimeler: IHA, Hava Soğutma Sistemi, Pistonlu Motor, Turboşarj, Arasoğutucu

ACKNOWLEDGEMENTS

I would like to express my gratitude to all the people and institutions who provided me with all kinds of support and contributions during the preparation of my master's thesis.
First of all, I would like to thank my thesis advisor, ASIST. PROF. Fatih Usta for guiding me with his knowledge and experience, his patience, understanding and all his help.
I would like to express my endless gratitude to my family, my daughter, my son and my wife, who supported me throughout my research.
I would also like to thank my friends Ibrahim Ethem Kazancı and Rifat Ramiz Aydın, who were always with me with their opinions, suggestions and support throughout my graduate education and thesis work.

TABLE OF CONTENTS

	Page
ABSTRACT	vi
ÖZET	vii
ACKNOWLEDGEMENTS	viii
TABLE OF CONTENTS	ix
LIST OF SYMBOLS AND ABBREVIATIONS	xi
LIST OF FIGURES	xiii
LIST OF TABLES	xix
1. INTRODUCTION	1
1.1.Unmanned Aerial Vehicles	1
1.1.1.Fixed-Wing UAVs	2
1.1.2.Rotary-Wing UAVs	6
1.1.3.Hybrid UAVs	8
1.2. Engıne Types of Unmanned Aerial Vehicles	11
1.2.1.Turbojet and Turbofan Engines	11
1.2.2 Turboprop Engines	13
1.2.3 Electric Engines	15
1.2.4 Piston Engines	16
1.3.Literature Survey	24
2. TURBOCHARGED PISTON ENGINE AIRCOOLING SYSTEMS	31
2.1. Air to Air Intercooler	31
2.1.1.Sub-Components of the Air to Air Intercoolers	32
2.1.2.Calculation Formulas for Air to Air Intercooler	35
2.2.Air to Water Intercooler	39
3. MALE UAV TURBOCHARGED HFE PISTON ENGINE AIRCOOLING SYSTEM OPTIMISATION	41
3.1 Engine Specifications And Intercooler Requirements	41
3.1.1.Engine Specifications	41
3.1.2.Engıne Air Cooling Requirements	41
3.1.3.Air Cooling Layout	42
3.2. Old Intercooler Design	43
3.2.1.HP Intercooler Specıfications	43
3.2.2.LP Intercooler Specifications	44
3.2.3.Flight Test Datas	45
3.3. By Pass System Integration	67
3.3.1.By Pass System Descriptions	67
3.3.2.By Pass System Layout & Design	68
3.3.3.Flight Test Results	69
3.4. Intercooler Resizing + By-Pass	81
3.4.1.New HP Intercooler Specifications	81
3.4.2.New LP Intercooler Specifications	82
3.4.3.Test Results	83
4. RESULTS	104
REFERENCES	109
BIOGRAPHY	112

LIST OF SYMBOLS AND ABBREVIATIONS

ρ	: Air density (kg/m³)
v	: Air velocity (m/s)
h_i	: Convective heat transfer coefficients of the air inside the tubes
h_o	: Convective heat transfer coefficients of the ambient air outside the tubes
A_c	: Cross-sectional area of the flow
μ	: Dynamic viscosity of the air (Pa·s)
EGT	: Exhaust Gas Temperature
D_{ext}	: External diameter of the tube (m)
n_f	: Fin Efficiency
f	: Friction factor
$Q_{SingleTube}$	: Heat transfer rate (W) of one Tube
Q_{fin}	: Heat transfer rate for a single fin (W)
h_{fin}	: Height of each fin (m)
h_c	: Height of the channel between the fins.
HALE	: High Altitude Long Endurance
HP	: High Pressure
D_h	: Hydraulic Diameter of one Tube
$T_{c,i}$	: Inlet temperature of the cold air (K)
$T_{h,i}$	: Inlet temperature of the hot air (K)
D_{int}	: Internal diameter of the tube (m)
L_{fin}	: Length of the fin (m)
L	: Length of the finned section (m)
ΔT_{lm}	: Logmean Temperature difference between the compressed air and ambient air (K)
LP	: Low Pressure
MAT	: Manifold Air Temperature
MALE	: Medium Altitude Long Endurance
n_{fin}	: Number of fins per tube
N	: Number of Tubes
$T_{c,o}$	: Outlet temperature of the cold air (K)
$T_{h,o}$	: Outlet temperature of the hot air (K)
U	: Overall heat transfer coefficient (W/m²·K)
ΔP	: Pressure drop (Pa)
Re	: Reynolds Number
A_{ST}	: Surface area of one tube (m²)
A_{fin}	: Surface area of the fin (m²)
A_{tube}	: Surface areas of external fin tubes (m²)
k	: Thermal conductivity of the tube material (W/m·K)
t_{fin}	: Thickness of the fin (m)
Q	: Total Heat transfer rate (W)
A	: Total Heat transfer surface area (m²)
ΔP_{total}	: Total Pressure drop across all tubes
L_{tube}	: Tube length (m)
UAV	: Unmanned Air Vehicles
t	: Wall thickness of the tube (m)
P_w	: Wetted perimeter of the flow channel

w_c : Width of the channel between the fins

LIST OF FIGURES

		Page
Figure 1.1:	Fixed Wings UAV , TUSAŞ - AKSUNGUR	3
Figure 1.2:	MALE UAV , TUSAŞ – ANKA	4
Figure 1.3:	HALE UAV , TUSAS-ANKA III	5
Figure 1.4:	Rotary Wings UAV , AIRBUS-VSR700.	7
Figure 1.5:	Single Rotor Cargo UAV , Skeldar V200	7
Figure 1.6:	Multi Rotor UAV , FlyingBasket –FB3	8
Figure 1.7:	Tilt Rotor UAV , BELL V-247.	10
Figure 1.8:	Tail-Sitter UAV , Lockheed Martin – Vector Hawk	10
Figure 1.9:	Quadplane UAV, Quantum Systems Trinity F90+	11
Figure 1.10:	Turbofan Engine , General Electric TF34	12
Figure 1.11:	Turbojet Engine , Pratt & Whitney J58	13
Figure 1.12:	Turboprop Engine , General Electric H-80	14
Figure 1.13:	Electric Engine , Siemens SP260D	16
Figure 1.14:	One Cylinder Two Stroke Engine , DLE-55	18
Figure 1.15:	Four-Stroke Turbocharged Heavy Fuel UAV Engine , TEI PD170	20
Figure 1.16:	Two pass cross flow intercooler with VFP	28
Figure 1.17:	Moving cylindrical shell on/off for the VFP.	28
Figure 3.1:	Air Cooling System Layout	42
Figure 3.2:	Inlet Ducts of UAV	43
Figure 3.3:	Old Intercooler Take-Off Test – Ambient Air Temperature Graph (°C - min)	45
Figure 3.4:	Old Intercooler Take-Off Test – Load Input Graph (% - min)	46
Figure 3.5:	Old Intercooler Take-Off Test- LP Turbo Compressor Output Temperature Graph (°C - min)	46
Figure 3.6:	Old Intercooler Take-Off Test - HP Turbo Compressor Inlet Temperature Graph (°C - min)	46
Figure 3.7:	Old Intercooler Take-Off Test – LP Intercooler Temperature Decrease Graph (°C - min)	47
Figure 3.8:	Old Intercooler Take-Off Test – HP Turbo Compressor Output Temperature Graph (°C - min)	47
Figure 3.9:	Old Intercooler Take-Off Test – Engine Manifold Air Temperature Graph (°C - min)	47
Figure 3.10:	Old Intercooler Take-Off Test – HP Intercooler Temperature Decrease Graph (°C - min)	48
Figure 3.11:	Old Intercooler Take-Off Test – LP Intercooler Pressure Drop Graph (mbar - min)	48
Figure 3.12:	Old Intercooler 30000ft Test – Ambient Air Temperature Graph (°C - min)	49
Figure 3.13:	Old Intercooler 30000ft Test – Load Input Graph (°C - min)	49
Figure 3.14:	Old Intercooler 30000ft Test – LP Turbo Compressor Output Temperature Graph (°C - min)	50
Figure 3.15:	Old Intercooler 30000ft Test - HP Turbo Compressor Inlet Temperature Graph (°C - min)	50
Figure 3.16:	Old Intercooler 30000ft Test – LP Intercooler Temperature Decrease Graph (°C - min)	51

Figure 3.17: Old Intercooler 30000ft Test – HP Turbo Compressor Output Temperature Graph (°C - min) 51
Figure 3.18: Old Intercooler 30000ft Test – Engine Manifold Air Temperature Graph (°C - min) 51
Figure 3.19: Old Intercooler 30000ft Test – HP Intercooler Temperature Decrease Graph (°C - min) 52
Figure 3.20: Old Intercooler 30000ft Test- LP Intercooler Pressure Drop Graph (mbar- min) 52
Figure 3.21: Old Intercooler 25000ft Test - Ambient Air Temperature Graph (°C - min) 53
Figure 3.22: Old Intercooler 25000ft Test - Load Input Graph (% - min) 53
Figure 3.23: Old Intercooler 25000ft Test - LP Turbo Compressor Output Temperature Graph (°C - min) 54
Figure 3.24: Old Intercooler 25000ft Test - HP Turbo Compressor Inlet Temperature Graph (°C - min) 54
Figure 3.25: Old Intercooler 25000ft Test - LP Intercooler Temperature Decrease Graph (°C - min). 54
Figure 3.26: Old Intercooler 25000ft Test - HP Turbo Compressor Output Temperature Graph (°C - min). 55
Figure 3.27: Old Intercooler 25000ft Test - Engine Manifold Air Temperature Graph (°C - min). 55
Figure 3.28: Old Intercooler 25000ft Test - HP Intercooler Temperature Decrease Graph (°C - min) 55
Figure 3.29: Old Intercooler 20000ft Test - Ambient Air Temperature Graph (°C - min) 56
Figure 3.30: Old Intercooler 20000ft Test - Load Input Graph (% - min) 57
Figure 3.31: Old Intercooler 20000ft Test - LP Turbo Compressor Output Temperature Graph (°C - min) 57
Figure 3.32: Old Intercooler 20000ft Test - HP Turbo Compressor Inlet Temperature Graph (°C - min) 57
Figure 3.33: Old Intercooler 20000ft Test – LP Intercooler Temperature Decrease Graph (°C - min) 58
Figure 3.34: Old Intercooler 20000ft Test – HP Turbo Compressor Output Temperature Graph (°C - min) 58
Figure 3.35: Old Intercooler 20000ft Test – Engine Manifold Air Temperature Graph (°C - min) 58
Figure 3.36: Old Intercooler 20000ft Test – HP Intercooler Temperature Decrease Graph (°C - min) 59
Figure 3.37: Old Intercooler Take-Off Test 2 – Ambient Air Temperature Graph (°C - min) 60
Figure 3.38: Old Intercooler Take-Off Test 2 – Load Input Graph (% - min) 60
Figure 3.39: Old Intercooler Take-Off Test 2 – LP Turbo Compressor Output Temperature Graph (°C - min) 60
Figure 3.40: Old Intercooler Take-Off Test 2 – HP Turbo Compressor Inlet Temperature Graph (°C - min) 61
Figure 3.41: Old Intercooler Take-Off Test 2 – LP Intercooler Temperature Decrease Graph (°C - min) 61
Figure 3.42: Old Intercooler Take-Off Test 2 – HP Turbo Compressor Output Temperature Graph (°C - min) 61

Figure 3.43: Old Intercooler Take-Off Test 2 – Engine Manifold Air Temperature Graph (°C - min) 62
Figure 3.44: Old Intercooler Take-Off Test 2 – HP Intercooler Temperature Decrease Graph (°C - min) 62
Figure 3.45: Old Intercooler Take-Off Test 2 – LP Intercooler Pressure Drop Graph (mbar – min) 62
Figure 3.46: Old Intercooler Take-Off Test 2 – HP Intercooler Pressure Drop Graph (mbar - min) 63
Figure 3.47: Old Intercooler 20000ft Test 2 - Ambient Air Temperature Graph (°C - min) 64
Figure 3.48: Old Intercooler 20000ft Test 2 – Load Input Graph (% - min) 64
Figure 3.49: Old Intercooler 20000ft Test 2 - LP Turbo Compressor Output Temperature Graph (°C - min) 64
Figure 3.50: Old Intercooler 20000ft Test 2- HP Turbo Compressor Inlet Temperature Graph (°C - min) 65
Figure 3.51: Old Intercooler 20000ft Test 2 – LP Intercooler Temperature Decrease Graph (°C - min) 65
Figure 3.52: Old Intercooler 20000ft Test 2 – HP Turbo Compressor Output Temperature Graph (°C - min) 65
Figure 3.53: Old Intercooler 20000ft Test 2 – Engine Manifold Air Temperature Graph (°C - min) 66
Figure 3.54: Old Intercooler 20000ft Test 2 – HP Intercooler Temperature Decrease Graph (°C - min) 66
Figure 3.55: Old Intercooler 20000ft Test 2 – LP Intercooler Pressure Drop Graph (mbar - min) 66
Figure 3.56: Old Intercooler 20000ft Test 2 – HP Intercooler Pressure Drop Graph (mbar - min) 67
Figure 3.57: Air Cooling System Layout with By Pass System 69
Figure 3.58 : Test -3, Take Off – Ambient Air Temperature Graph (°C - min) 70
Figure 3.59 : Test -3, Take Off – Load Input Graph (% - min) 71
Figure 3.60: Test -3, Take Off - LP Turbo Compressor Output Temperature Graph (°C - min) 71
Figure 3.61: Test -3, Take Off - HP Turbo Compressor Inlet Temperature Graph (°C - min) 71
Figure 3.62: Test -3, Take Off – LP Intercooler Temperature Decrease Graph (°C - min) 72
Figure 3.63: Test -3, Take Off – HP Turbo Compressor Output Temperature Graph (°C - min) 72
Figure 3.64: Test -3, Take Off – Engine Manifold Air Temperature Graph (°C - min) 72
Figure 3.65: Test -3, Take Off – HP Intercooler Temperature Decrease Graph (°C-min) 73
Figure 3.66: Test -3, Take Off – HP Intercooler Pressure Drop Graph (bar - min) 73
Figure 3.67: Test -3, Take Off - LP Intercooler Pressure Drop Graph (bar - min) 73
Figure 3.68 : Test -3, By Pass Opening – Ambient Air Temperature Graph (°C - min) 74
Figure 3.69 : Test -3, By Pass Opening – Load Input Graph (% - min) 75

Figure 3.70: Test -3, By Pass Opening – LP Turbo Compressor Output Temperature Graph (°C - min) 75
Figure 3.71: Test -3, By Pass Opening – HP Turbo Compressor Inlet Temperature Graph (°C - min) 75
Figure 3.72: Test -3, By Pass Opening – LP Intercooler Temperature Decrease Graph (°C - min) 76
Figure 3.73: Test -3, By Pass Opening – Engine Manifold Air Temperature Graph (°C - min) 76
Figure 3.74: Test -3, By Pass Opening – HP Turbo Compressor Output Temperature Graph (°C - min) 76
Figure 3.75: Test -3, By Pass Opening – HP Intercooler Temperature Decrease Graph (°C - min) 77
Figure 3.76: Test -3, By Pass Opening –HP Intercooler Pressure Drop (mbar-min) 77
Figure 3.77: Test -3, By Pass Opening –LP Intercooler Pressure Drop (mbar-min) 77
Figure 3.78: Test -4, Take-off – Ambient Air Temperature Graph (°C - min) 78
Figure 3.79: Test -4, Take-off – Load Input Graph (%- min) 79
Figure 3.80: Test -4, Take-off – Engine Manifold Air Temperature Graph (°C – min) 79
Figure 3.81: Test -4, By Pass Opening – Ambient Air Temperature Graph (°C - min) 80
Figure 3.82: Test -4, By Pass Opening – Load Input Graph (%- min) 80
Figure 3.83: Test -4, By Pass Opening – Engine Manifold Air Temperature Graph (°C - min) 81
Figure 3.84: Test -5, Take Off – Ambient Air Temperature Graph (°C - min) 84
Figure 3.85: Test -5, Take Off – Load Input Graph (% - min) 84
Figure 3.86: Test -5, Take Off – LP Turbo Compressor Output Temperature Graph (°C - min) 84
Figure 3.87: Test -5, Take Off – HP Turbo Compressor Inlet Temperature Graph (°C - min) 85
Figure 3.88: Test -5, Take Off – LP Intercooler Temperature Decrease Graph (°C - min) 85
Figure 3.89: Test -5, Take Off – HP Turbo Compressor Output Temperature Graph (°C - min) 85
Figure 3.90: Test -5, Take Off – Engine Manifold Air Temperature Graph (°C - min) 86
Figure 3.91: Test -5, Take Off – HP Intercooler Temperature Decrease Graph (°C - min) 86
Figure 3.92: Test -5, Take Off – LP Intercooler Pressure Drop (mbar-min) 86
Figure 3.93: Test -5, Take Off – HP Intercooler Pressure Drop (mbar-min) 87
Figure 3.94 : Test -5, By Pass Opening – Ambient Air Temperature Graph (°C -min) 88
Figure 3.95: Test -5, By Pass Opening – Load Input Graph (% - min) 88
Figure 3.96: Test -5, By Pass Opening – LP Turbo Compressor Output Temperature Graph (°C – min) 88
Figure 3.97: Test -5, By Pass Opening – HP Turbo Compressor Inlet Temperature Graph (°C - min) 89
Figure 3.98: Test -5, By Pass Opening – LP Intercooler Temperature Decrease Graph (°C - min) 89

Figure 3.99: Test -5, By Pass Opening – HP Turbo Compressor Output Temperature Graph (°C – min) 89
Figure 3.100: Test -5, By Pass Opening – Engine Manifold Air Temperature Graph (°C - min) 90
Figure 3.101: Test -5, By Pass Opening – HP Intercooler Temperature Decrease Graph (°C - min) 90
Figure 3.102: Test -5, By Pass Opening – LP Intercooler Pressure Drop (mbar-min) 90
Figure 3.103: Test -5, By Pass Opening – HP Intercooler Pressure Drop (mbar-min) 91
Figure 3.104: Test -5, 30kft Idle – Ambient Air Temperature Graph (°C - min) 92
Figure 3.105: Test -5, 30kft Idle – Load Input Graph (% - min) 92
Figure 3.106: Test -5, 30kft Idle – LP Turbo Compressor Output Temperature Graph (°C - min) 92
Figure 3.107: Test -5, 30kft Idle – HP Turbo Compressor Inlet Temperature Graph (°C - min) 93
Figure 3.108: Test -5, 30kft Idle – LP Intercooler Temperature Decrease Graph (°C - min) 93
Figure 3.109: Test -5, 30kft Idle – HP Turbo Compressor Output Temperature Graph (°C - min) 94
Figure 3.110: Test -5, 30kft Idle – Engine Manifold Air Temperature Graph (°C - min) 94
Figure 3.111: Test -5, 30kft Idle – HP Intercooler Temperature Decrease Graph (°C - min) 94
Figure 3.112: Test -5, 30kft Idle – LP Intercooler Pressure Drop (mbar-min) 95
Figure 3.113: Test -5, 30kft Idle – HP Intercooler Pressure Drop (mbar-min) 95
Figure 3.114: Test -5, 25kft Idle – Ambient Air Temperature Graph (°C - min) 96
Figure 3.115: Test -5, 25kft Idle – Load Input Graph (% - min) 96
Figure 3.116: Test -5, 25kft Idle – LP Turbo Compressor Output Temperature Graph (°C - min) 97
Figure 3.117: Test -5, 25kft Idle – HP Turbo Compressor Inlet Temperature Graph (°C - min) 97
Figure 3.118: Test -5, 25kft Idle – LP Intercooler Temperature Decrease Graph (°C - min) 97
Figure 3.119: Test -5, 25kft Idle – HP Turbo Compressor Output Temperature Graph (°C - min) 98
Figure 3.120: Test -5, 25kft Idle – Engine Manifold Air Temperature Graph (°C - min) 98
Figure 3.121: Test -5, 25kft Idle – HP Intercooler Temperature Decrease Graph (°C - min) 98
Figure 3.122: Test -5, 25kft Idle – LP Intercooler Pressure Drop (mbar-min) 99
Figure 3.123: Test -5, 25kft Idle – HP Intercooler Pressure Drop (mbar-min) 99
Figure 3.124: Test -5, 20kft Idle – Ambient Air Temperature Graph (°C - min) 100
Figure 3.125: Test -5, 20kft Idle – Load Input Graph (% - min) 100
Figure 3.126: Test -5, 20kft Idle – LP Turbo Compressor Output Temperature Graph (°C - min) 101
Figure 3.127: Test -5, 20kft Idle – HP Turbo Compressor Inlet Temperature Graph (°C - min) 101

Figure 3.128: Test -5, 20kft Idle – LP Intercooler Temperature Decrease Graph (°C - min) 101
Figure 3.129: Test -5, 20kft Idle – HP Turbo Compressor Output Temperature Graph (°C - min) 102
Figure 3.130: Test -5, 20kft Idle – Engine Manifold Air Temperature Graph (°C - min) 102
Figure 3.131: Test -5, 20kft Idle – HP Intercooler Temperature Decrease Graph (°C - min) 103
Figure 3.132: Test -5, 20kft Idle – LP Intercooler Pressure Drop (mbar-min) 103
Figure 3.133: Test -5, 20kft Idle – HP Intercooler Pressure Drop (mbar-min) 103
Figure 4.1: Take-Off Manifold Air Temp Comparison Btw Old & New Air Cooling Systems 104
Figure 4.2: Take Off- Ambient Air Temp Comparison Btw Old & New Air Cooling System 105
Figure 4.3: 30kft Manifold Air Temp Comparison Btw Old & New Air Cooling Systems 105
Figure 4.4: 30kft Ambient Air Temp Comparison Btw Old & New Air Cooling Systems 106
Figure 4.5: 25kft Manifold Air Temp Comparison Btw Old & New Air Cooling Systems 106
Figure 4.6: 25kft Ambient Air Temp Comparison Btw Old & New Air Cooling Systems 107
Figure 4.7: 20kft Manifold Air Temp Comparison Btw Old & New Air Cooling Systems 107
Figure 4.8: 20kft Ambient Air Temp Comparison Btw Old & New Air Cooling Systems 108

LIST OF TABLES

		Page
Table 3.1:	Engine Performance Datas	41
Table 3.2:	HP Intercooler Requirements	41
Table 3.3:	LP Intercooler Requirements	42
Table 3.4:	Old HP Intercooler Technical Specifications	43
Table 3.5:	Old HP Intercooler Supplier Analysis Results	44
Table 3.6:	Old LP Intercooler Technical Specifications	44
Table 3.7:	Old LP Intercooler Supplier Analysis Data	44
Table 3.8:	New HP Intercooler Technical Specifications	81
Table 3.9:	New HP Intercooler Supplier Analysis	82
Table 3.10:	New LP Intercooler Technical Specifications	82
Table 3.11:	New LP Intercooler Supplier Analysis	82

1. INTRODUCTION

Air Cooling systems used in aircraft must have the performance to cover all mission profiles and be as light as possible. In an aircraft with an internal combustion two-turbocharged diesel engine, two separate intercoolers are used to cool the compressed and heated air in each turbocharger. The capacity of this two-intercooler system must be large enough to support takeoff in the hottest ground conditions, but small enough to avoid overcooling of the engine at high altitude.

In the thesis study, an intercooler system was designed for an aircraft with a two-turbocharged diesel engine flight at subsonic speeds and a maximum service altitude of 30000 feet. It is aimed to verify the design and optimization of two intercoolers and By-Pass systems with flight tests to be carried out.

Civil aviation aircraft using piston engines have a service altitude between 15 000 feet and 20 000 feet and the most of these aircrafts have a single turbocharger system. There are many direct or indirect studies on intercooler design and performance evaluation for these aircraft. There are not enough test-verified system design studies for HFE-powered aircraft with piston engines and two turbochargers that climb to altitudes above 20,000 feet. With this thesis, the air cooling system design of aircraft serving at altitudes of 30 000 feet and above will be validated with flight test data and added to the literature.

1.1. Unmanned Aerial Vehicles

Unmanned Aerial Vehicles (UAVs), commonly known as drones, are aircraft that operate without a human pilot onboard. These sophisticated machines are remotely controlled or autonomously piloted using pre-programmed flight plans or more complex dynamic automation systems. UAVs come in a variety of sizes and configurations, tailored for diverse applications ranging from military operations to commercial and recreational use.

In military settings, UAVs are used for surveillance, reconnaissance, and targeted missions. They offer the advantage of reducing risk to human life while providing real-

time intelligence and strike capabilities in hostile environments. Some military drones are equipped with advanced sensors, cameras, and weaponry, enabling them to carry out complex operations with high precision.

In the commercial sector, UAVs are revolutionizing industries such as agriculture, logistics, and environmental monitoring. Agricultural drones help farmers monitor crop health, optimize irrigation, and manage pests, leading to improved yields and resource efficiency. Logistics companies are exploring drone deliveries to enhance the speed and efficiency of their services, particularly in remote or congested areas. Environmental agencies use UAVs to track wildlife, monitor forest health, and assess the impacts of climate change.

Recreationally, drones have become popular among hobbyists and photographers, offering unique perspectives for capturing stunning aerial footage and engaging in competitive flying.

Technological advancements have significantly enhanced UAV capabilities. Modern drones are equipped with GPS navigation, high-resolution cameras, and sophisticated sensors, enabling precise control and data collection. Innovations in battery technology and materials science have extended their flight times and payload capacities.

However, the proliferation of UAVs also raises concerns about privacy, security, and airspace management. Regulatory bodies worldwide are developing frameworks to address these issues, ensuring safe and responsible drone operations.

Overall, UAVs represent a transformative technology with vast potential across various fields, continually evolving to meet the growing demands and challenges of modern society.

1.1.1. Fixed-Wing UAVs

Fixed-wing Unmanned Aerial Vehicles (UAVs) are designed with wings similar to those of traditional airplanes, providing superior aerodynamics that allow for efficient long-distance flight. These UAVs are generally powered by internal combustion engines or electric motors, enabling them to maintain high speeds and extended flight times. The aerodynamic efficiency of fixed-wing UAVs makes them ideal for applications requiring coverage of vast areas, such as surveying, mapping, and large-scale surveillance.

One of the primary advantages of fixed-wing UAVs is their ability to stay airborne for prolonged periods, often exceeding several hours. This endurance is particularly beneficial in agricultural monitoring, where they can cover large fields to assess crop health, soil conditions, and irrigation needs. Environmental monitoring is another key application, with fixed-wing UAVs used to track wildlife, monitor deforestation, and assess the impact of natural disasters.

However, fixed-wing UAVs do have limitations. They require a runway or a catapult system for takeoff and landing, which can be a constraint in rugged or confined environments. Additionally, their design limits their ability to hover in place, making them less suitable for tasks that require stationary observation or precise maneuvering. Despite these limitations, their speed, range, and fuel efficiency make them indispensable in many fields, including military reconnaissance, where they can cover large operational areas with minimal energy consumption.

Fixed-wing UAVs are categorized based on their altitude and endurance capabilities, with Medium Altitude Long Endurance (MALE) and High Altitude Long Endurance (HALE) being two significant types.

Figure 1.1: Fixed Wings UAV , TUSAŞ - AKSUNGUR, **[Web 1, 2024]**.

1.1.1.1. Medium Altitude Long Endurance (MALE) UAVs

Medium Altitude Long Endurance (MALE) UAVs are a class of unmanned aerial vehicles specifically designed for sustained flight durations at medium altitudes, typically ranging from 10,000 to 30,000 feet. These UAVs can remain airborne for extended periods, often between 24 to 48 hours, making them ideal for missions that require persistent monitoring and surveillance.

Operating at medium altitudes allows MALE UAVs to cover vast areas while staying below the higher, more congested airspace. Their long endurance is facilitated by efficient aerodynamics and advanced propulsion systems.

They are equipped to carry a variety of payloads, including high-resolution cameras, infrared sensors, radar systems, and communication equipment. This versatility enables.

MALE UAVs are primarily used for ISR (Intelligence, Surveillance, and Reconnaissance) missions, providing real-time data and imagery to military and civilian operators. Their ability to loiter over target areas for extended periods makes them ideal for continuous observation. In addition to ISR, these UAVs support military operations by offering target acquisition, battle damage assessment, and, in some cases, precision strike capabilities with onboard munitions.

MALE UAVs are critical tools for a wide range of applications, offering the endurance and capabilities necessary to perform prolonged and complex missions efficiently. Their contributions to military, environmental, and security operations highlight their importance in contemporary aerial strategies.

Figure 1.2: MALE UAV , TUSAŞ – ANKA, **[Web 2, 2024]**.

1.1.1.2. High Altitude Long Endurance (HALE) UAVs

High Altitude Long Endurance (HALE) UAVs are a specialized class of unmanned aerial vehicles designed to operate at very high altitudes, often exceeding 30,000 feet, and to sustain prolonged flight durations, frequently lasting several days. These UAVs are equipped with sophisticated technology to support extensive missions over vast areas, providing invaluable data and surveillance capabilities.

HALE UAVs fly at altitudes typically between 30,000 to 65,000 feet. Their design focuses on maximizing endurance, allowing them to stay aloft for extended periods, often for several days without the need for refueling. These UAVs can carry substantial payloads, including advanced sensors, radar systems, high-resolution cameras, and communication equipment. This capability enables them to perform multiple, complex tasks simultaneously.

HALE UAVs are pivotal in strategic military and intelligence missions. Their high-altitude operation allows them to cover large geographic areas, providing continuous, real-time surveillance and reconnaissance data critical for national security. These UAVs are also used in atmospheric research, climate monitoring, and environmental science. Their ability to fly at high altitudes for extended periods makes them ideal for collecting data on weather patterns, air quality, and other atmospheric phenomena.

HALE UAVs can act as high-altitude communication relays, extending the reach and reliability of communication networks, especially in remote or disaster-affected areas where ground infrastructure is lacking.

HALE UAVs are indispensable for missions requiring prolonged high-altitude operations. Their advanced technological capabilities support a wide range of applications, from military and intelligence operations to scientific research and communication networks, highlighting their critical role in modern aerial strategies.

Figure 1.3: HALE UAV , TUSAS-ANKA III, **[Web 3, 2024]**.

1.1.2. Rotary-Wing UAVs

Single-rotor drones are similar to manned helicopters and feature a single large rotor plus a tail rotor to control heading. These UAVs are more efficient than multi-rotors when it comes to long-duration flights and can carry heavier loads. They are often used in scenarios where helicopters are typically employed, such as aerial lifting of heavy goods or in search and rescue operations where flight time and payload capacity are critical.

Rotary-wing UAVs, commonly referred to as drones or quadcopters, are equipped with multiple rotors that provide vertical takeoff and landing (VTOL) capabilities. This design allows for exceptional maneuverability and the ability to hover in place, making them ideal for tasks that require precision and stability. Rotary-wing UAVs are powered by electric motors, which offer the benefits of quieter operation and easier maintenance compared to combustion engines.

The VTOL capability of rotary-wing UAVs makes them highly versatile and easy to deploy in a variety of environments, from urban areas to remote locations. They are widely used in aerial photography and videography, enabling stunning overhead shots and dynamic filming angles. Inspection tasks, such as examining infrastructure, power lines, and pipelines, benefit from the UAV's ability to access hard-to-reach areas and provide detailed visual data. Search and rescue operations also rely on rotary-wing UAVs to locate and assist individuals in distress, especially in challenging terrains.

Despite their versatility, rotary-wing UAVs have some drawbacks, including shorter flight times and limited range compared to fixed-wing UAVs. Their battery life constraints necessitate frequent recharges or battery swaps during extended missions. Nonetheless, their ease of use, portability, and precise control make them popular for commercial, industrial, and recreational applications.

Figure 1.4: Rotary Wings UAV , AIRBUS-VSR700. **[Web 4, 2024]**.

1.1.2.1. Single-Rotor UAVs

Single-rotor UAVs resemble traditional helicopters with one main rotor and a tail rotor for stability and control. The main rotor provides lift, while the tail rotor counters torque and provides directional control. More efficient in forward flight compared to multi-rotor UAVs, with longer flight times.

Single Rotor UAVs Used for cargo transport, crop monitoring, spraying pesticides, and surveying land. Effective in search and rescue missions due to their ability to hover and maneuver in tight spaces.

Figure 1.5: Single Rotor Cargo UAV , Skeldar V200, **[Web 5, 2024]**.

1.1.2.2. Multi-Rotor UAVs

Multi-rotor UAVs have multiple rotors, typically ranging from three to eight, which provide lift and control. Highly stable and easy to control, making them suitable for precise maneuvers and stationary hovering. Can take off and land vertically, requiring minimal space. Multi-rotor UAV is also Mechanically simpler than single-rotor UAVs, with fewer moving parts.

Multi-rotor UAVs widely used in filmmaking, journalism, and real estate for capturing high-quality aerial footage. Ideal for inspecting infrastructure such as power lines, bridges, and wind turbines.

Figure 1.6: Multi Rotor UAV , FlyingBasket –FB3, **[Web 6, 2024]**.

1.1.3. Hybrid UAVs

Hybrid UAVs combine the features of both fixed-wing and rotary-wing designs, offering a versatile solution that leverages the strengths of each type. These UAVs can take off and land vertically like rotary-wing UAVs, thanks to their multiple rotors. Once airborne, they transition to efficient fixed-wing flight for longer distances and durations, utilizing their wings for sustained forward flight.

The dual capability of hybrid UAVs makes them highly adaptable to a wide range of applications. In surveillance and reconnaissance missions, they can perform vertical takeoffs in confined spaces, then switch to fixed-wing mode for extensive area

coverage. This flexibility is particularly useful in delivery services, where hybrid UAVs can navigate urban environments with VTOL and then transition to faster fixed-wing flight for longer hauls.

Hybrid UAVs are also valuable in disaster response scenarios, where they can quickly deploy, hover to assess damage, and then travel significant distances to survey affected areas. Their ability to perform in diverse operational contexts, from precision tasks to endurance flights, makes them increasingly popular in both commercial and military sectors.

While hybrid UAVs offer significant advantages, they also come with complexity and cost considerations. Their design and operational requirements are more sophisticated, leading to higher production and maintenance costs. However, the operational flexibility and enhanced capabilities they provide often justify these investments, particularly in applications that demand both the precision of rotary-wing and the endurance of fixed-wing UAVs.

These UAVs are designed to perform a wide range of tasks, benefiting from the flexibility and efficiency of both flight modes. Here are the primary types of hybrid UAVs:

1.1.3.1 Tilt-Rotor UAVs

Tilt-rotor UAVs have rotors that can tilt from a horizontal orientation for vertical takeoff and landing to a vertical orientation for forward flight.

Can take off and land vertically like a helicopter, making them ideal for operations in confined spaces. Transition to fixed-wing mode for more efficient forward flight, allowing for longer range and higher speeds.

Tilt-rotor UAVs combines the maneuverability of rotary-wing UAVs with the endurance and speed of fixed-wing UAVs.

Used for reconnaissance, surveillance, and transport missions that require rapid deployment and long-range capabilities. Suitable for search and rescue, medical supply delivery, and disaster response due to their ability to quickly reach remote areas. Utilized for cargo delivery, especially in areas lacking infrastructure for traditional aircraft.

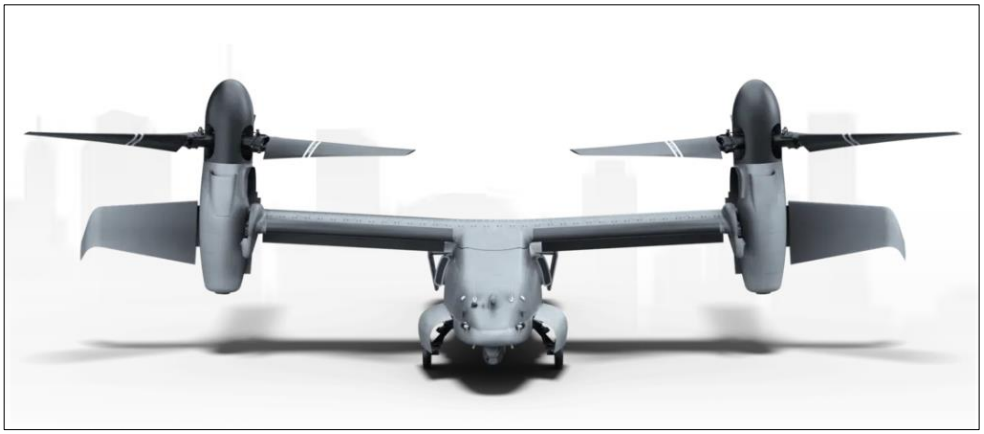

Figure 1.7: Tilt Rotor UAV , BELL V-247. **[Web 7, 2024]**.

1.1.3.2 Tail-Sitter UAVs

Tail-sitter UAVs take off and land on their tail, then transition to horizontal flight by pitching forward. Typically simpler than tilt-rotor UAVs, with fewer moving parts, enhancing reliability. Capable of vertical takeoff and landing, allowing operation in confined or unprepared areas. Once transitioned to horizontal flight, they perform like conventional fixed-wing UAVs, offering greater range and speed.

Used for precision agriculture tasks such as crop monitoring and spraying, benefiting from their ability to cover large areas efficiently. Ideal for also monitoring wildlife, forests, and other environmental parameters in remote areas.

Figure 1.8: Tail-Sitter UAV , Lockheed Martin – Vector Hawk **[Web 8, 2024]**.

1.1.3.3 Quadplane UAVs

Quadplane UAVs combine a traditional fixed-wing aircraft with vertical lift motors, similar to those found on quadcopters. Equipped with both fixed wings for efficient forward flight and vertical lift motors for VTOL operations.

Transition seamlessly between rotary-wing and fixed-wing modes, optimizing for both vertical takeoff/landing and long-endurance flight.

Quadplane UAVs used for land surveying, infrastructure inspection, and environmental monitoring, providing high-resolution data over large areas. Employed in crop monitoring, precision farming, and aerial spraying, leveraging their ability to hover and cover extensive fields efficiently. Also ideal for delivering packages in urban and rural areas, benefiting from their VTOL capabilities and long-range flight.

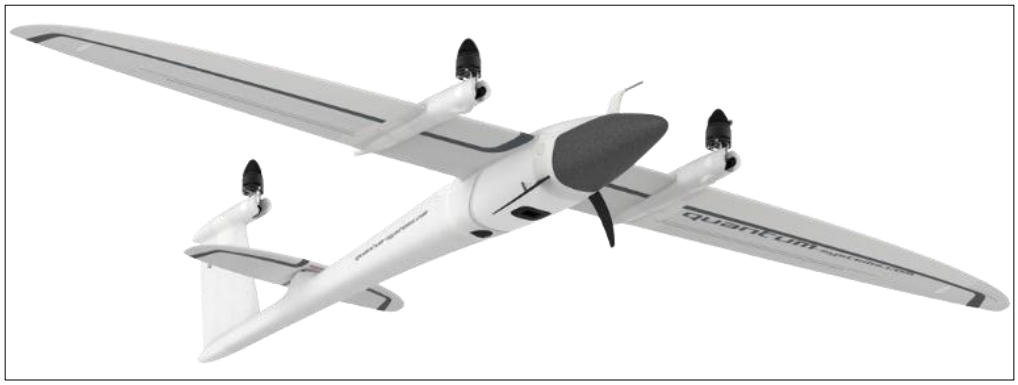

Figure 1.9: Quadplane UAV, Quantum Systems Trinity F90+ , **[Web 9, 2024]**.

1.2. Engine Types of Unmanned Aerial Vehicles

1.2.1. Turbojet and Turbofan Engines

Turbofan and turbojet engines are jet propulsion systems used in high-speed and high-altitude unmanned aerial vehicles (UAVs). These engines leverage advanced aerodynamics and thermodynamics to generate thrust, enabling UAVs to perform demanding missions.

1.2.1.1. Turbofan Engines

The large fan at the front of a turbofan engine draws in air. A portion of this air bypasses the core engine, providing additional thrust. Compressor compresses the

incoming air to high pressures before it enters the combustion chamber. Combustion chamber mixes the compressed air with fuel and ignites it, generating high-temperature, high-pressure gases. Turbine extracts energy from the exhaust gases to drive the compressor and the fan. From exhaust, remaining gases are expelled, generating thrust. The combination of bypass air and exhaust gases produces efficient thrust.

Turbofans have a high bypass ratio, meaning a significant portion of the air bypasses the core engine. This design improves fuel efficiency and reduces noise. The fan-generated bypass air adds to the thrust produced by the core engine, making turbofans efficient at subsonic speeds.

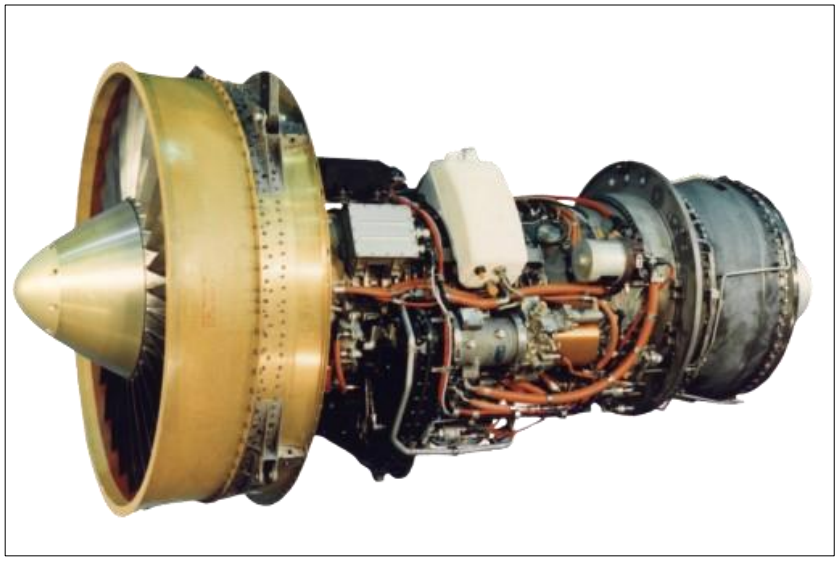

Figure 1.10: Turbofan Engine , General Electric TF34, **[Web 10, 2024]**.

1.2.1.2. Turbojet Engines

Turbojet engines are a type of jet propulsion system widely used in high-speed unmanned aerial vehicles (UAVs). These engines are known for their ability to generate significant thrust and operate efficiently at high speeds, making them ideal for applications requiring rapid acceleration and sustained supersonic flight. This description outlines the working principle of turbojet engines, focusing on their key components and the thermodynamic processes involved.

Incoming air is directed by air intake ducts, into the engine, ensuring a smooth and steady flow. Compressor compresses the incoming air to high pressures, increasing its

temperature and density. The compressor typically consists of multiple stages of rotating blades and stationary vanes. Combustion chamber mixes the high-pressure air with fuel and ignites the mixture. The combustion process significantly increases the energy of the air, converting chemical energy into thermal energy. Turbine extracts energy from the high-temperature, high-pressure exhaust gases to drive the compressor. The turbine consists of multiple stages of blades, similar to the compressor but designed to extract energy rather than impart it. Nozzle accelerates the exhaust gases to very high velocities, generating thrust. The nozzle's design is crucial for maximizing the efficiency of the thrust generation process.

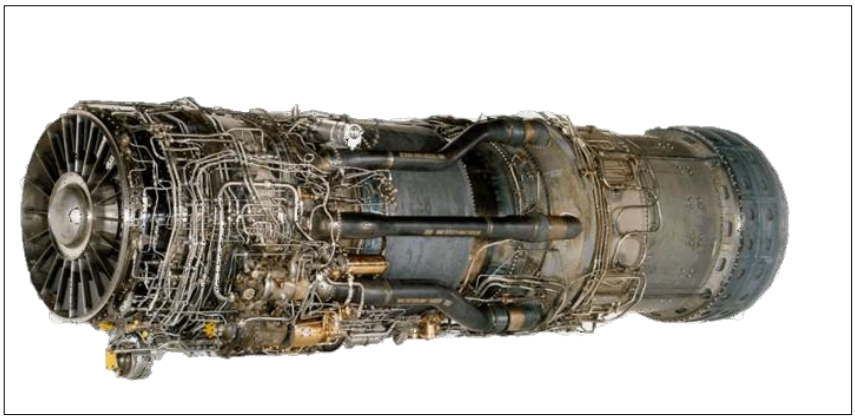

Figure 1.11: Turbojet Engine , Pratt & Whitney J58, **[Web 11, 2024]**.

1.2.2 Turboprop Engines

Turboprop engines are a type of gas turbine engine used in unmanned aerial vehicles (UAVs) that combine the high-speed capabilities of jet engines with the fuel efficiency and operational versatility of propeller-driven systems. These engines are particularly valued in UAV applications for their ability to provide significant thrust and endurance, making them ideal for long-range and high-altitude missions.

The core of the turboprop engine consists of a compressor, combustion chamber, and turbine. The gas generator's primary function is to produce high-pressure, high-temperature gas. Compressor compresses incoming air to high pressures before delivering it to the combustion chamber. Combustion chamber mixes compressed air with fuel and ignites the mixture, producing high-energy exhaust gases. Turbine extracts energy from the exhaust gases to drive the compressor and the propeller. Propeller is connected to the gas generator via a reduction gearbox. The propeller

provides the primary thrust by converting the engine's rotational energy into aerodynamic force. Reduction gearbox reduces the high rotational speed of the turbine to a suitable speed for the propeller, optimizing efficiency and performance. Exhaust system directs the flow of exhaust gases out of the engine, contributing to additional thrust and improving overall engine efficiency.

Air is drawn into the engine through the intake and compressed by the compressor stages, increasing its pressure and temperature. The compressed air is mixed with fuel in the combustion chamber and ignited, resulting in high-temperature, high-pressure gases. These gases pass through the turbine stages, where energy is extracted to drive both the compressor and the propeller. The reduction gearbox reduces the turbine's high rotational speed to an appropriate level for the propeller. The propeller then generates thrust by accelerating a large mass of air at a lower velocity, which is more efficient than jet propulsion for lower-speed flight.

Turboprop engines are more fuel-efficient than turbojet engines, especially at lower speeds and altitudes, making them suitable for long-endurance UAV missions. Turboprop engines capable of providing significant thrust and power, allowing UAVs to carry heavier payloads and perform demanding tasks. These engines effective at a wide range of altitudes, from low-level flight to high-altitude operations, providing flexibility for various mission profiles.

Turboprop engines are built to withstand harsh operating conditions and offer high reliability and long service intervals, which are critical for UAV operations. Turboprop engines offer a blend of efficiency, power, and versatility, making them an ideal choice for a wide range of UAV applications.

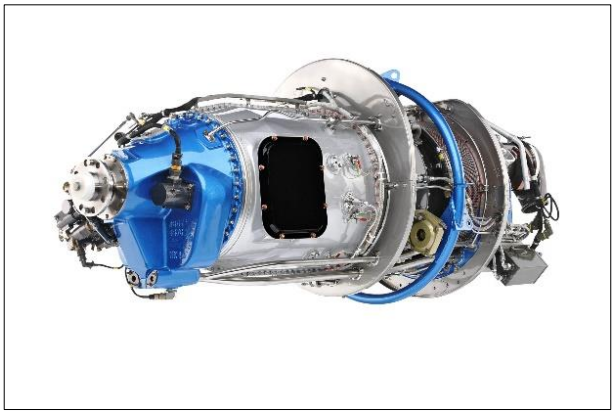

Figure 1.12: Turboprop Engine , General Electric H-80, **[Web 12, 2024]**.

1.2.3 Electric Engines

Electric engines, or electric motors, are becoming increasingly popular in unmanned aerial vehicles (UAVs) due to their efficiency, reliability, and environmental benefits. These engines convert electrical energy into mechanical energy, providing a clean and efficient propulsion system. This scientific description delves into the design, operation, and applications of electric engines in UAVs.

Electric Motor is primary component that converts electrical energy into mechanical motion. Stator is the stationary part of the motor that produces a rotating magnetic field. Rotor is the rotating part that interacts with the magnetic field to produce torque and rotational motion. Battery stores the electrical energy required to power the motor. UAVs typically use lithium-polymer (LiPo) or lithium-ion (Li-ion) batteries due to their high energy density and lightweight properties. Electronic Speed Controller (ESC) regulates the power to the motor, controlling the motor's speed and direction. ESC adjusts the speed of the motor based on input from the UAV's control system, allowing precise control of thrust and flight dynamics. Power Management System manages the distribution and usage of electrical power, ensuring optimal performance and battery health. Propellers are attached to the motor shaft, converting the motor's rotational energy into thrust.

Electrical energy is supplied from the battery pack to the ESC. ESC regulates the current flow to the stator windings, creating a rotating magnetic field. Magnetic field induces a torque on the rotor, causing it to rotate. This rotation is transferred to the propeller, generating thrust. Some advanced systems can recover energy during deceleration, extending the overall flight time.

Electric engines are highly efficient, often exceeding 90% efficiency in converting electrical energy to mechanical energy. This efficiency translates to longer flight times and lower operational costs. Fewer moving parts compared to internal combustion engines, leading to lower maintenance requirements and higher reliability.

Electric engines offer a combination of efficiency, reliability, and environmental benefits, making them an excellent choice for a wide range of UAV applications.

Figure 1.13: Electric Engine , Siemens SP260D, **[Web 13, 2024]**.

1.2.4 Piston Engines

Unmanned Aerial Vehicles (UAVs) utilize a variety of propulsion systems to meet the demands of diverse operational environments. Among these, piston engines are one of the most common, particularly in small to medium-sized UAVs. Piston engines, also known as reciprocating engines, operate on the principle of converting chemical energy from fuel into mechanical energy through a series of controlled combustions within cylinders.

The core components include one or more cylinders in which pistons move up and down. Each cylinder comprises an intake valve, exhaust valve, spark plug, and fuel injector. The pistons are connected to the crankshaft via connecting rods. The crankshaft converts the linear motion of the pistons into rotational motion. The space at the top of each cylinder where the fuel-air mixture is compressed and ignited to produce power.

Piston engines in UAVs typically use aviation gasoline (avgas) or heavy fuels like JP-8. The choice of fuel affects the engine's performance, efficiency, and operational altitude.

The power output of a piston engine depends on the number of cylinders, engine displacement, and the efficiency of the combustion process. In UAVs, this power is translated into thrust via a propeller connected to the crankshaft.

Piston engines generate significant heat during operation, necessitating efficient cooling systems. Air-cooled and liquid-cooled systems are common, with air-cooled systems being lighter and simpler, and liquid-cooled systems providing better temperature control.

Piston engines are generally more fuel-efficient compared to turbine engines, particularly at lower speeds and altitudes. They are less expensive to manufacture and maintain, making them suitable for a wide range of UAV applications. Piston engines have a proven track record of reliability, crucial for missions requiring long endurance and operational readiness.

1.2.4.1 Two-Stroke Piston Engines

Two-stroke piston engines are a popular choice for small to medium-sized UAVs due to their simplicity, high power-to-weight ratio, and ease of maintenance. Unlike four-stroke engines, two-stroke engines complete a power cycle in just two strokes of the piston (one crankshaft revolution), which makes them lighter and more powerful relative to their size.

The engine typically has one or more cylinders with pistons that move up and down to compress and ignite the fuel-air mixture. Instead of valves, two-stroke engines use ports for intake and exhaust, which are opened and closed by the movement of the piston. Crankcase functions as a pump to manage the intake of air-fuel mixture and expulsion of exhaust gases. Sparkplug ignites the compressed fuel-air mixture, initiating the combustion process.

Two-stroke engines typically use a mix of fuel and oil. The oil mixed with the fuel lubricates the engine components, reducing the need for a separate lubrication system.

These engines have fewer moving parts and a simpler design, which translates to easier and quicker maintenance. However, they require regular maintenance due to higher wear rates from their operational cycle.

Two-stroke engines perform the complete engine cycle in two strokes. At the first stroke (Compression and Combustion); the upward movement of the piston

compresses the fuel-air mixture. Near the top of the stroke, the spark plug ignites the mixture, forcing the piston downward (power stroke). Second stroke (Exhaust and Intake) ; as the piston moves down, it uncovers the exhaust port, allowing the exhaust gases to escape. Simultaneously, the intake port is uncovered, allowing a fresh fuel-air mixture to enter the cylinder.

Two-stroke engines are less fuel-efficient than four-stroke engines because of the overlap in the intake and exhaust processes, leading to some unburned fuel escaping with the exhaust gases. Despite this, their high power output and lightweight design make them efficient for specific applications.

Two-stroke engines in UAVs can operate on a variety of fuel types, each offering unique advantages. Gasoline and mixed-fuel (gasoline-oil mix) are commonly used due to their high energy density and simplicity. Methanol-based fuels provide higher performance and cooler combustion, making them suitable for high-performance applications. Synthetic fuels offer customized performance characteristics, ideal for advanced and environmentally sensitive applications. Heavy fuels like JP-8 or diesel provides significant logistical and operational advantages. These engines offer a balance of durability, fuel efficiency, and power, making them suitable for long-endurance missions and heavy payload applications. Understanding these fuel types helps in selecting the appropriate propulsion system to meet specific UAV mission requirements.

Figure 1.14: One Cylinder Two Stroke Engine , DLE-55, **[Web 14, 2024]**.

1.2.4.2 Four-Stroke Piston Engines

Four-stroke piston engines are a common propulsion choice for Unmanned Aerial Vehicles (UAVs) due to their efficiency, reliability, and balanced performance characteristics. These engines operate on the four-stroke cycle—intake, compression, power, and exhaust—which makes them more fuel-efficient and durable than two-stroke engines.

Cylinders are the central component where the air-fuel mixture is compressed and ignited. UAV engines typically range from single-cylinder to multi-cylinder configurations. Pistons move up and down within the cylinders to compress the air-fuel mixture and transfer the force of combustion to the crankshaft. Crankshaft converts the linear motion of the pistons into rotational motion, which drives the propeller. Intake valves allow the air-fuel mixture to enter the cylinder. Exhaust valves expel the burned gases from the cylinder after combustion. Camshafts control the opening and closing of the intake and exhaust valves. The camshaft is driven by the crankshaft through a timing belt or chain, ensuring the valves operate in sync with the pistons. Carburetors or fuel injectors deliver the precise amount of fuel into the cylinders. Fuel injectors are more common in modern UAV engines due to their efficiency and accuracy. Spark Plugs ignite the compressed air-fuel mixture within the cylinders for Gasoline and AVGAS engines. Lubrication system ensures all moving parts are properly lubricated to reduce friction and wear. This system circulates oil throughout the engine.

The four-stroke cycle consists of four distinct phases; At the intake stroke, intake valve opens, and the piston moves down, drawing a mixture of air and fuel into the cylinder. At compression stroke, intake valve closes, and the piston moves up, compressing the air-fuel mixture. At power stroke, compressing mixture if engine is gasoline or avgas, spark plugs ignites also, explosion occurs than forces the piston down, generating power. At exhaust stroke, exhaust valve opens, and the piston moves up again, expelling the exhaust gases from the cylinder. This cycle repeats continuously, providing a smooth and efficient power delivery to the UAV.

Four-stroke engines are more fuel-efficient than two-stroke engines because they burn fuel more completely and have a dedicated exhaust stroke to expel combustion by-products. While they produce less power per unit of displacement compared to two-

stroke engines, they provide more consistent and reliable power output over longer periods.

The design of four-stroke engines generally leads to less wear and tear on components, resulting in longer engine life and lower maintenance requirements.

Four-stroke piston engines are a versatile and reliable choice for UAV propulsion, offering a balance of efficiency, durability, and performance. Their well-established technology and design make them suitable for a wide range of applications, from surveillance and reconnaissance to agricultural and environmental monitoring. Understanding the technical aspects and operational benefits of four-stroke engines helps in selecting the right propulsion system to meet specific UAV mission requirements.

Figure 1.15: Four-Stroke Turbocharged Heavy Fuel UAV Engine , TEI PD170, **[Web 15, 2024]**.

There are more than one classification type of piston engines. Since our thesis topic is on the air cooling system, the types of piston engines according to their air intake systems are mentioned below.

Naturally Aspirated Piston Engines

Naturally aspirated engines are internal combustion engines that rely solely on atmospheric pressure to draw air into the combustion chambers. These engines do not

utilize turbochargers or superchargers to force air into the engine, making them simpler in design and operation. Naturally aspirated engines have been widely used in various types of aircraft, particularly in general aviation and light aircraft. One of the primary advantages of naturally aspirated engines in aircraft is their mechanical simplicity. The absence of forced induction components reduces the overall complexity of the engine, leading to lower maintenance requirements and potentially longer service intervals. This simplicity can be particularly beneficial in remote or less-developed regions where maintenance facilities may be limited. Another advantage is the immediate throttle response and linear power delivery. Without the lag associated with turbocharged or supercharged systems, pilots can enjoy a more direct and predictable control over the engine's power output. This can enhance the flying experience and provide a sense of reliability and confidence in engine performance. Naturally aspirated engines are also generally lighter than their forced induction counterparts. This weight advantage can contribute to better overall aircraft performance, including improved fuel efficiency and greater payload capacity.

However, naturally aspirated engines come with certain disadvantages, particularly in the aviation context. One significant drawback is their limited performance at higher altitudes. As altitude increases, air density decreases, leading to a reduction in the amount of oxygen available for combustion. This results in a decrease in engine power output, which can be a critical factor for aircraft operating in mountainous regions or requiring high-altitude performance. Furthermore, naturally aspirated engines may struggle to match the power-to-weight ratio of turbocharged or supercharged engines. To achieve higher power outputs, naturally aspirated engines often need to be larger and may require more complex intake and exhaust systems, potentially negating some of their weight advantages.

In summary, naturally aspirated engines for aircraft offer reliability, simplicity, and a direct flying experience but are limited by their performance at higher altitudes and power-to-weight ratio compared to forced induction engines. Despite these limitations, they remain a popular choice in general aviation for their ease of maintenance and straightforward operation.

Turbocharged Piston Engines

This type of piston engines for aircraft utilize turbochargers to increase the engine's power and efficiency by compressing the intake air.

Turbocharger systems for piston engines operate by using exhaust gases to drive a turbine connected to a compressor. Exhaust gases from the engine pass through the turbine side of the turbocharger. The force of the exhaust gases spins the turbine wheel. The turbine wheel is connected to a compressor wheel by a shaft. As the turbine spins, it drives the compressor. The compressor draws in outside air and compresses it, increasing its density. The compressed air is then fed into the engine, providing more oxygen for combustion. With more oxygen, the engine can burn more fuel, resulting in increased power output and efficiency. This process boosts engine performance, particularly at higher altitudes, while optimizing fuel use and enhancing overall engine efficiency.

One of the primary advantages of turbocharged piston engines is their superior performance at high altitudes. As an aircraft ascends, the atmospheric pressure and air density decrease, leading to a natural reduction in engine power for naturally aspirated engines. Turbocharged engines counteract this effect by forcing more air into the combustion chamber, maintaining power output even as the aircraft climbs. This capability is particularly beneficial for aircraft operating in mountainous regions or requiring high-altitude cruise capabilities. Another significant advantage is the improved power-to-weight ratio. Turbocharged engines can produce more power from a smaller displacement compared to naturally aspirated engines. This means that aircraft can achieve better performance without a substantial increase in engine size or weight. Consequently, turbocharged engines often contribute to improved fuel efficiency and higher overall performance metrics. Moreover, turbocharging can enhance the versatility of an aircraft, allowing it to operate efficiently across a wider range of altitudes and conditions. This adaptability can be crucial for missions that involve varied flight profiles, such as search and rescue operations or cross-country flights.

However, turbocharged piston engines also come with certain disadvantages. The process of compressing air raises its temperature, necessitating effective cooling systems to prevent overheating and ensure reliable engine operation. This can add

weight and complexity to the aircraft's design. The added complexity of the turbocharging system increases maintenance requirements and can lead to higher operational costs. Components such as the turbocharger itself, intercoolers, and additional piping introduce more potential points of failure and necessitate more frequent inspections and upkeep. Additionally, turbocharged engines can suffer from turbo lag, a delay in power delivery caused by the time it takes for the turbocharger to spool up. While this is less of an issue in steady flight conditions, it can be a consideration during rapid power changes, such as during takeoff or landing.

In summary, turbocharged piston engines for aircraft offer significant advantages in high-altitude performance, power-to-weight ratio, and operational versatility. However, these benefits come with trade-offs in terms of increased complexity, maintenance requirements, and potential turbo lag. Despite these challenges, turbocharged engines remain a popular choice in aviation for their ability to deliver enhanced performance and efficiency.

Supercharged Piston Engines

Supercharged piston engines for aircraft utilize superchargers to boost engine performance by compressing the intake air, which increases the amount of oxygen available for combustion. Unlike turbochargers, which are powered by exhaust gases, superchargers are mechanically driven by the engine itself, usually through a belt connected to the crankshaft. This direct drive system allows superchargers to provide immediate and consistent power increases across the engine's RPM range. One of the primary advantages of supercharged piston engines is their ability to deliver instant power without the lag associated with turbochargers. Because the supercharger is mechanically driven, it provides a consistent boost in air pressure as soon as the engine is running, which translates to immediate throttle response. This is particularly beneficial during critical phases of flight, such as takeoff and climb, where rapid power availability is essential. Supercharged engines also offer enhanced performance at higher altitudes. As altitude increases, air density decreases, which can reduce engine power. A supercharger helps mitigate this by compressing the intake air, ensuring sufficient oxygen for optimal combustion even at high altitudes. Additionally, the mechanical simplicity of superchargers compared to turbochargers can be an advantage. Superchargers do not rely on the exhaust system, reducing the complexity

and potential failure points associated with turbocharging. This can lead to increased reliability and easier maintenance.

However, supercharged piston engines also have their drawbacks. One significant disadvantage is the additional mechanical load on the engine. Since the supercharger is driven by the engine, it consumes some of the engine's power to operate, which can reduce overall efficiency. This can lead to higher fuel consumption compared to naturally aspirated or even some turbocharged engines. Another disadvantage is the increased weight and complexity of the supercharging system, which can add to the aircraft's overall weight and maintenance requirements. The need for robust cooling systems to manage the heat generated by the supercharger also adds to the complexity and weight.

In summary, Supercharged piston engines for aircraft provide immediate power, improved high-altitude performance, and mechanical simplicity, but they come with trade-offs in terms of fuel efficiency, added weight, and increased maintenance complexity. Despite these challenges, they remain a popular choice for applications where rapid and reliable power delivery is crucial.

1.3. Literature Survey

The paper titled "The Effect of Turbocharger Pressure and Intercooler Temperature on Engine Performance" by Mohamed S. Oun, Salem A. Farhat, and Mohammed A. l Rabeei, investigates the impact of turbocharger pressure and intercooler temperature on the performance of diesel engines. This research addresses the critical issues of engine emissions and fuel consumption, proposing the utilization of turbochargers and intercoolers to enhance engine efficiency and reduce harmful emissions. This research underscores the importance of turbochargers and intercoolers in enhancing diesel engine performance. By optimizing turbocharger pressure and intercooler temperature, engines can achieve higher power output, better fuel efficiency, and lower emissions. The findings support the ongoing development and implementation of advanced turbocharging and intercooling technologies to meet the increasing demand for efficient and environmentally friendly engines.

Intercoolers are crucial in cooling the compressed air from the turbocharger, improving its density and the combustion process. The study by Eyub Canli et al. (2010)

highlighted the significance of intercoolers in conventional supercharging systems, showing improvements in engine power and fuel efficiency.

The study uses thermodynamic analysis based on C.R. Ferguson's "Internal Combustion Engine Applied Thermodynamics" to model the effects of turbocharger pressure and intercooler temperature. It was found that increasing turbocharger pressure and decreasing intercooler temperature significantly enhanced engine power output and reduced specific fuel consumption.

Mifdal et al. (2015) developed an automatic turbo intercooler cooling system that operates based on the intercooler's temperature. The system uses an Arduino Uno microcontroller to detect temperature increases and trigger a water spray to cool the intercooler. This automatic system ensures that the intercooler operates efficiently without manual intervention, maintaining optimal engine performance even during long runs.

The paper "Improving the Performance of CI Engine by Using Turbo-charger with an Inter-cooler" by Fatima M. Elafi, Abdurrauf Mohamed Naas, and Salem Farhat explores the enhancements in performance and efficiency of a compression ignition (CI) engine through the integration of a turbocharger and an intercooler. The study focuses on a medium-speed diesel engine, modeling and simulating the effects of cooled intake air on engine performance using theoretical thermodynamic analysis. Turbochargers are utilized to increase the density of intake air by compressing it, which boosts the volumetric efficiency and power output of the engine. However, the compression process also raises the air temperature, reducing its density. To counteract this, intercoolers are employed to cool the compressed air, enhancing engine efficiency and performance (Jadhao & Thombare, 2013; Patil et al., 2015). Cooling the intake air using an intercooler significantly improves volumetric efficiency. The study found that volumetric efficiency increased by about 98% when the intake air temperature was reduced from 370 K to 300 K (Ellafi et al., 2020). The engine's indicated power (Pi) showed a notable increase with the use of a turbocharger and intercooler. The indicated power increased by approximately 107%, highlighting the substantial performance gains achievable through effective charge air cooling (Ellafi et al., 2020). The study illustrated the relationship between crank angle and pressure, showing that maximum cylinder pressure increased significantly with cooler intake air. This increase in pressure contributes to higher power output and efficiency (Ellafi et al., 2020).

The paper titled "Performance of an Agricultural Engine Using Turbocharger and Intercooler" by Marcelo Silveira de Farias et al. explores the effects of air and fuel supercharging on an agricultural engine. This study evaluates key variables such as torque, power, and specific fuel consumption using a dynamometer through the power take-off of an agricultural tractor. The research is motivated by the need to improve engine performance and efficiency while reducing fuel consumption and emissions. The study conducted by Farias et al. (2021) involved testing six engine configurations: natural aspiration, natural aspiration with increased fuel flow (service), turbocharger, turbocharger with increased fuel flow, turbocharger with intercooler, and turbocharger with increased fuel flow and intercooler. The results showed that configurations with both turbocharger and increased fuel flow significantly improved torque and power by approximately 30% and reduced specific fuel consumption by up to 10%.

The efficiency of combustion is influenced by altitude, as air density decreases with higher altitudes. Turbochargers help mitigate this issue by maintaining air density, ensuring consistent engine performance. Agudelo et al. (2009) highlighted that turbocharging is essential to prevent efficiency loss at high altitudes.

Intercoolers are vital for reducing the temperature of compressed air from the turbocharger, thereby increasing its density and oxygen content. This cooling effect leads to improved combustion efficiency and engine performance. Lima (2018) found that engines equipped with intercoolers demonstrated higher torque and power compared to those without.

The study "Experimental Study on Thermal Balance of Regulated Two-Stage Turbocharged Diesel Engine at Variable Altitudes" investigates the thermal balance of a regulated two-stage turbocharged (RTST) diesel engine under different variable geometry turbocharger (VGT) vane openings at various altitudes. The research aims to understand how altitude and VGT adjustments affect engine heat distribution, load management, and thermal efficiency. High altitudes significantly challenge diesel engines due to reduced intake air density, which results in decreased power and efficiency and increased heat load. Liu and Liu (2021) highlight that two-stage turbocharging technology effectively addresses these issues by optimizing intake air density using exhaust energy.

The paper titled " Effects of Altitude and Temperature on the Performance and Efficiency of Turbocharged Direct Injection Gasoline Engine " S. Motahari and I. Chitsaz, investigates the impact of altitude and temperature variations on the performance and efficiency of turbocharged direct injection gasoline engines. Specifically, the research focuses on how these environmental factors influence engine performance metrics such as brake specific fuel consumption (BSFC), brake mean effective pressure (BMEP), and engine torque. High altitudes reduce the density of intake air, which can lead to a decrease in engine power output and efficiency. Various studies have highlighted that altitude increments result in significant reductions in engine performance and increases in fuel consumption. For example, a naturally aspirated diesel engine experiences approximately 8% power reduction with every 1000 meters increase in altitude. Turbocharging is a common method to counteract the negative effects of high altitude by increasing the intake air pressure. However, at high altitudes, turbochargers approach their operational limits, which can lead to issues such as compressor surge and reduced effectiveness. Additionally, higher compressor outlet temperatures can exacerbate the risk of knock. Various empirical studies and simulations have been conducted to assess the impact of altitude and temperature on engine performance. For instance, experimental data combined with GT power simulations have been used to validate models that predict engine behavior under different environmental conditions. These studies often reveal that low-end torque is not significantly affected due to turbocharging compensation, but high-end torque and overall engine efficiency can drop considerably at elevated temperatures and altitudes.

The study "Aero Engıne Intercoolıng Optımızatıon Usıng A Varıable Flow Path" by Xin Zhao and Tomas Grönstedt, presented at ISABE-2015, focuses on optimizing the intercooling process in aero engines using a variable flow path (VFP) concept. This research aims to enhance fuel efficiency and reduce emissions by improving the thermal management of the engine, particularly during different flight conditions. The VFP concept involves controlling the flow path of the intercooler’s hot side during different flight phases. By allowing part of the hot flow to bypass the intercooler at cruise, the system can reduce the pressure loss and improve specific fuel consumption (SFC) (Zhao et al., 2014).

The VFP system uses a moving cylindrical shell to switch the flow path on and off, allowing for dynamic adjustment of the intercooling process based on the flight conditions (Figure 1.16, Figure 1.17).

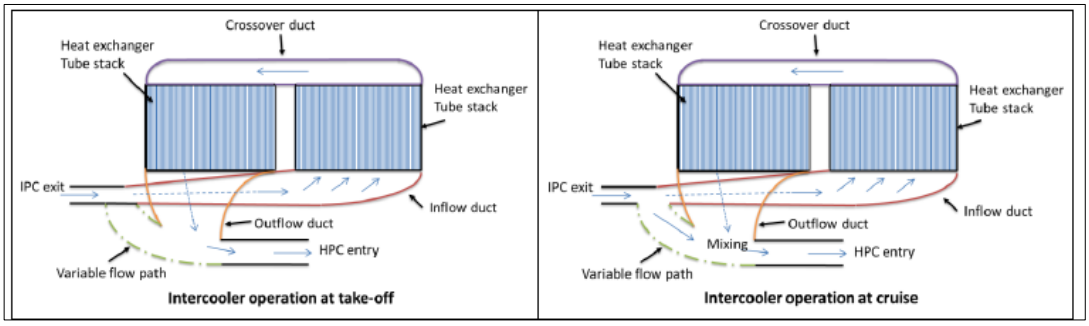

Figure 1.16: Two pass cross flow intercooler with VFP

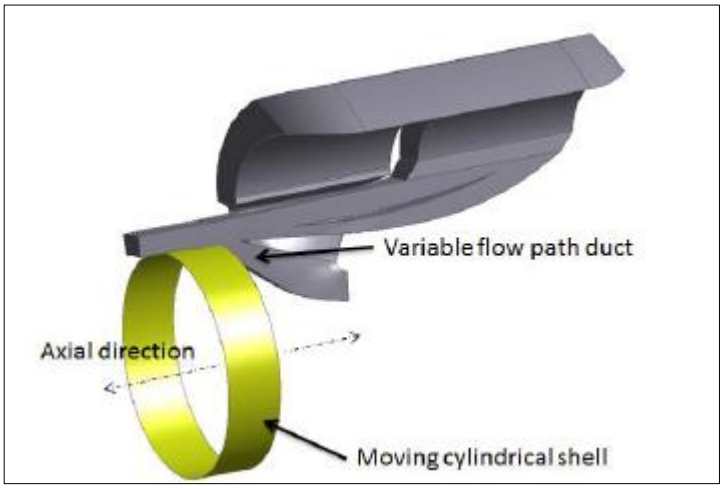

Figure 1.17: Moving cylindrical shell on/off for the VFP.

Intercooling involves cooling the compressed air between compression stages in an engine, which can lead to lower combustor entry temperatures and reduced NOx emissions. This process is particularly beneficial in achieving higher overall pressure ratios (OPR) and turbine inlet temperatures (TIT) without compromising engine efficiency (Wilfert et al., 2007; Rolt & Kyprianidis, 2010).

The paper "Assessment of the Performance Potential for a Two-Pass Cross Flow Intercooler for Aero Engine Applications" by Xin Zhao, Tomas Grönstedt, and Konstantinos G. Kyprianidis examines the performance potential of a two-pass cross flow intercooler in geared turbofan engines. This research aims to enhance aero engine efficiency, reduce fuel consumption, and minimize emissions by optimizing

intercooler design and integration. Intercoolers have gained significant attention for their potential to improve engine specific fuel consumption (SFC) and reduce nitrogen oxide (NOx) emissions. They achieve this by lowering compressor exit temperatures, which in turn reduces the cooling air requirements for the turbine (Wilfert et al., 2007; Rolt & Kyprianidis, 2010).

The paper "Study and Comparison of Charge Air Cooling Techniques and their Effects on Efficiency of Automobile Engine" by Ravindra Kapse and Dr. R. R. Arakerimath focuses on various charge air cooling methods and their impact on the efficiency of automotive engines. The study emphasizes the importance of cooling the intake air to improve engine performance, reduce emissions, and meet stringent regulatory standards like BSVI. Turbochargers increase the density of intake air, improving volumetric efficiency. However, compressing air raises its temperature, reducing its density and the engine's efficiency. Intercoolers cool this compressed air, increasing its density and thus the engine's power output and efficiency. This process also helps in reducing the risk of engine knocking and improving durability (Veneţia Sandu, 2014). Air-to-air intercoolers rely on ambient air to cool the charge air. While effective, their efficiency is limited in high ambient temperature conditions, which reduces their ability to cool the intake air effectively. Additionally, their performance diminishes at lower vehicle speeds where less air flows through the intercooler fins (Sandu, 2014). Indirect (water-cooled) intercoolers offer better thermal management by using a coolant to transfer heat from the charge air. This method provides more consistent cooling regardless of ambient temperatures and vehicle speeds, enhancing overall engine performance (Sankar & Kishore, 2013). Studies have explored integrating existing air conditioning systems with intercoolers to provide additional cooling. This method involves routing cooled air from the air conditioning system through the intercooler, which can significantly reduce the intake air temperature and improve engine performance (Muqeem & Kumar, 2013). The research includes simulation models and practical testing to compare the performance of direct (air-to-air) and indirect (water-cooled) intercoolers. Simulations help predict heat rejection capabilities and pressure drops, while practical tests validate these models under real-world conditions (Brouillard et al., 2015).

The study titled "Condensation within a Charge Air Cooler" by Tomás Roseiro Murcela addresses the challenge of water condensation in charge air coolers (CACs)

used in automotive engines. This condensation can cause significant engine damage when large amounts of water are expelled into the combustion chamber. The study, conducted in collaboration with the JDEUS company, aims to identify the conditions under which condensation occurs and to propose solutions to mitigate this issue. The study uses both theoretical models and experimental tests to validate the predictions of condensation within the intercooler. Tests conducted in a wind tunnel with a modified intercooler prototype showed that certain design changes could effectively reduce or eliminate condensation without compromising thermal efficiency or increasing pressure drop. A device designed to reduce or eliminate condensation was developed and tested. The modified intercooler prototype demonstrated a significant reduction in condensation while maintaining performance. This solution involves adjusting the temperature profile within the intercooler to prevent temperatures from dropping below the dew point.

The paper "Knock (and pre-ignition) damage on engine components: case studies" by E. Balducci, S. Parisi, F. Boccia, M. Barichello, and L. Ceschini explores the effects of knocking and pre-ignition on various components of internal combustion engines. This study emphasizes the need to understand and mitigate knock-induced damage to enhance engine performance and longevity, especially in high-performance engines where higher compression ratios and turbocharging are common. The study focuses on pistons, cylinder heads, liners, and spark plugs, which are most susceptible to knock-induced damage. The analysis uses high-resolution digital and 3D microscopes, scanning electron microscopy (SEM), and energy-dispersive X-ray spectroscopy (EDS) to examine the damage mechanisms. Persistent knocking can lead to pre-ignition, a more destructive form of abnormal combustion. Pre-ignition causes excessive heat and pressure, resulting in severe damage such as piston seizure, ring locking, and significant wear on all combustion chamber components (Cavina et al., 2016).

2. TURBOCHARGED PISTON ENGINE AIRCOOLING SYSTEMS

Air cooling systems for turbocharged piston engines are essential for managing the additional heat generated by the turbocharging process. Turbochargers compress the intake air, which increases its temperature. Without effective cooling, this hot, dense air can lead to engine knocking, reduced performance, and potential engine damage. Therefore, air cooling systems play a crucial role in maintaining engine efficiency and longevity. Air Cooling systems significantly improves engine performance and efficiency by reducing the temperature of the intake air, increasing its density, and allowing more oxygen to enter the combustion chamber. This results in better fuel combustion, increased power output, and enhanced overall engine performance.

However, air cooling systems also come with disadvantages. They add weight and complexity to the aircraft, which can affect overall performance and maintenance requirements. Air-to-water intercoolers, in particular, require additional components like radiators and coolant systems, increasing both weight and maintenance complexity. Furthermore, ensuring adequate airflow to air-to-air intercoolers can be challenging, especially in compact engine compartments.

The primary types of air cooling systems for turbocharged piston engines are listed and described below.

2.1. Air to Air Intercooler

Air-to-air intercoolers are crucial components in turbocharged piston engines, designed to enhance performance and efficiency by cooling the compressed intake air. By reducing the temperature of the air charge before it enters the combustion chamber, air-to-air intercoolers increase air density, leading to more efficient fuel combustion and improved engine power output.

The primary function of an air-to-air intercooler is to remove heat from the compressed air exiting the turbocharger before it enters the engine's intake manifold.

The turbocharger compresses the intake air, raising its temperature significantly due to the ideal gas law

$$\frac{P1 \times V1}{T1} = \frac{P2 \times V2}{T2} \tag{2.1}$$

The hot, compressed air flows through the intercooler, which is a type of heat exchanger. The intercooler has a network of internal tubes and external fins. Ambient air flows over the external fins of the intercooler, absorbing heat from the compressed air inside the tubes. This process reduces the temperature of the compressed air. The cooled, denser air is then directed into the engine's intake manifold, where it mixes with fuel for combustion.

Air-to-air intercoolers do not require additional liquid cooling circuits, reducing complexity. Generally lighter than liquid-based cooling systems. Additionally Air to Air Intercoolers are efficient at reducing intake air temperatures, especially in conditions with high ambient airflow.

However their effectiveness relies heavily on the availability of ambient air, which can be a limitation at low speeds or in specific operating conditions. Proper placement is essential for optimal performance, which can be challenging in confined engine compartments.

Air-to-air intercoolers are typically constructed from materials with high thermal conductivity, such as aluminum, to maximize heat transfer efficiency.

The challenge for Air to Air Intercooler design is optimizing the balance between cooling efficiency and pressure drop and reserved space.

2.1.1. Sub-Components of the Air to Air Intercoolers

Air-to-air intercoolers are composed of several sub-components that work together to effectively cool the compressed air before it enters the engine. The main components are Core and End Tanks. The core part consists of tube and fin.

2.1.1.1. Tubes

Air-to-air intercooler tubes are critical components within the intercooler system, designed to transfer heat from the compressed intake air to the ambient air, enhancing the efficiency and performance of turbocharged piston engines. The design and selection of these tubes are essential for optimizing cooling performance, minimizing pressure drop, and ensuring durability.

High thermal conductivity materials, such as aluminum, are preferred to maximize heat transfer efficiency. Materials must withstand exposure to various environmental conditions and corrosive intake air. Also Tubes must withstand high pressures without deforming or leaking.

Adequate support and mounting is important also for tubes to resist vibrations and thermal expansion.

The shape (cylindrical, oval, flat) affects both the pressure drop and heat transfer efficiency. Maximizing the surface area through internal and external fins improves heat dissipation. Pressure Drop and Flow Distribution is important parameters for tube selection.

Types of Intercooler Tubes;

Straight Tubes: Simple cylindrical or oval tubes that allow air to flow directly from one end to the other. Common in basic intercooler designs where simplicity and cost are key considerations.

Bar-and-Plate Tube: Comprises flat tubes separated by finned plates. Offers robust construction and high heat transfer efficiency, suitable for high-performance and heavy-duty applications. Can be more complex and expensive to manufacture.

Tube-and-Fin: Consists of round or oval tubes with external fins attached. Provides a balance between weight and cooling efficiency, commonly used in automotive and aviation applications.

2.1.1.2. Fins

Fins are a critical component of air-to-air intercoolers in turbocharged piston engines, playing a vital role in the heat exchange process. They increase the surface area available for heat transfer, enhancing the efficiency of cooling the compressed intake

air. Proper design and selection of fins are crucial for maximizing intercooler performance while minimizing pressure drop and weight. Fins can also accumulate dirt and debris, reducing their effectiveness over time and requiring maintenance.

External Fins located outside the tubes, they enhance heat transfer to the ambient air. Internal Fins are located Inside the tubes, they increase the internal surface area to improve heat transfer from the air to the tube walls.

Types of Intercooler Fins

Straight Fins: Simple, straight fins that run parallel to the airflow. Straight fins are easy to manufacture and provide a low-pressure drop. However they are less effective in maximizing surface area compared to other fin types.

Louvered Fins: Fins with small slits or louvers cut into them to increase turbulence.

These fins enhance heat transfer by increasing air turbulence. But this fin type causes higher pressure drop and they more complex for manufacturing.

Wavy Fins: Fins with a wavy pattern to increase surface area. Wavy fins have better heat transfer efficiency due to increased surface area and airflow disruption. But this fin type cause increased pressure drop compared to straight fins.

Perforated Fins: Fins with small holes to create additional turbulence. Increases heat transfer by enhancing airflow mixing. But the main disadvantage of this fins are higher manufacturing complexity and potential for higher pressure drop.

Offset Strip Fins: Short strips of fins offset from each other to create turbulent airflow. Excellent heat transfer performance due to induced turbulence. To manufacture these fin types is olsa harder than staraight fins.

2.1.1.3. End Tanks

Located at each end of the core, they direct the flow of air into and out of the intercooler. Ensures uniform airflow across the intercooler core, enhancing cooling efficiency. Provides mechanical strength to the intercooler assembly. The end tank design promotes even airflow distribution across the intercooler core. The design must withstand the operating pressures and thermal stresses. The shape and internal geometry must be optimized to minimize pressure losses.

Types of End Tanks

Stamped End Tanks: Manufactured by stamping sheets of metal into the desired shape. These type of tanks are cost effective, lightweight, and suitable for high-volume production. However, limited design flexibility and potential for weaker structural integrity compared to other methods.

Cast End Tanks: Produced by pouring molten metal into a mold. These types of tanks are strong and durable, with high design flexibility. However, these tanks are heavier and more expensive to manufacture. Especially molding costs are higher.

Fabricated End Tanks: Assembled by welding or brazing individual metal pieces. These tanksa re highly customizable and strong. But they are more expensive due to welding requirements.

2.1.2. Calculation Formulas for Air to Air Intercooler

2.1.2.1. Single Tube Calculation Formulas

Heat Transfer Rate of Tube (Q_single):

$$Q_{singleTube} = U \cdot A_{ST} \cdot \Delta T_{lm} \tag{2.2}$$

$$\Delta T_{lm} = \frac{\left(T_{h,i} - T_{c,o}\right) - \left(T_{h,o} - T_{c,i}\right)}{\ln\left(\frac{T_{h,i} - T_{c,o}}{T_{h,o} - T_{c,i}}\right)} \tag{2.3}$$

$$A_{ST} = \pi \cdot D_{ext} \cdot L_{tube} \tag{2.4}$$

$$\frac{1}{U} = \frac{1}{h_i} + \frac{t}{k} + \frac{1}{h_o}$$

(2.5)

Airflow and Pressure Drop of Tube:

$$Darcy - Weisbach\ Equation:\ \Delta P = f \cdot \frac{L}{D_h} \cdot \frac{\rho . v^2}{2}$$

(2.6)

For a circular tube, the hydraulic diameter (D_h) is simply the internal diameter of the tube (D_{int})

$$D_h = D_{int}$$

(2.7)

$$Re = \frac{\rho \cdot v \cdot D_h}{\mu}$$

(2.8)

The friction factor depends on the Reynolds number (Re) and the relative roughness of the tube

- For laminar flow (Re<2000), the friction factor can be calculated as:

  $f = \frac{64}{Re}$

- For turbulent flow (Re>4000), the Colebrook-White equation or empirical correlations such as the Moody chart can be used. An approximation for smooth pipes is:

  $f = 0.316 \cdot Re^{-0.25}$

2.1.2.2. Single Fin Calculation Formulas

Heat Transfer Rate (Q) of Fin:

$$Q_{fin} = h \cdot A_{fin} \cdot \Delta T . n_f$$

(2.9)

$$n_f = \frac{tanh(m \cdot L)}{m \cdot L}$$

(2.10)

$$m = \sqrt{\frac{2h}{k \cdot t}}$$

(2.11)

$$A_{fin} = 2.(h_{fin}.L + t_{fin}.L)$$

(2.12)

Airflow and Pressure Drop (ΔP) of Fin:

$$\Delta P = f \cdot \frac{L}{D_h} \cdot \frac{\rho . v^2}{2}$$

(2.13)

$$D_h = \frac{4.A_c}{P_w}$$

(2.14)

For a simple rectangular channel between fins:

$$A_c = w_c \cdot h_c$$

(2.15)

$$P_w = 2.(w_c + h_c)$$

(2.16)

$$Re = \frac{\rho \cdot v \cdot D_h}{\mu}$$

(2.17)

The friction factor depends on the Reynolds number (Re) and the relative roughness of the tube

- For laminar flow (Re<2000), the friction factor can be calculated as:

$$f = \frac{64}{Re}$$

- For turbulent flow (Re>4000), the Colebrook-White equation or empirical correlations such as the Moody chart can be used. An approximation for smooth pipes is:

$$f = 0.316 \cdot Re^{-0.25}$$

2.1.2.3 Air to Air Intercooler with Multiple Tubes and Fins Calculation Formulas

$$Q = U \cdot A \cdot \Delta T_{lm} \cdot n_f$$

(2.18)

$$\Delta T_{lm} = \frac{\left(T_{h,i} - T_{c,o}\right) - \left(T_{h,o} - T_{c,i}\right)}{\ln\left(\frac{T_{h,i} - T_{c,o}}{T_{h,o} - T_{c,i}}\right)}$$

(2.19)

$$A_{tube} = N \times (\pi \cdot D_{ext} \cdot L_{tube})$$

(2.20)

$$A_{fin} = N \times n_{fin} \times (2 \cdot h_{fin} \cdot t_{fin})$$

(2.21)

$$A = A_{tube} + A_{fin}$$

(2.22)

$$\frac{1}{U} = \frac{1}{h_i} + \frac{t}{k} + \frac{1}{h_o}$$

(2.23)

$$n_f = \frac{tanh(m \cdot L_{fin})}{m \cdot L_{fin}}$$

(2.24)

$$m = \sqrt{\frac{2h_o}{k_{fin} \cdot t_{fin}}}$$

(2.25)

$$\Delta P_{total} = N.f \cdot \frac{L}{D_h} \cdot \frac{\rho . v^2}{2}$$

(2.26)

2.2. Air to Water Intercooler

Air-to-water intercoolers are advanced cooling systems used primarily in turbocharged and supercharged engines to manage the temperature of the compressed intake air. These intercoolers operate by transferring heat from the hot compressed air to a cooling medium, which is water, thereby reducing the air temperature before it enters the engine. This cooling process increases the air density, enhancing engine performance and efficiency.

The core of intercooler, made of high thermal conductivity materials like aluminum, contains internal tubes or fins through which the hot compressed air passes. The surrounding water absorbs the heat from the air. Water Pump circulates the water

through the intercooler core and a separate heat exchanger (radiator). The heated water is then cooled in the radiator, where the heat is dissipated into the ambient air before the water is recirculated back to the intercooler. A reservoir stores extra coolant, ensuring the system remains full and accommodates coolant expansion and contraction. Thermostat and Control Valves regulate the coolant flow, maintaining optimal operating temperatures by controlling when the coolant circulates based on the air temperature.

Air-to-water intercoolers are widely used in high-performance automotive applications, marine engines, and aviation where space is limited, and consistent cooling is critical. Their ability to manage thermal loads effectively makes them suitable for environments with varying operating conditions and high-performance requirements.

More complex due to the additional components required like water pump, reservoir etc. Additional components and coolant weight is main disadvantage of the Air to water intercooler compared with air to air intercoolers. The initial cost and maintanence cost of the system is also higher than the air to air intercooler systems

3. MALE UAV TURBOCHARGED HFE PISTON ENGINE AIRCOOLING SYSTEM OPTIMISATION

3.1. Engine Specifications and Intercooler Requirements

3.1.1. Engine Specifications

Table 3.1: Engine Performance Datas

Nomenclature	Value
Bore	83.00 mm
Stroke	99.00 mm
Compression Ratio	16.2:1
Firing Order	1-3-4-2
Max Takeoff Power	165 hp
Min Manifold Air Temperature	0 °C
Max Manifold Air Temperature	70 °C
Max Manifold Pressure	2650 mbar
Max Rail Pressure	1500 mbar

3.1.2. Engıne Air Cooling Requirements

Table 3.2: HP Intercooler Requirements

Nomenclature	Value
External Fluid Inlet Temperature	43 °C
Internal Fluid Inlet Temperature	160 °C
Internal Fluid Flow (%100 Load)	660 kg/h
Max. Pressure Loss Limit Between HP Compressor and Engine Inlet	150 mbar
Internal Fluid Inlet Pressure (absolute)	3 bars
External Fluid Inlet Pressure (absolute)	1 bar
Max Manifold Air Temperature	70 °C
Min Manifold Air Temperature	0 °C

Table 3.3: LP Intercooler Requirements

Nomenclature	Value
External Fluid Inlet Temperature	43 °C
Internal Fluid Inlet Temperature	155°C
Internal Fluid Flow (%100 Load)	660 kg/h
Max. Pressure Loss Limit Between LP Compressor and HP Compressor Inlet	250 mbar
Internal Fluid Inlet Pressure (absolute)	2 bars
External Fluid Inlet Pressure (absolute)	1 bar
Max HP Compressor Inlet Temperature	75 °C

3.1.3. Air Cooling Layout

Our engine, which is the subject of our study, has a two stage turbocharger system, these turbochargers work serially with each other. Exhaust gases from the engine are directed to the LP and HP turbo turbines via two different wastegates mounted on the exhaust manifold. The air compressed and simultaneously heated in the LP turbo compressor is cooled over the LP intercooler before reaching the intake port of the HP compressor. This cooled air is then compressed and heated in the HP compressor before being sent to the HP intercooler. The air cooled in the HP intercooler is then delivered to the combustion chamber through the engine's intake manifold. In our design optimization study, we conducted tests to observe the effects of the modifications made, measuring temperature and pressure at multiple points. You can see the measurement sensor locations and the air cooling system layout below.

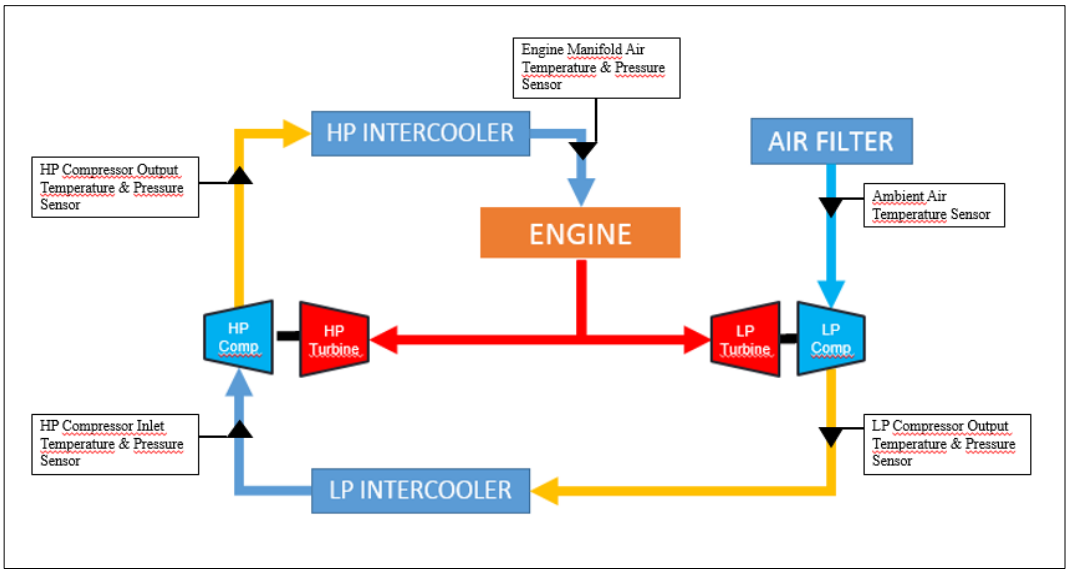

Figure 3.1: Air Cooling System Layout

When we look at the propeller on the aircraft from the front, the HP Intercooler is located on the left side of the engine and the LP intercooler is located on the right side of the engine. In this optimization study, no changes were made on the aircraft and the air intake ducts of the intercoolers.

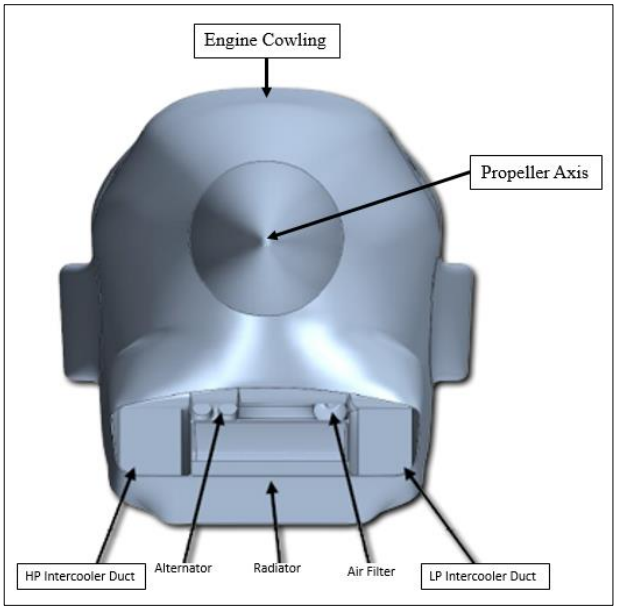

Figure 3.2: Inlet Ducts of UAV

3.2. Old Intercooler Design

3.2.1. HP Intercooler Specıfications

Table 3.4: Old HP Intercooler Technical Specifications

Nomenclature	**Value**
Core Length	485 mm
Core Height	150 mm
Core Depth	80 mm
Tube Dimensions	80x10 mm
Number Of Tube	7
Fin Type	Straight Fin
Flow Type	I Flow

Table 3.5: Old HP Intercooler Supplier Analysis Results

Nomenclature	Value	Units
Total Heat Transfer Rate	19,4	kW
Warm Fluid		
Flow	0,1833	kg/s
Temperature In	160	°C
Temperature Out	61,5	°C
Inlet Pressure (abs.)	3	bar
Pressure Drop	109,8	mbar
Cold Fluid		
Flow Rate	0,8142	kg/s
Temperature In	43	°C
Temperature Out	66,7	°C
Inlet Pressure	1013,25	mbar
Pressure Drop	11	mbar

3.2.2. LP Intercooler Specifications

Table 3.6: Old LP Intercooler Technical Specifications

Nomenclature	Value
Core Length	485 mm
Core Height	130 mm
Core Depth	80 mm
Tube Dimensions	80x10 mm
Number Of Tube	6
Fin Type	Straight Fin
Flow Type	I Flow

Table 3.7: Old LP Intercooler Supplier Analysis Data

Nomenclature	Value	Units
Total Heat Transfer Rate	19,8	kW
Warm Fluid		
Flow	0,1833	kg/s
Temperature In	155	°C
Temperature Out	57,7	°C
Inlet Pressure (abs.)	2	bar
Pressure Drop	160,84	mbar
Cold Fluid		
Flow Rate	0,7233	kg/s
Temperature In	43	°C
Temperature Out	56,4	°C
Inlet Pressure	1013,25	mbar
Pressure Drop	11	mbar

3.2.3. Flight Test Datas

3.2.3.1. Test Flight-1 with Old Intercoolers

Flight Test 1 was performed under ISA +15 weather conditions. During the test, throttle sweep tests were performed at 20,000, 25,000, and 30,000 feet. The purpose of this test was to observe the minimum Manifold Air Temperature achieved at high altitude with the old intercoolers.

Full Load Take-off Section Test Datas:

The data regarding the Take-off phase of Test 1 performed with the old intercoolers is presented below. The take-off occurred when the outside air temperature was 22 °C (Figure 3-3). Climbing was performed at full throttle (100% throttle) (Figure 3-4). The exit air temperatures at the LP turbo compressor increased to approximately 90 °C. (Figure 3-5). After passing through the LP intercooler, the temperatures dropped to around 35 °C (Figure 3-6), resulting in a temperature decrease of approximately 55 °C in the LP intercooler (Figure 3-7). The air entering the HP compressor at 35 °C was compressed, causing the temperatures to rise to around 120 °C. (Figure 3-8). In the HP intercooler, these temperatures were reduced to around 36 °C (Figure 3-9). The approximate temperature decrease in the HP intercooler was 84 °C (Figure 3-10). The pressure drop measurement was reliably taken from the LP intercooler, and it was approximately 85 mbar (Figure 3-11).

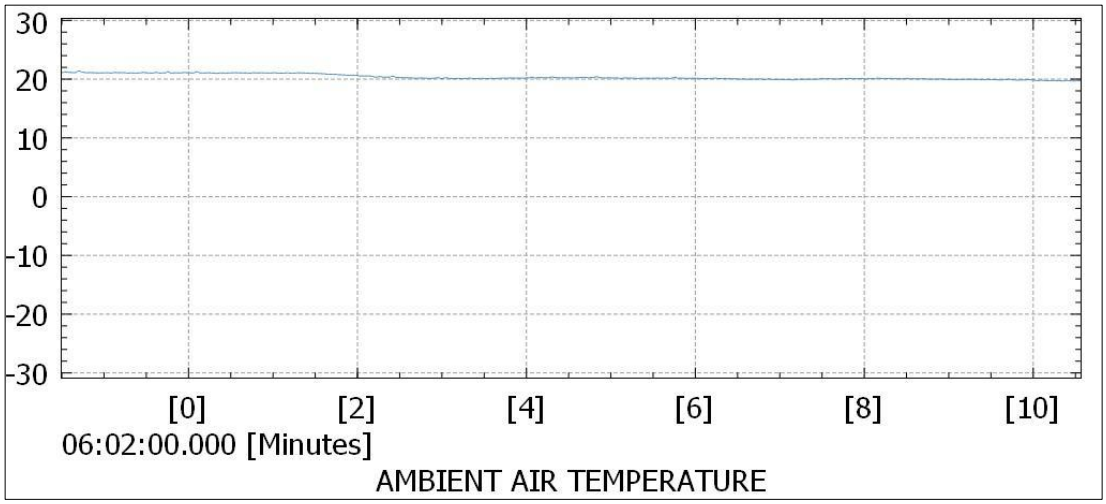

Figure 3.3: Old Intercooler Take-Off Test – Ambient Air Temperature Graph (°C - min)

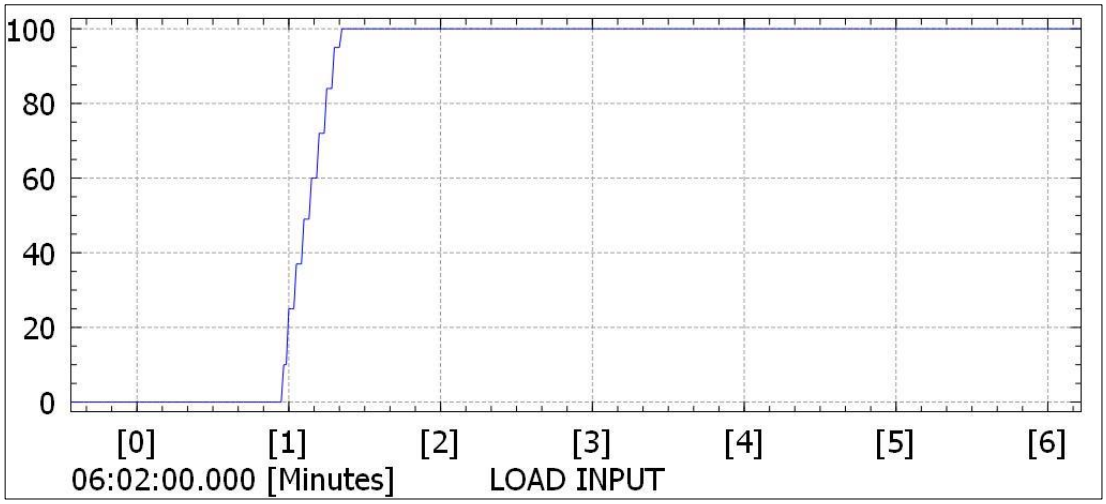

Figure 3.4: Old Intercooler Take-Off Test – Load Input Graph (% - min)

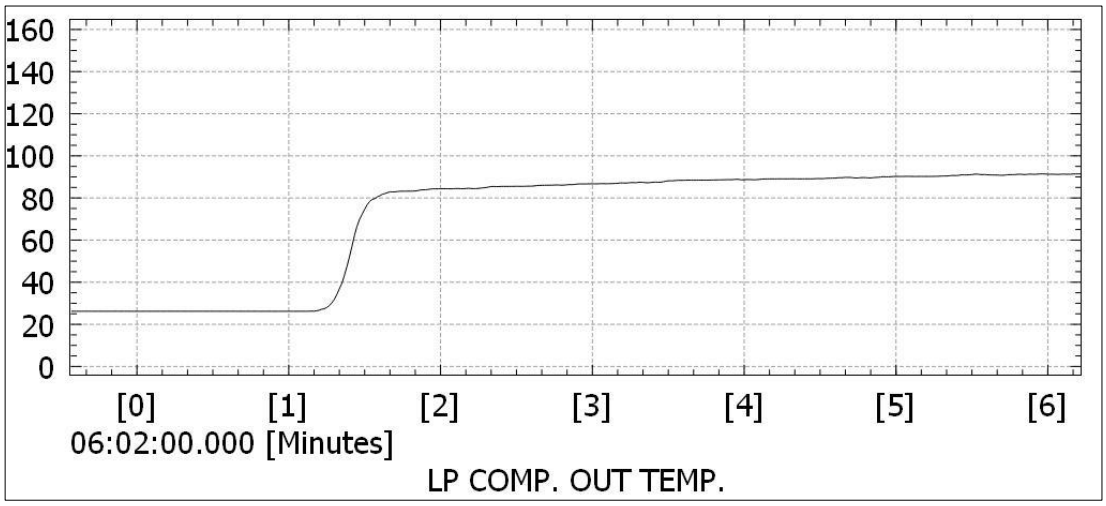

Figure 3.5: Old Intercooler Take-Off Test- LP Turbo Compressor Output Temperature Graph (°C - min)

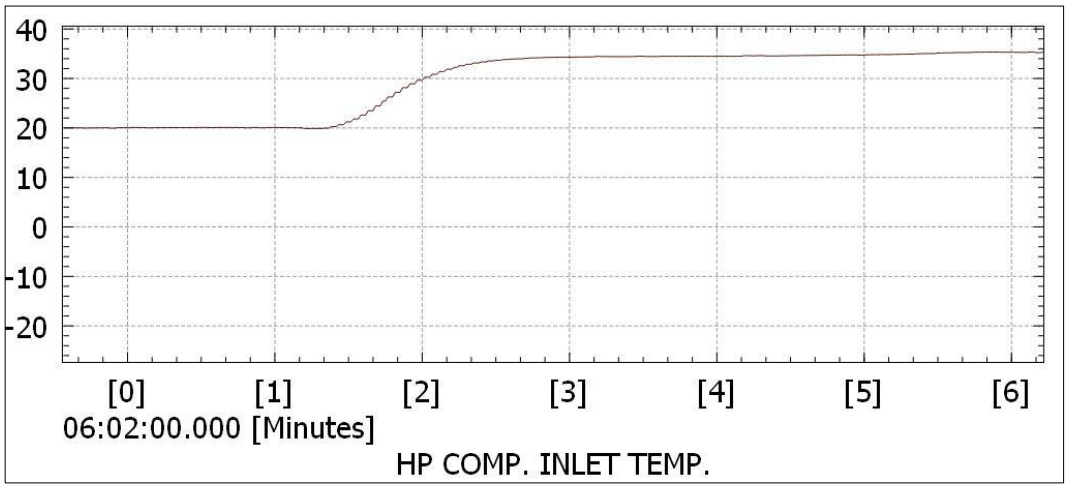

Figure 3.6: Old Intercooler Take-Off Test - HP Turbo Compressor Inlet Temperature Graph (°C - min)

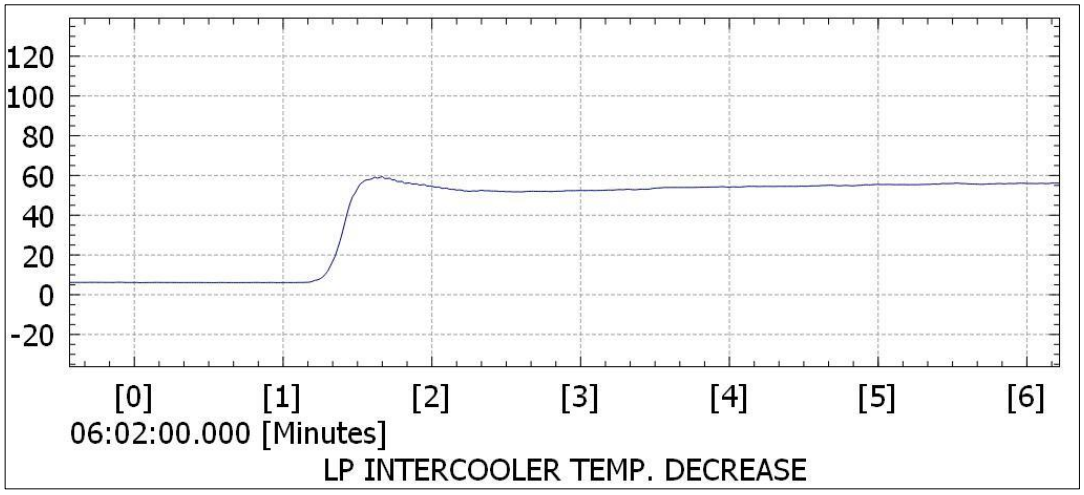

Figure 3.7: Old Intercooler Take-Off Test – LP Intercooler Temperature Decrease Graph (°C - min)

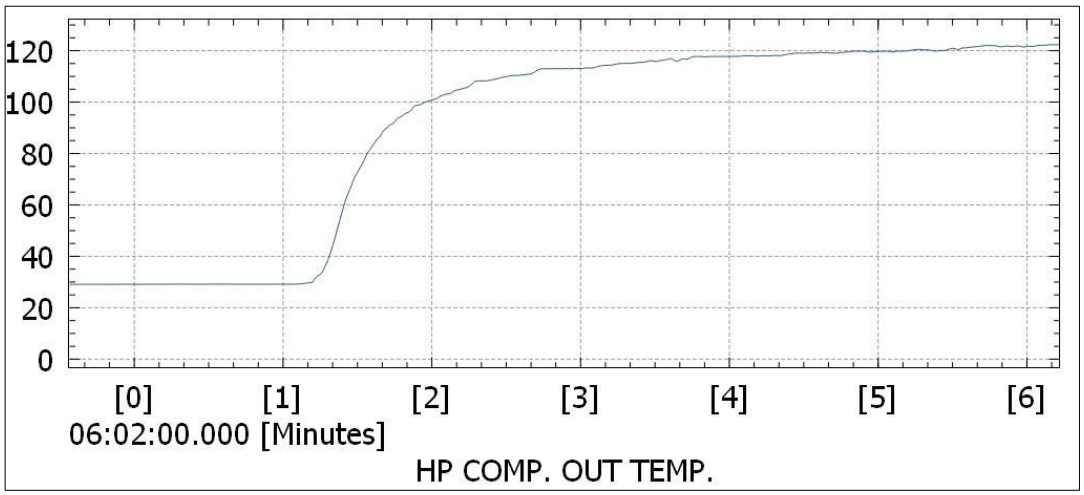

Figure 3.8: Old Intercooler Take-Off Test – HP Turbo Compressor Output Temperature Graph (°C - min)

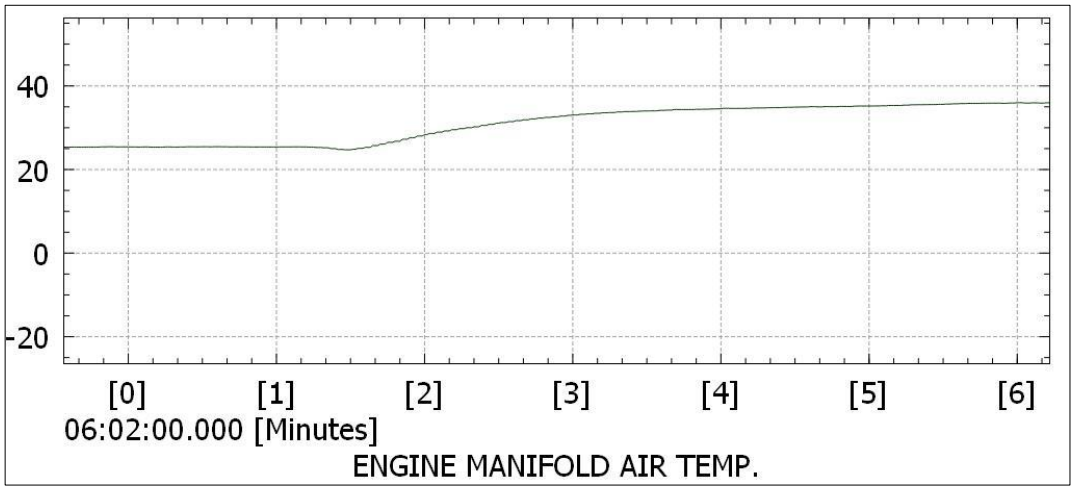

Figure 3.9: Old Intercooler Take-Off Test – Engine Manifold Air Temperature Graph (°C - min)

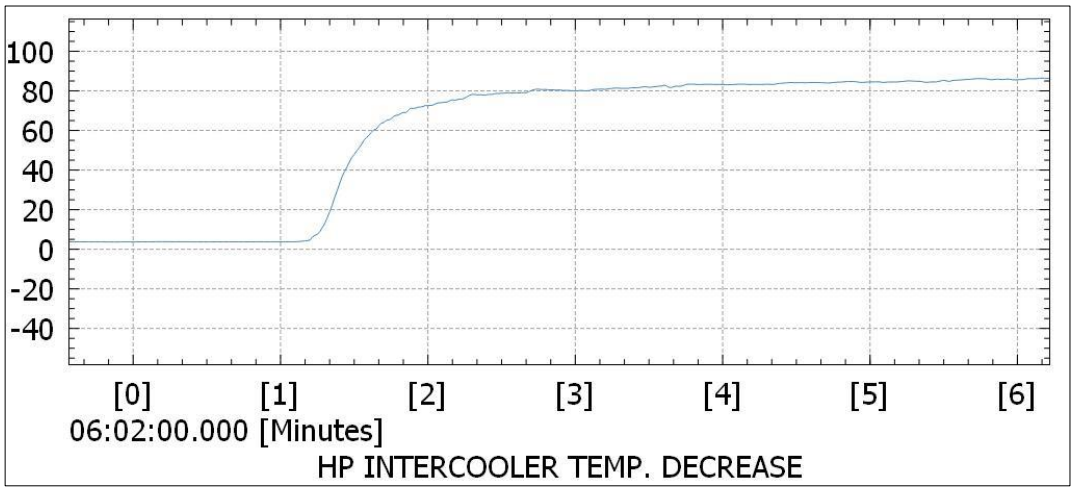

Figure 3.10: Old Intercooler Take-Off Test – HP Intercooler Temperature Decrease Graph (°C - min)

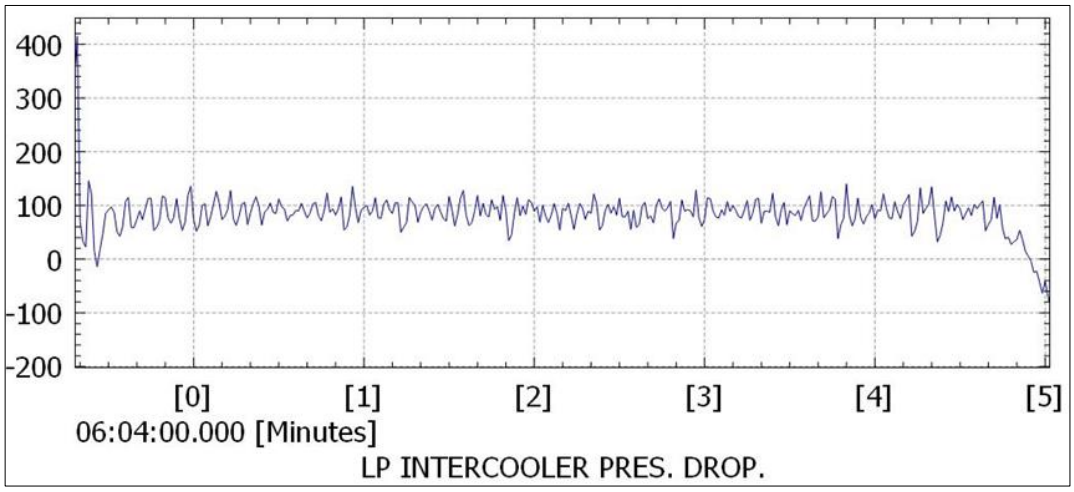

Figure 3.11: Old Intercooler Take-Off Test – LP Intercooler Pressure Drop Graph (mbar - min)

30000ft Test Section with %100 and %0 Load Input:

The data regarding the 30000 ft phase of Test 1 conducted with the old intercoolers is presented below. The outside air temperature was around -30 °C (Figure 3-12). 30000ft test was performed at full throttle (100% throttle) and idle. (Figure 3-13). The exit air temperatures at the LP turbo compressor increased to approximately 120 °C at full throttle phase and decreases 60 °C at idle throttle. (Figure 3-14). After passing through the LP intercooler, the temperatures dropped to around -24 °C at idle throttle and increased 2 °C at %100 throttle. (Figure 3-15), resulting in a temperature decrease of approximately 80 °C at idle throttle, and 120 °C at %100 throttle phase in the LP

intercooler (Figure 3-16). The air entering the HP compressor at was compressed, causing the temperatures to rise to around 45 °C at idle throttle and 85 °C at %100 throttle. (Figure 3-17). In the HP intercooler, these temperatures were reduced to around -24 °C for idle throttle and -12 °C for %100 throttle (Figure 3-18). The approximate temperature decrease in the HP intercooler was 70 °C for idle and 100 °C for %100 throttle (Figure 3-19). The pressure drop measurement was reliably taken from the LP intercooler, and it was approximately 10 mbar for idle and 60 mbar for %100 throttle (Figure 3-20).

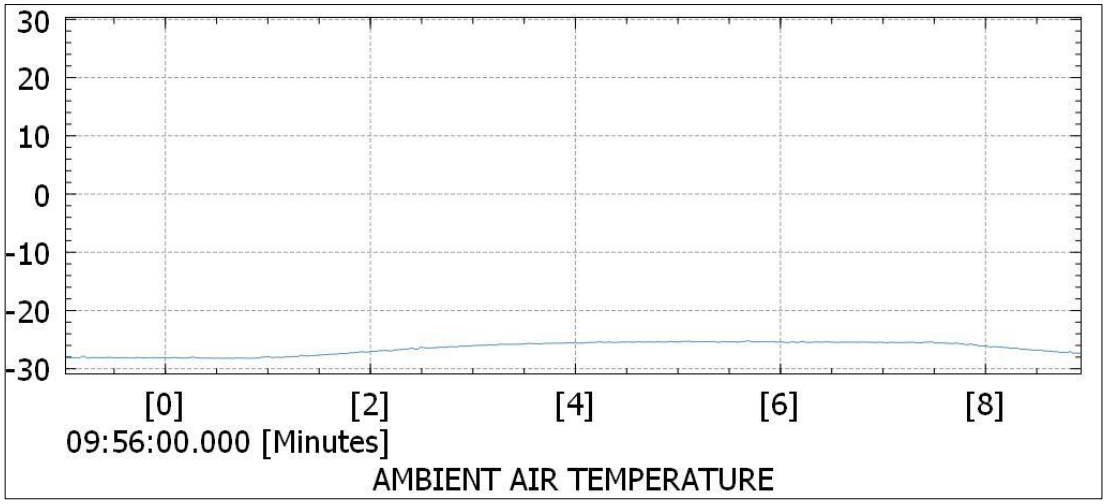

Figure 3.12: Old Intercooler 30000ft Test – Ambient Air Temperature Graph (°C - min)

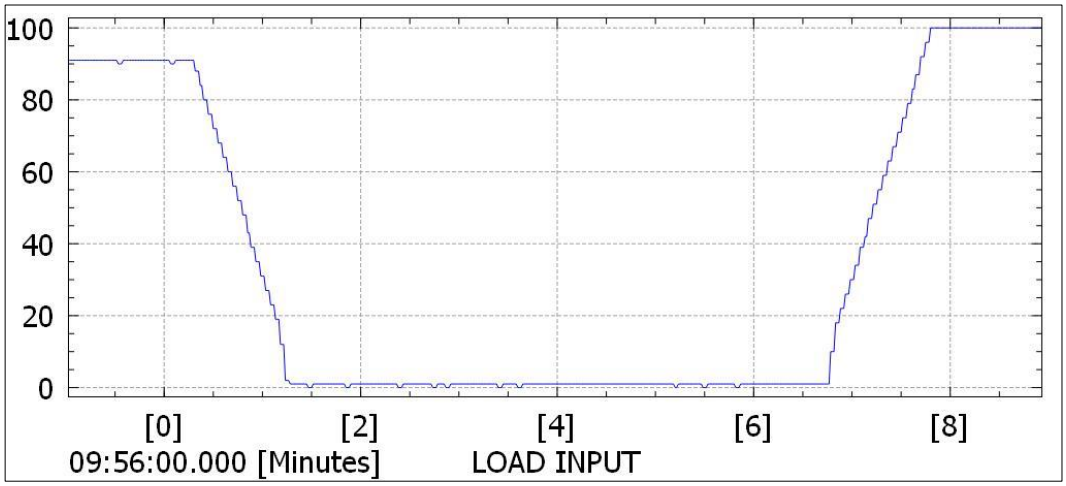

Figure 3.13: Old Intercooler 30000ft Test – Load Input Graph (°C - min)

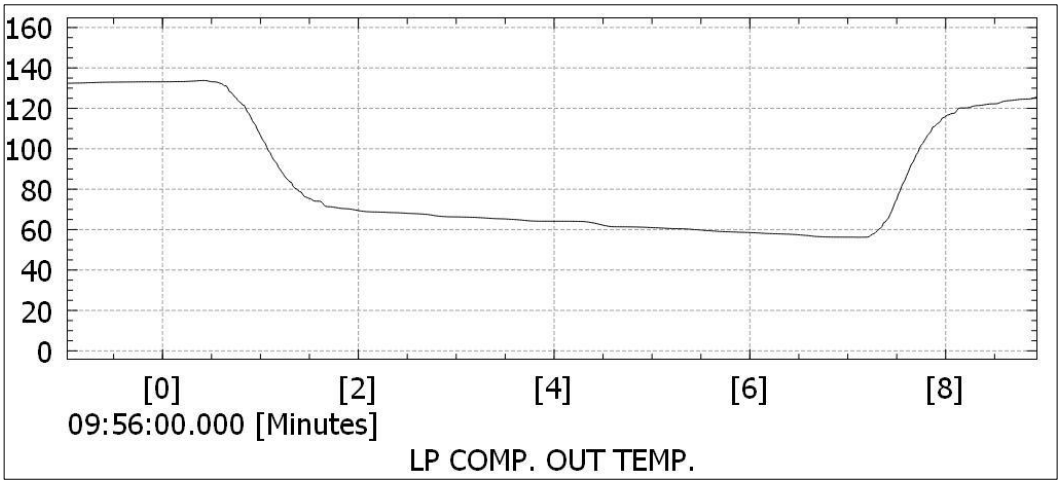

Figure 3.14: Old Intercooler 30000ft Test – LP Turbo Compressor Output Temperature Graph (°C - min)

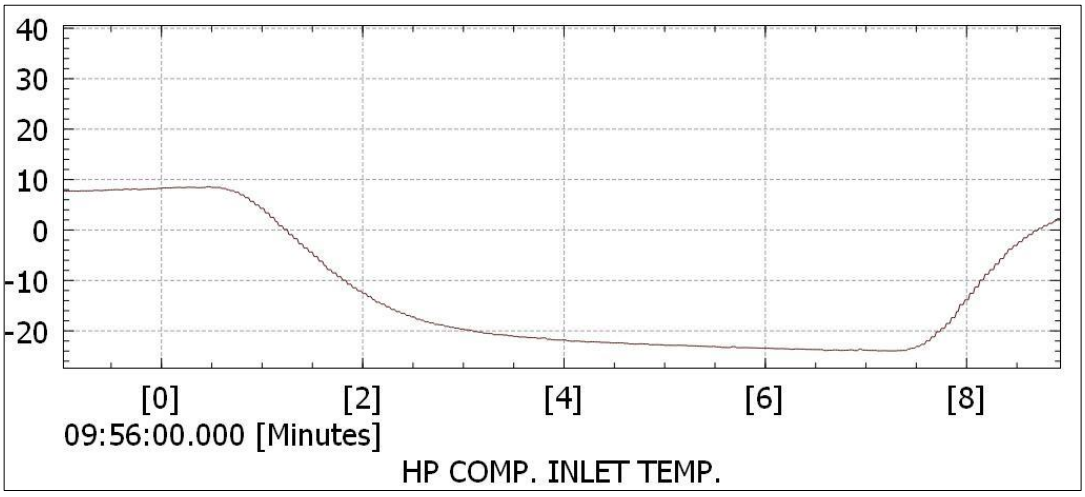

Figure 3.15: Old Intercooler 30000ft Test - HP Turbo Compressor Inlet Temperature Graph (°C - min)

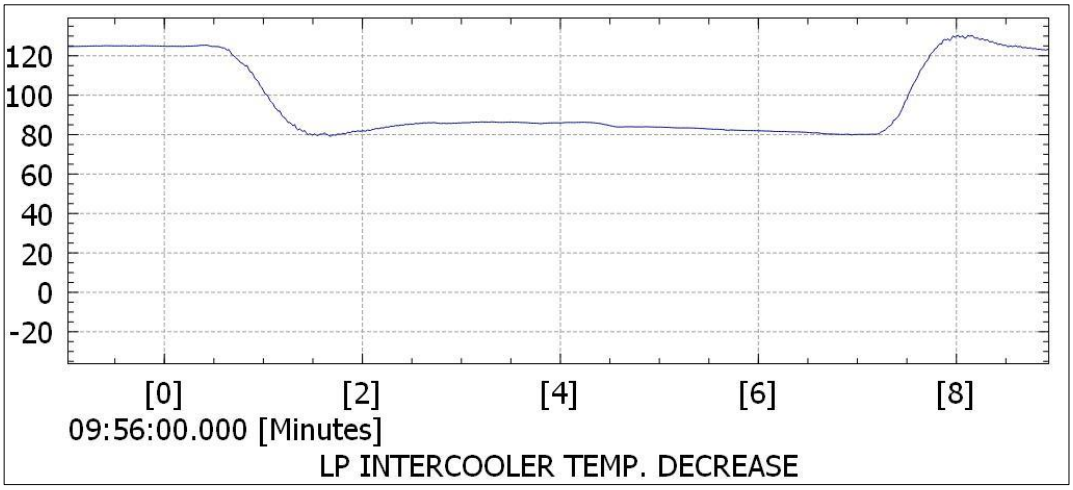

Figure 3.16: Old Intercooler 30000ft Test – LP Intercooler Temperature Decrease Graph (°C - min)

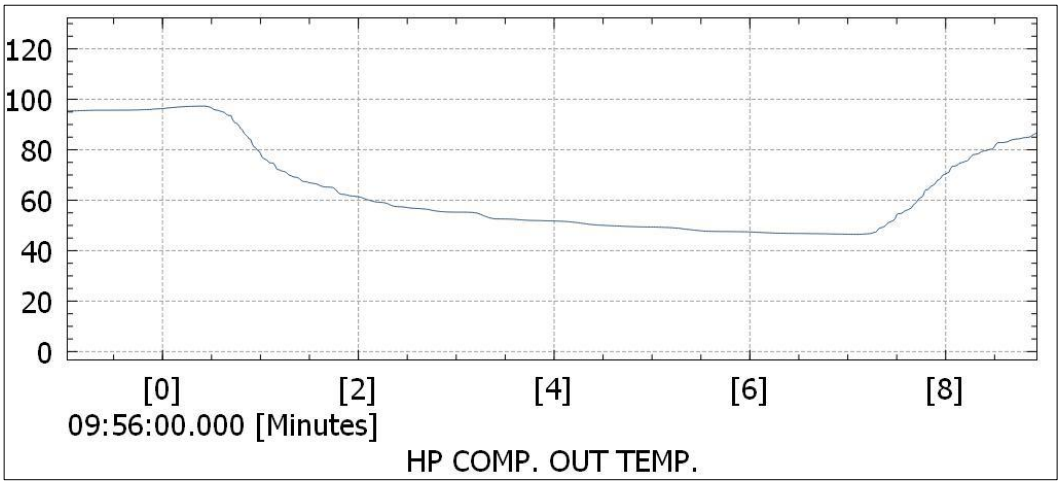

Figure 3.17: Old Intercooler 30000ft Test – HP Turbo Compressor Output Temperature Graph (°C - min)

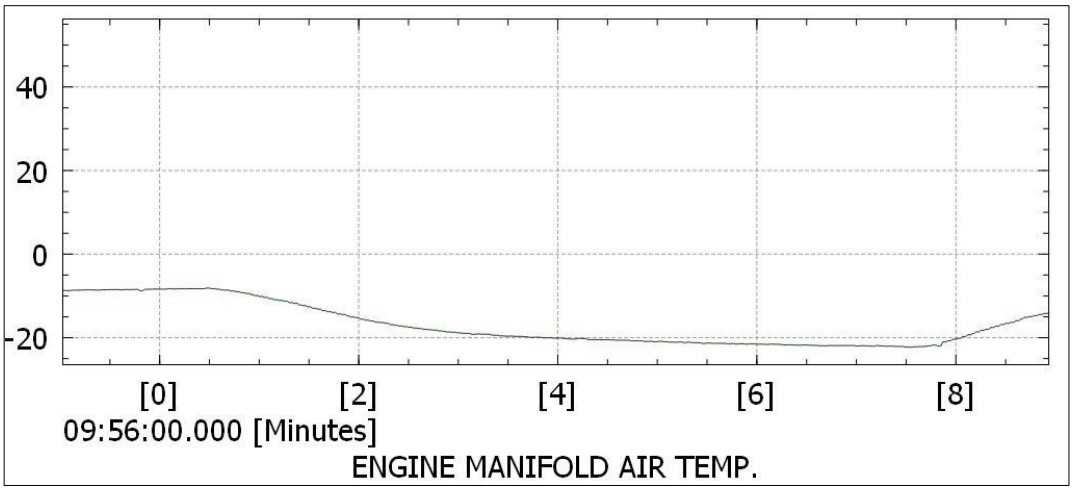

Figure 3.18: Old Intercooler 30000ft Test – Engine Manifold Air Temperature Graph (°C - min)

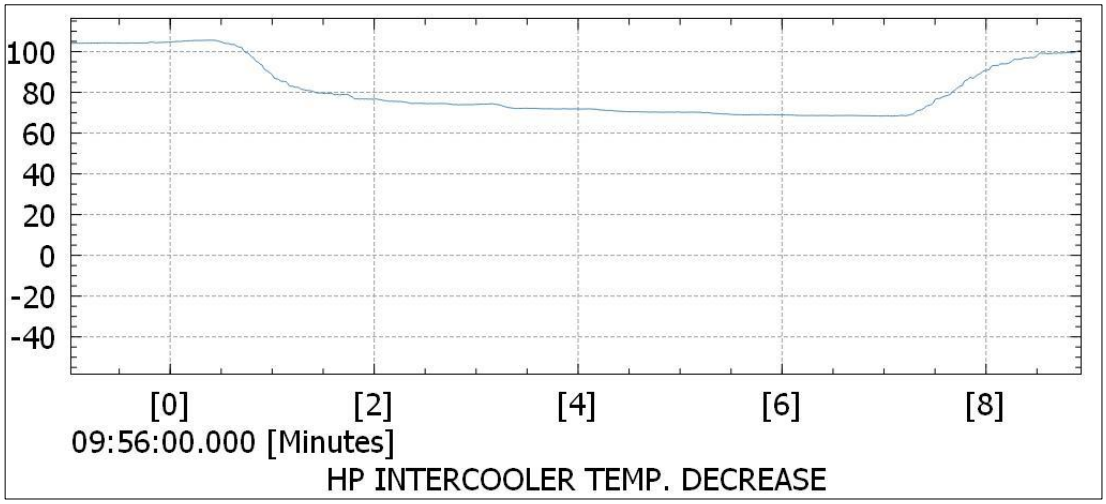

Figure 3.19 : Old Intercooler 30000ft Test – HP Intercooler Temperature Decrease Graph (°C - min)

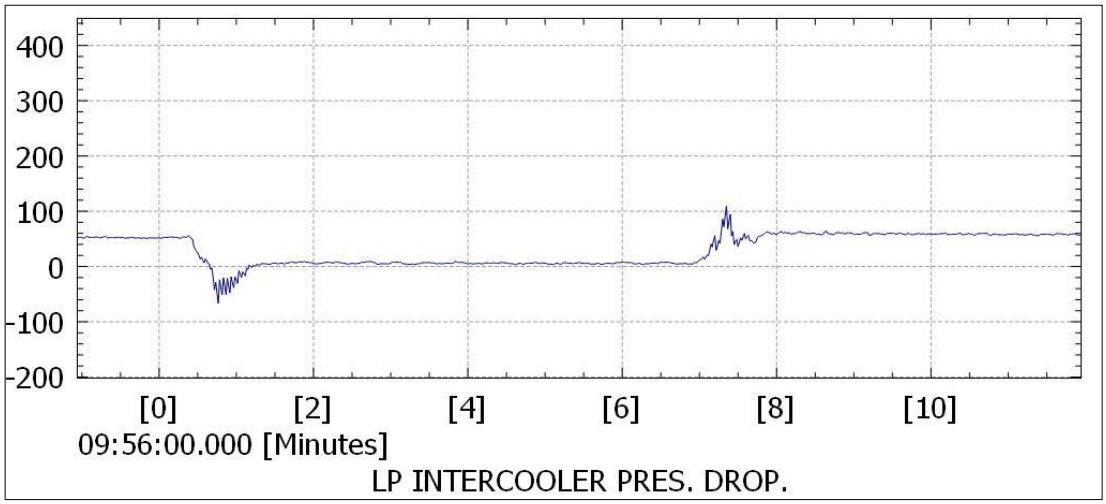

Figure 3.20 : Old Intercooler 30000ft Test- LP Intercooler Pressure Drop Graph (mbar- min)

25000ft Test Section Datas with %100 and %0 Load Input:

The data regarding the 25000 ft phase of Test 1 conducted with the old intercoolers is presented below. The outside air temperature was around -18 °C (Figure 3-21). 25000ft test was performed at full throttle (100% throttle) and idle. (Figure 3-22). The exit air temperatures at the LP turbo compressor increased to approximately 140 °C at full throttle phase and decreases 45 °C at idle throttle. (Figure 3-23). After passing through the LP intercooler, the temperatures dropped to around -15 °C at idle throttle and increased 20 °C at %100 throttle. (Figure 3-24), resulting in a temperature decrease of approximately 60 °C at idle throttle, and 120 °C at %100 throttle phase in the LP intercooler (Figure 3-25). The air entering the HP compressor at was compressed,

causing the temperatures to rise to around 45 °C at idle throttle and 100 °C at %100 throttle. (Figure 3-26). In the HP intercooler, these temperatures were reduced to around -14 °C for idle throttle and 2 °C for %100 throttle (Figure 3-27). The approximate temperature decrease in the HP intercooler was 60°C for idle and 100 °C for %100 throttle (Figure 3-28).

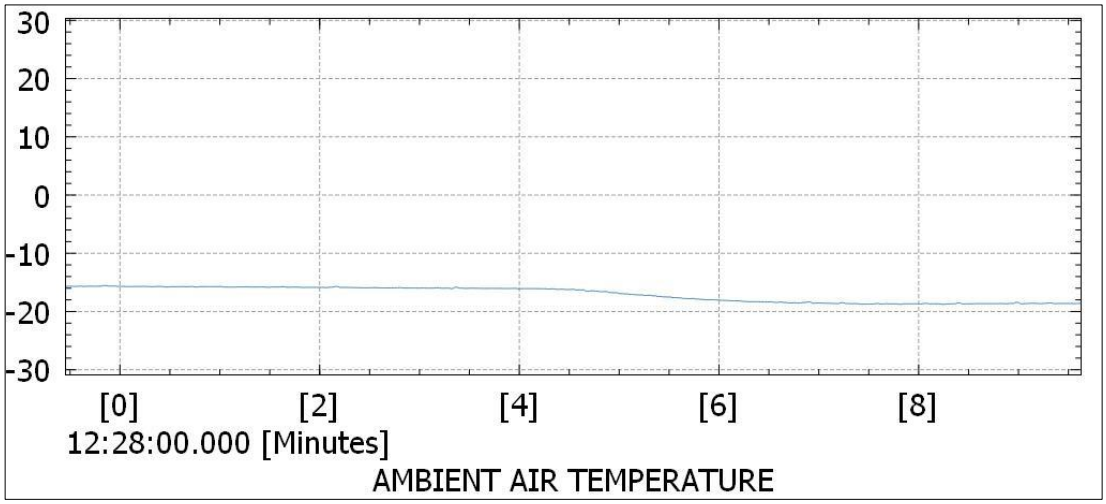

Figure 3.21: Old Intercooler 25000ft Test - Ambient Air Temperature Graph (°C - min)

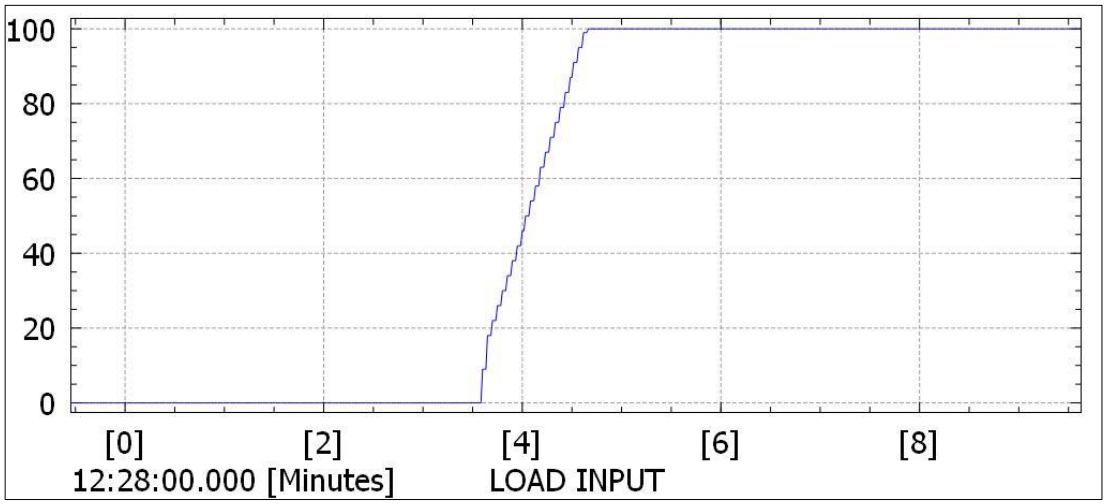

Figure 3.22: Old Intercooler 25000ft Test - Load Input Graph (% - min)

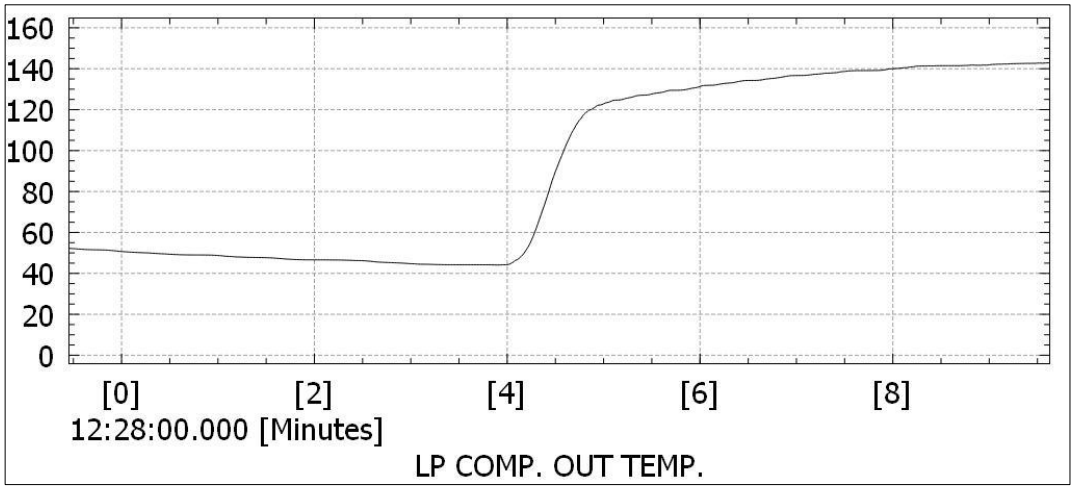

Figure 3.23: Old Intercooler 25000ft Test - LP Turbo Compressor Output Temperature Graph (°C - min)

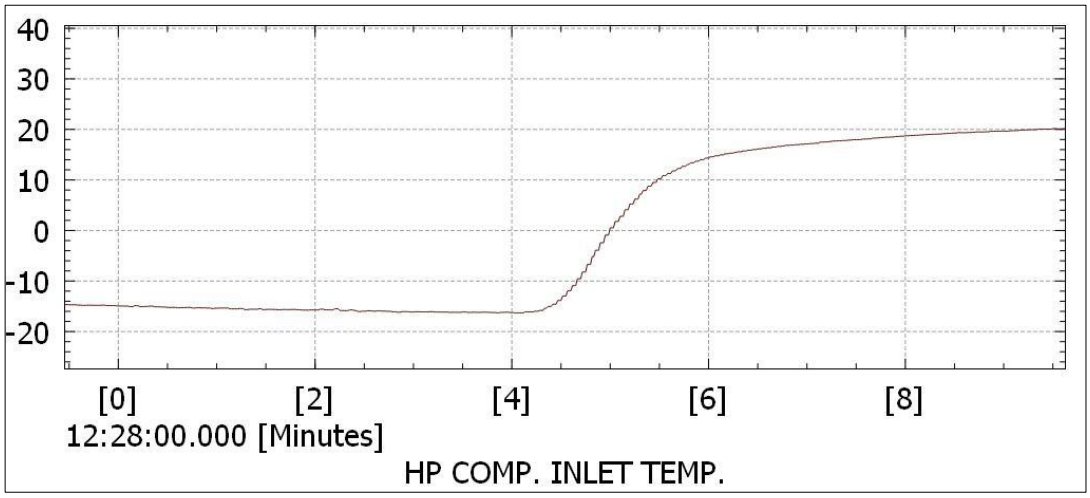

Figure 3.24: Old Intercooler 25000ft Test - HP Turbo Compressor Inlet Temperature Graph (°C - min)

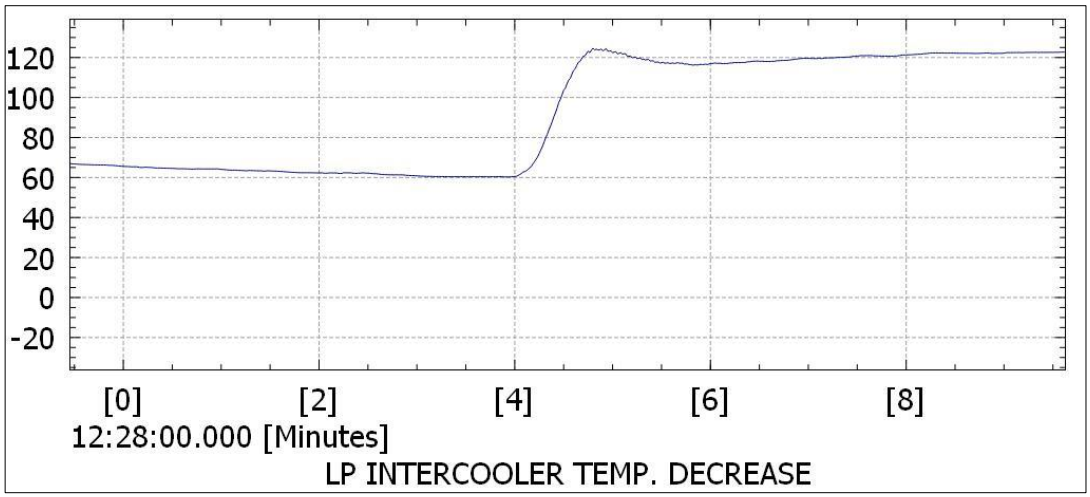

Figure 3.25: Old Intercooler 25000ft Test - LP Intercooler Temperature Decrease Graph (°C - min).

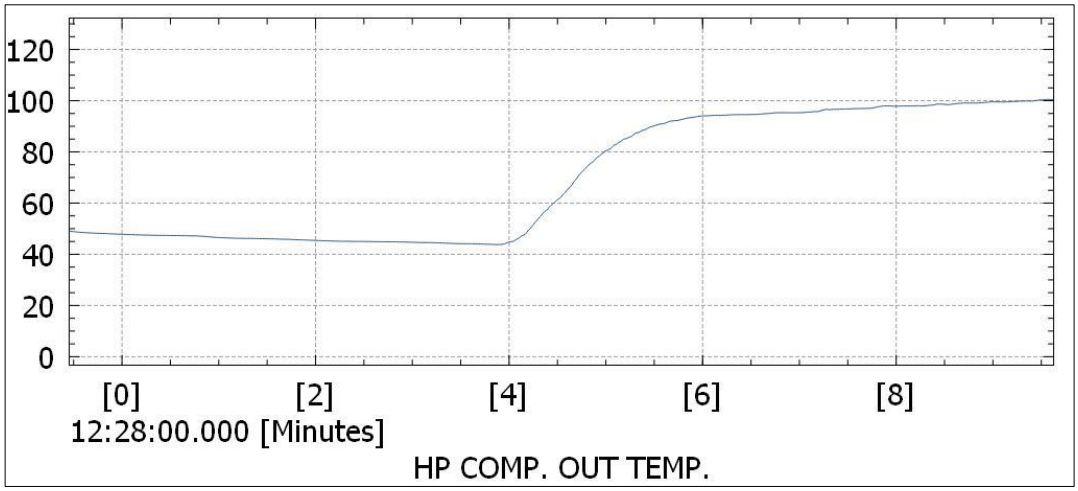

Figure 3.26: Old Intercooler 25000ft Test - HP Turbo Compressor Output Temperature Graph (°C - min).

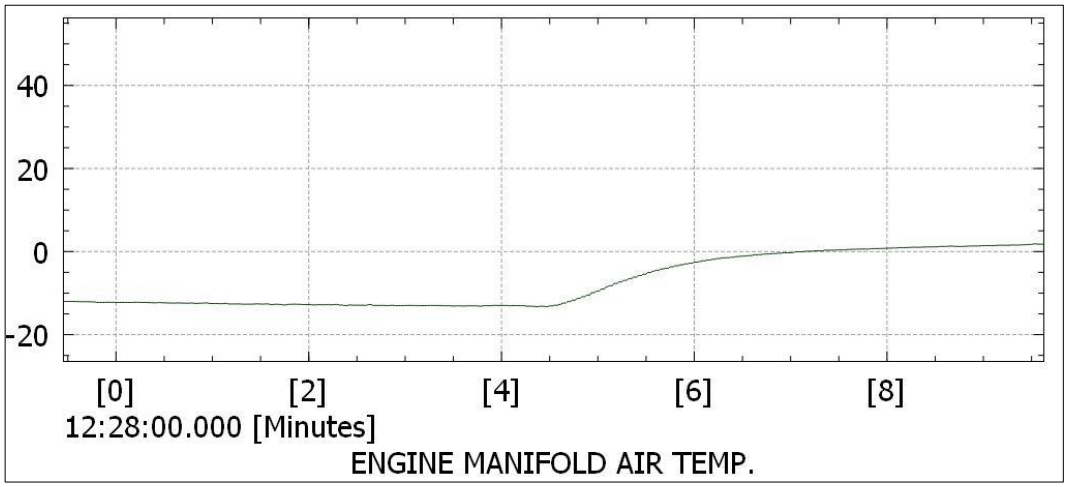

Figure 3.27: Old Intercooler 25000ft Test - Engine Manifold Air Temperature Graph (°C - min).

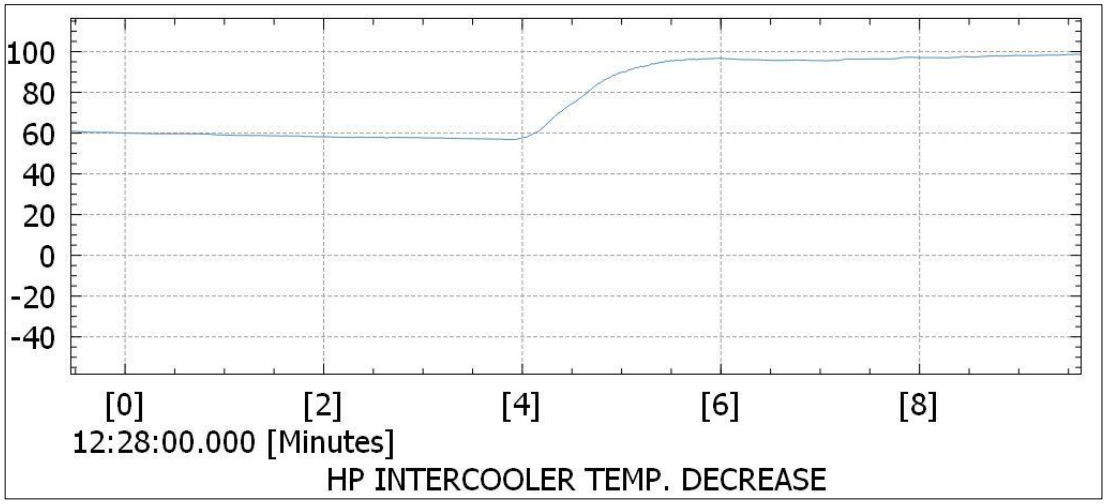

Figure 3.28: Old Intercooler 25000ft Test - HP Intercooler Temperature Decrease Graph (°C - min)

20000ft Test Section Datas with %100 and %0 Load Input:

The data regarding the 20000 ft phase of Test 1 conducted with the old intercoolers is presented below. The outside air temperature was around -5 °C (Figure 3-29). 20000ft test was performed at full throttle (100% throttle) and idle. (Figure 3-30). The exit air temperatures at the LP turbo compressor increased to approximately 140 °C at full throttle phase and decreases 40 °C at idle throttle. (Figure 3-31). After passing through the LP intercooler, the temperatures dropped to around -5 °C at idle throttle and increased 32°C at %100 throttle. (Figure 3-32), resulting in a temperature decrease of approximately 60 °C at idle throttle, and 120 °C at %100 throttle phase in the LP intercooler (Figure 3-33). The air entering the HP compressor at was compressed, causing the temperatures to rise to around 45 °C at idle throttle and 115 °C at %100 throttle. (Figure 3-34). In the HP intercooler, these temperatures were reduced to around 0 °C for idle throttle and 15 °C for %100 throttle (Figure 3-35). The approximate temperature decrease in the HP intercooler was 45°C for idle and 100 °C for %100 throttle (Figure 3-36).

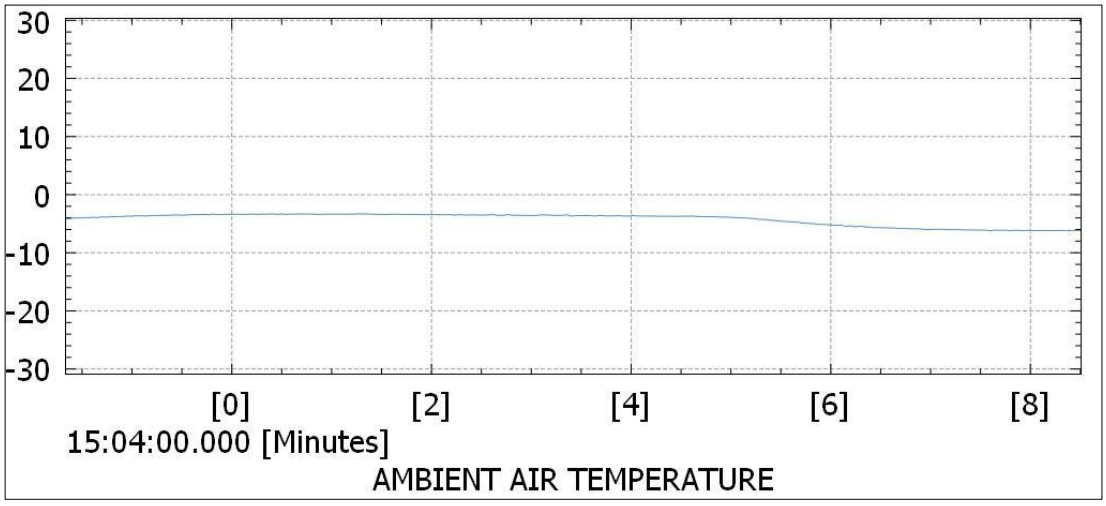

Figure 3.29: Old Intercooler 20000ft Test - Ambient Air Temperature Graph (°C - min)

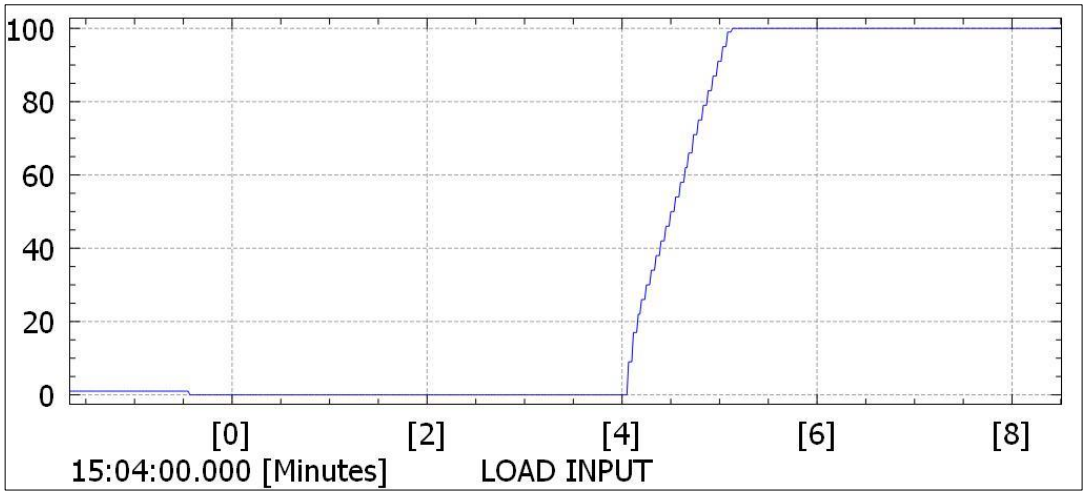

Figure 3.30: Old Intercooler 20000ft Test - Load Input Graph (% - min)

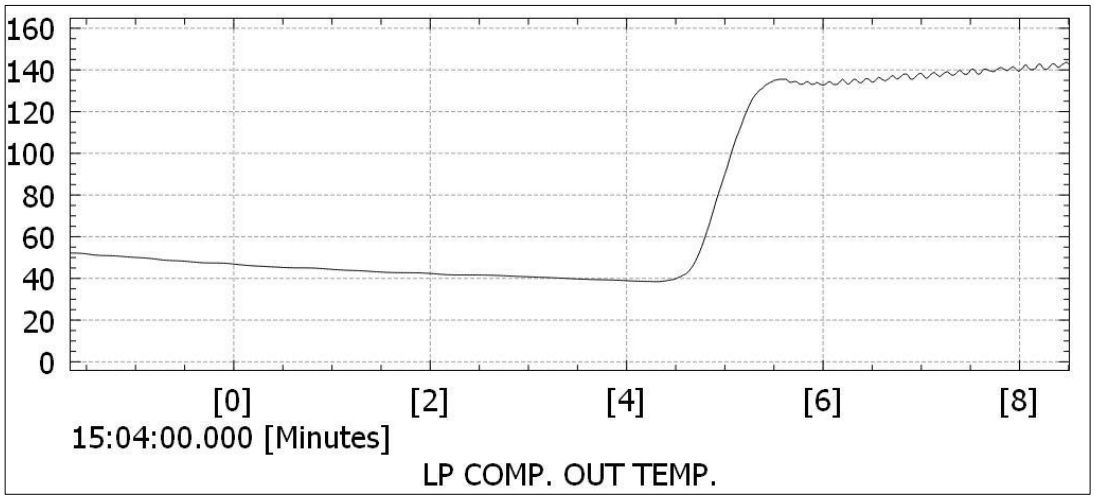

Figure 3.31: Old Intercooler 20000ft Test - LP Turbo Compressor Output Temperature Graph (°C - min)

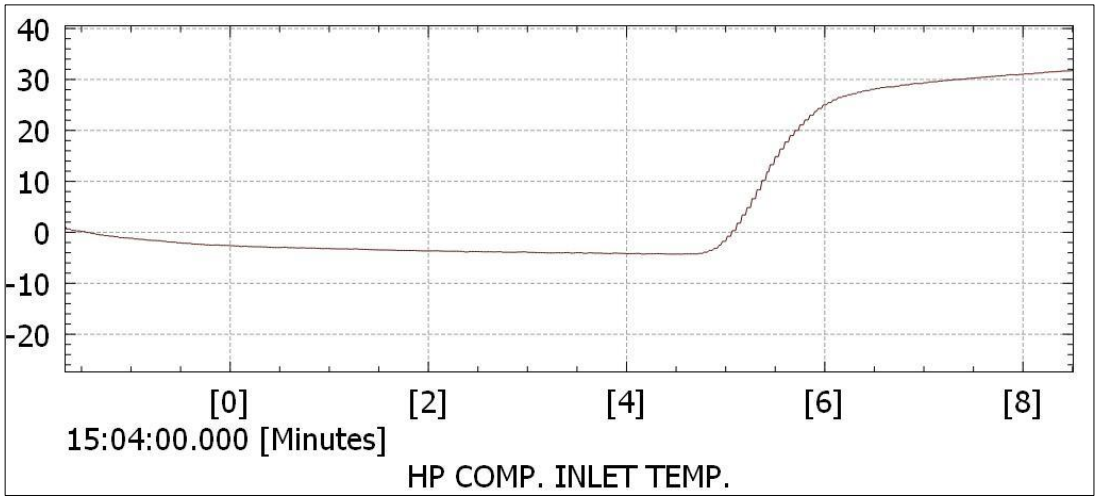

Figure 3.32: Old Intercooler 20000ft Test - HP Turbo Compressor Inlet Temperature Graph (°C - min)

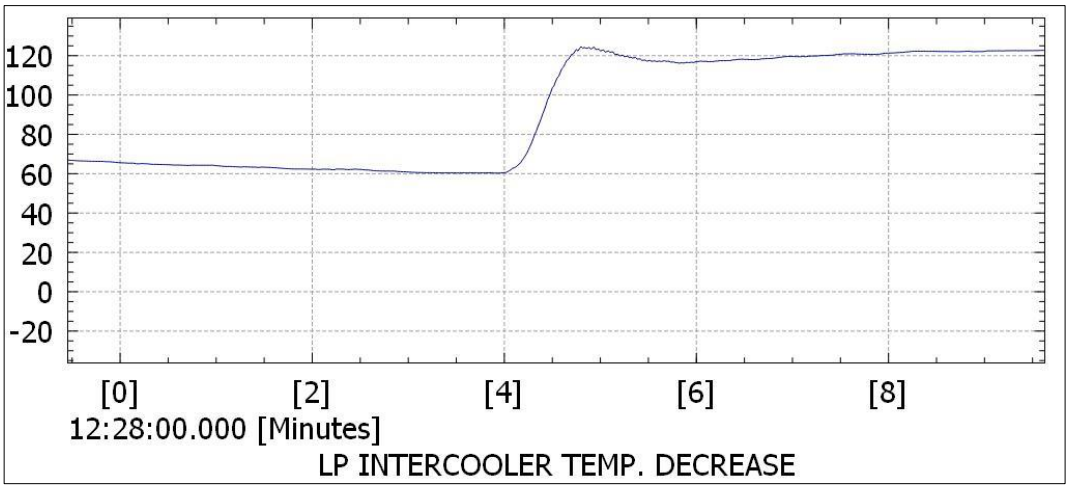

Figure 3.33: Old Intercooler 20000ft Test – LP Intercooler Temperature Decrease Graph (°C - min)

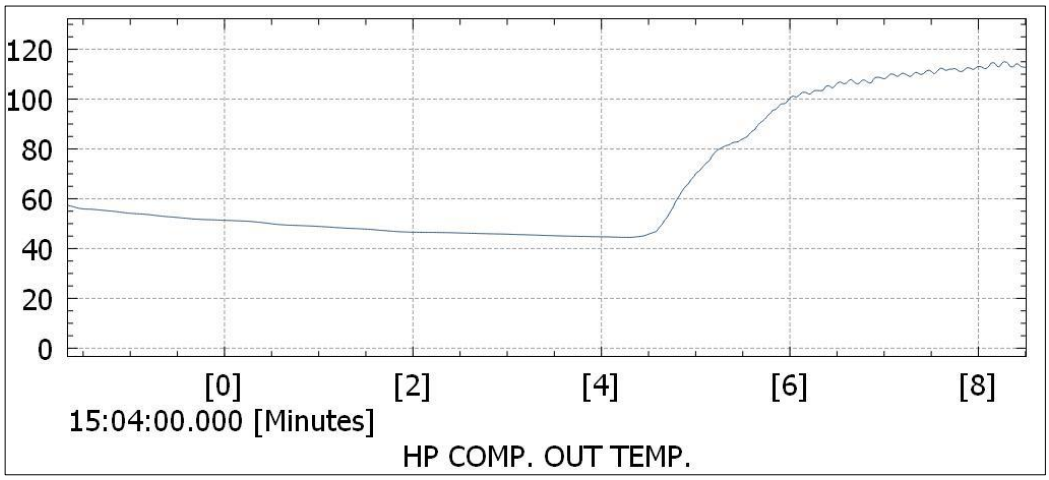

Figure 3.34: Old Intercooler 20000ft Test – HP Turbo Compressor Output Temperature Graph (°C - min)

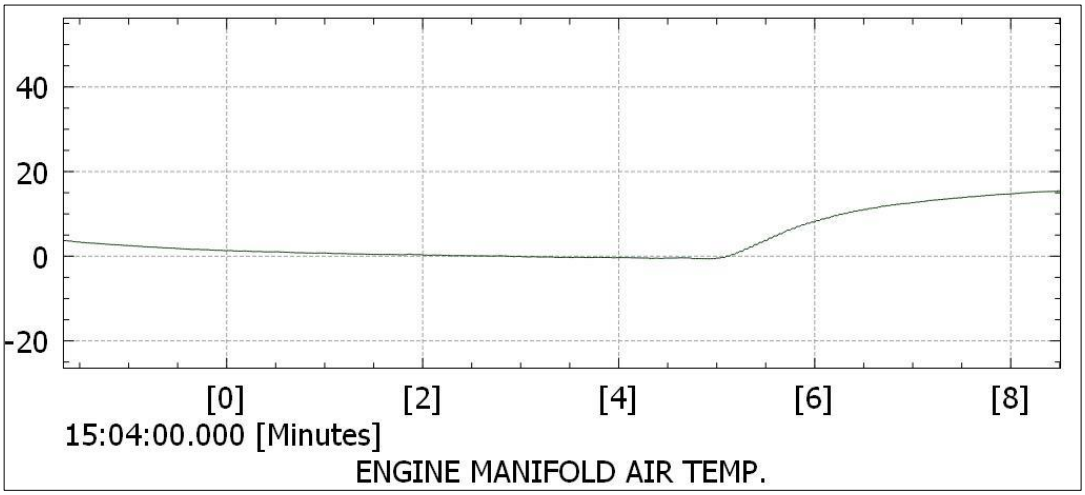

Figure 3.35: Old Intercooler 20000ft Test – Engine Manifold Air Temperature Graph (°C - min)

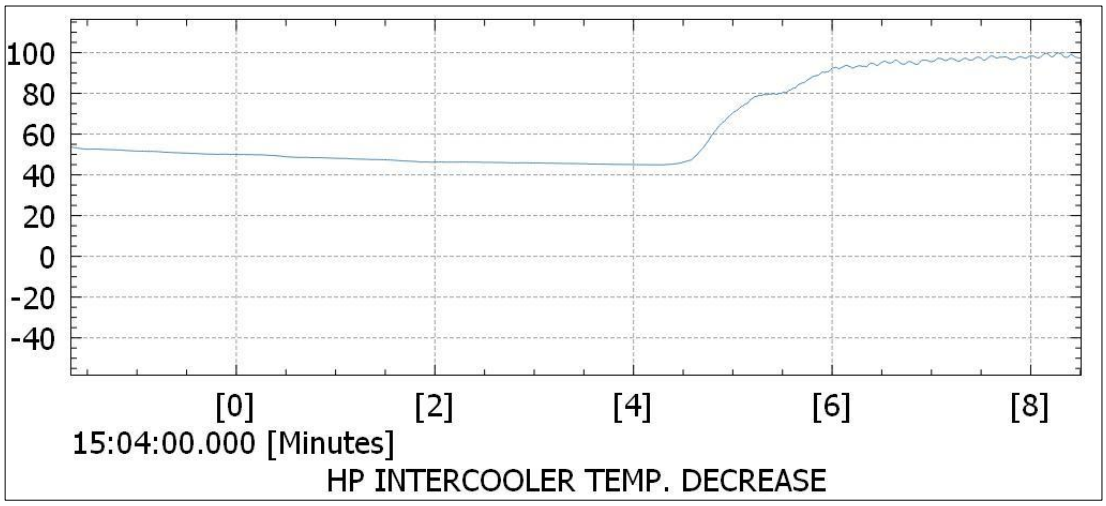

Figure 3.36: Old Intercooler 20000ft Test – HP Intercooler Temperature Decrease Graph (°C - min)

3.2.3.2. Test Flight-2 with Old Intercoolers

Flight Test 2 was performed under ISA +28 weather conditions. During the test, throttle sweep tests were performed at 20,000 feet. The purpose of this test was to observe the maximum Manifold Air Temperature achieved at take-off with the old intercoolers.

Full Load Take-off Section Test Datas:

The data regarding the Take-off phase of Test 2 performed with the old intercoolers is presented below. The take-off occurred when the outside air temperature was 38 °C (Figure 3-37). Climbing was performed at full throttle (100% throttle) (Figure 3-38). The exit air temperatures at the LP turbo compressor increased to approximately 117 °C. (Figure 3-39). After passing through the LP intercooler, the temperatures dropped to around 52 °C (Figure 3-40), resulting in a temperature decrease of approximately 65 °C in the LP intercooler (Figure 3-41). The air entering the HP compressor at 65 °C was compressed, causing the temperatures to rise to around 143 °C. (Figure 3-42). In the HP intercooler, these temperatures were reduced to around 53 °C (Figure 3-43). The approximate temperature decrease in the HP intercooler was 90 °C (Figure 3-44). The pressure drop measurement was reliably taken from the LP intercooler, and it was approximately 90 mbar (Figure 3-45). HP compressor output pressure sensor is not

worked properly, because of that pressure drop measurements of Hp intercooler is not reliable (Figure 3-46).

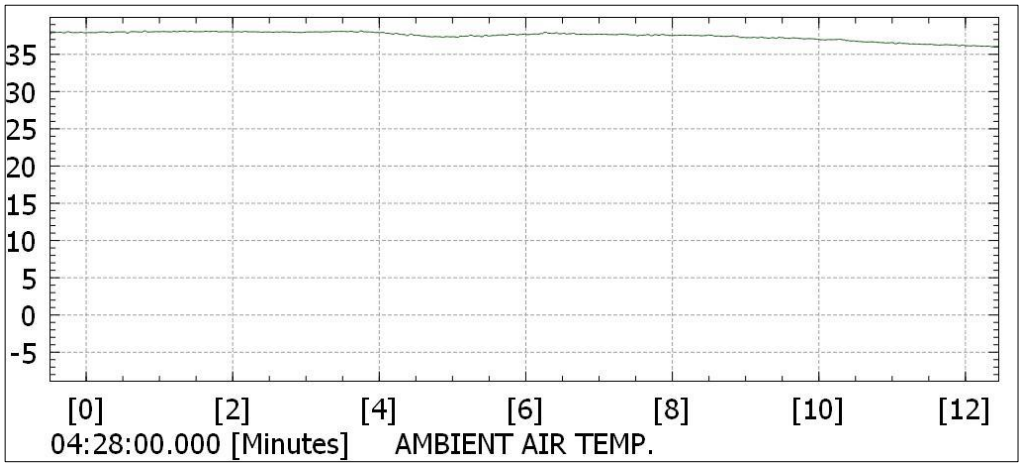

Figure 3.37 : Old Intercooler Take-Off Test 2 – Ambient Air Temperature Graph (°C - min)

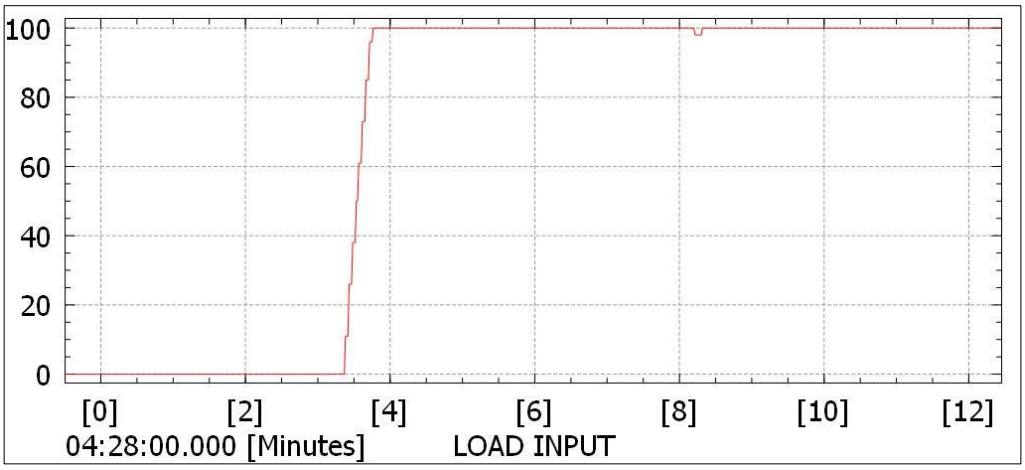

Figure 3.38: Old Intercooler Take-Off Test 2 – Load Input Graph (% - min)

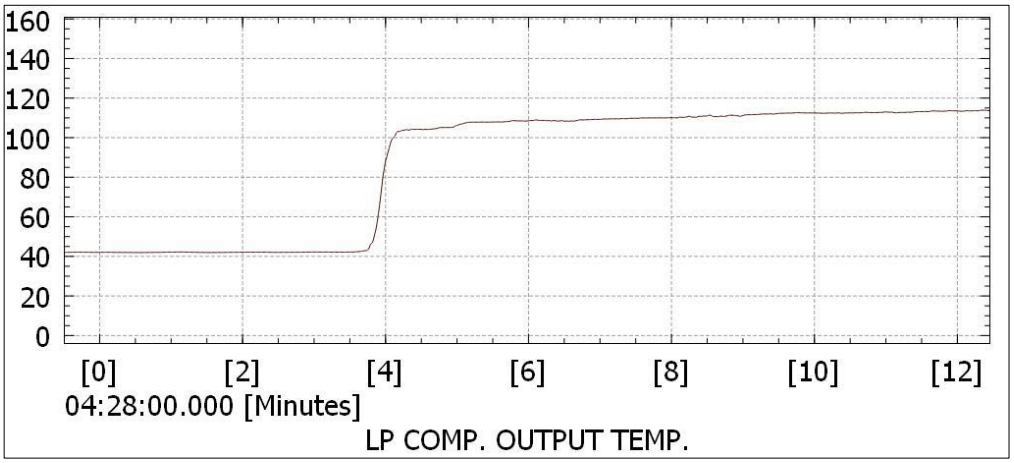

Figure 3.39: Old Intercooler Take-Off Test 2 – LP Turbo Compressor Output Temperature Graph (°C - min)

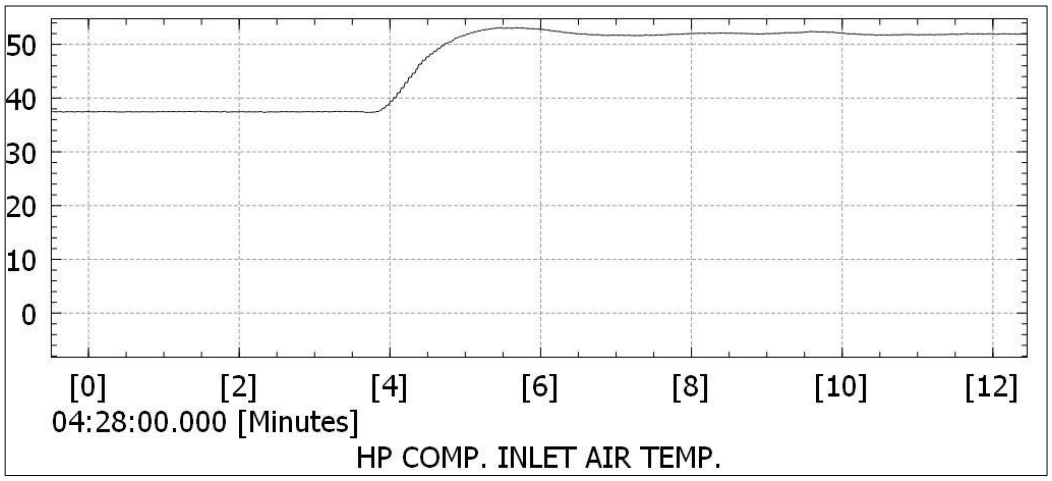

Figure 3.40: Old Intercooler Take-Off Test 2 – HP Turbo Compressor Inlet Temperature Graph (°C - min)

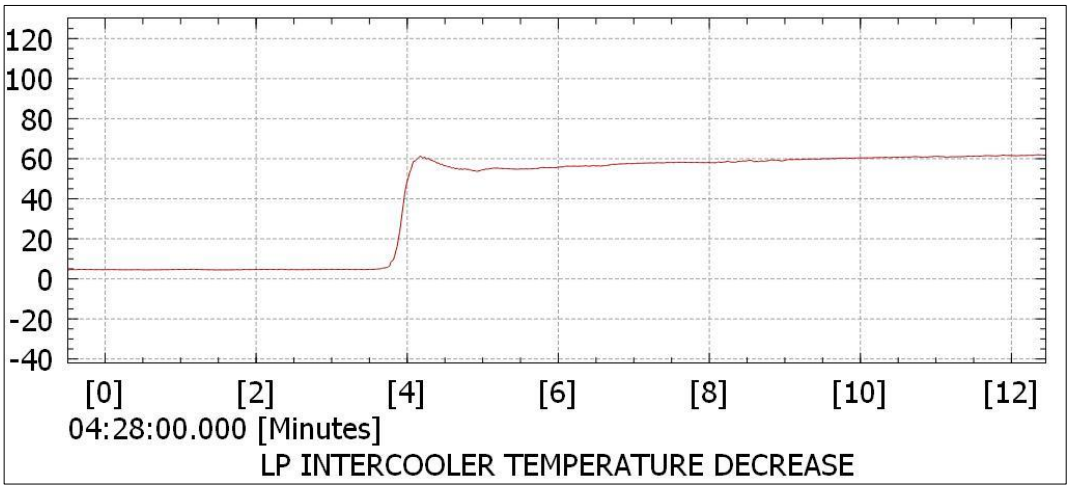

Figure 3.41: Old Intercooler Take-Off Test 2 – LP Intercooler Temperature Decrease Graph (°C - min)

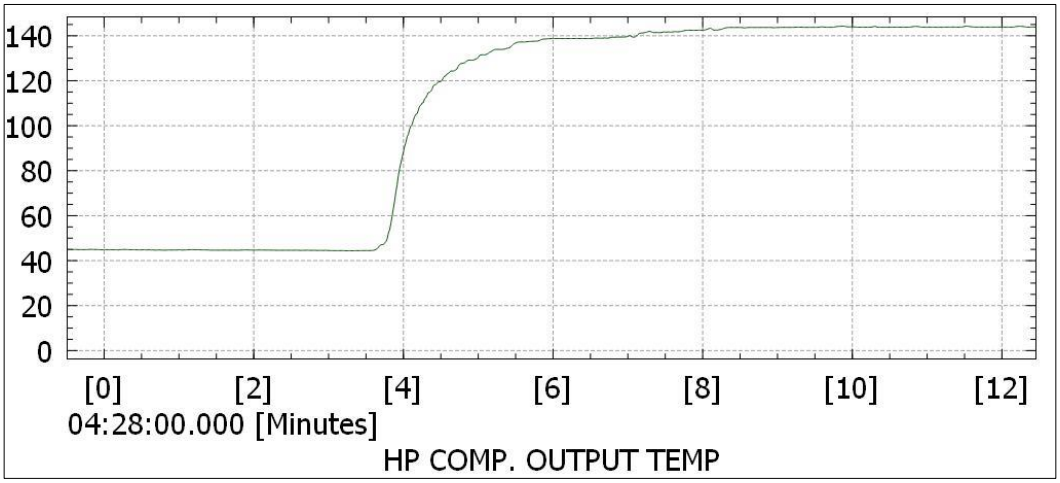

Figure 3.42: Old Intercooler Take-Off Test 2 – HP Turbo Compressor Output Temperature Graph (°C - min)

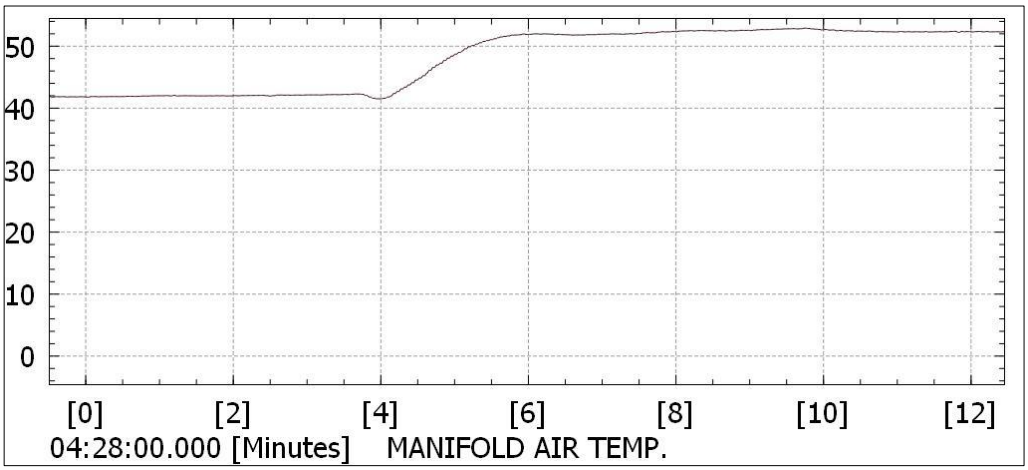

Figure 3.43: Old Intercooler Take-Off Test 2 – Engine Manifold Air Temperature Graph (°C - min)

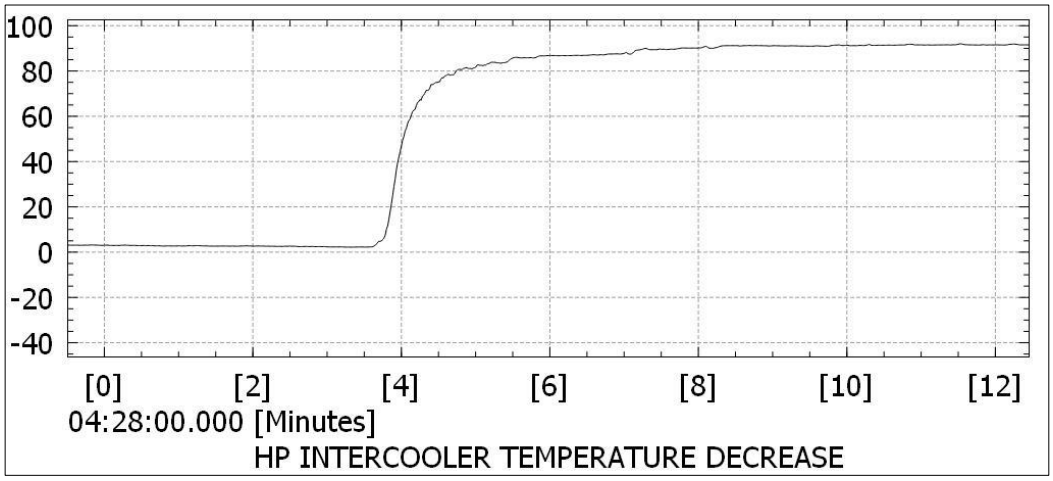

Figure 3.44: Old Intercooler Take-Off Test 2 – HP Intercooler Temperature Decrease Graph (°C - min)

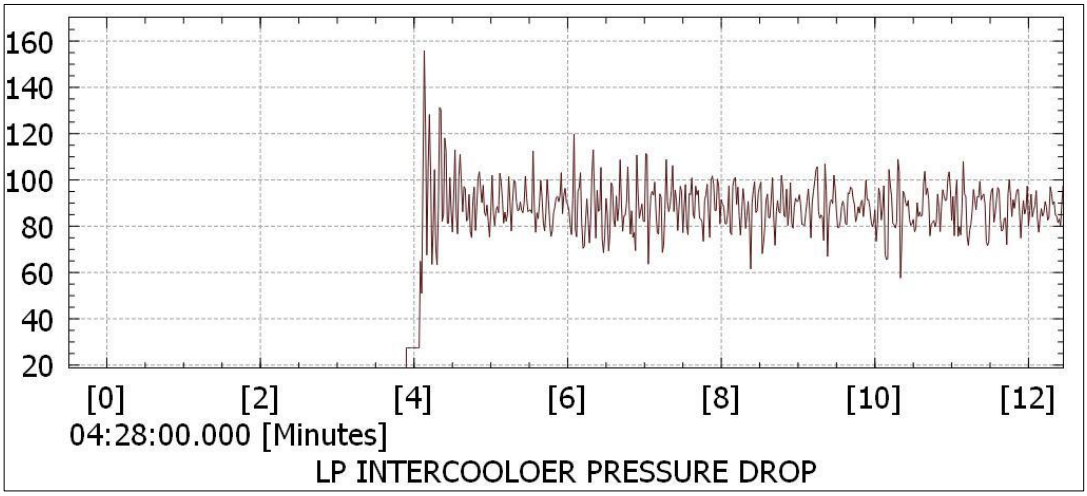

Figure 3.45: Old Intercooler Take-Off Test 2 – LP Intercooler Pressure Drop Graph (mbar – min)

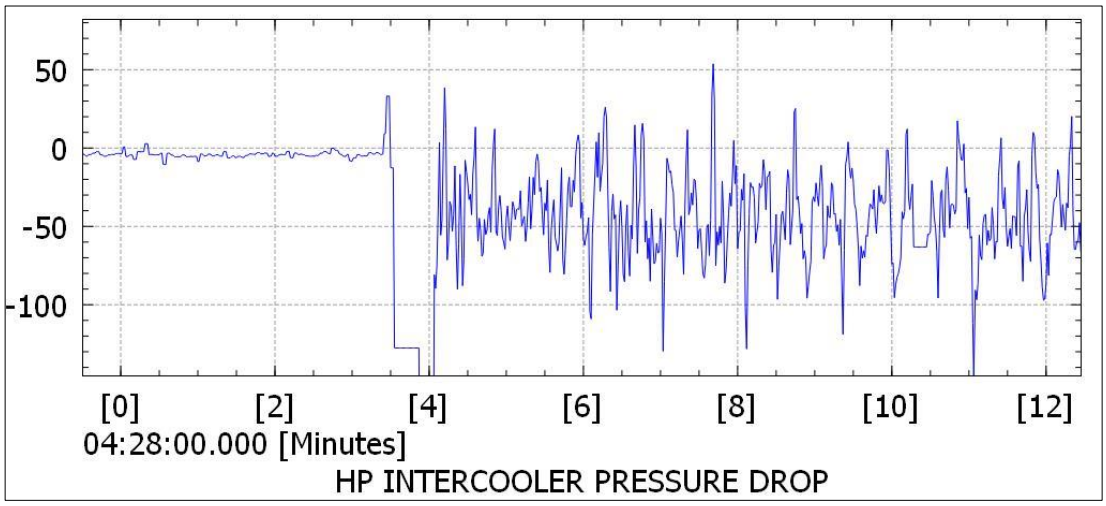

Figure 3.46: Old Intercooler Take-Off Test 2 – HP Intercooler Pressure Drop Graph (mbar - min)

20000ft Test Section Datas with %100 and %0 Load Input:

The data regarding the 20000 ft phase of Test 2 performed with the old intercoolers is presented below. The outside air temperature was around -5 °C (Figure 3-47). 20000ft test was performed at full throttle (100% throttle) and idle. (Figure 3-48). The exit air temperatures at the LP turbo compressor increased to approximately 140 °C at full throttle phase and decreases 45 °C at idle throttle. (Figure 3-49). After passing through the LP intercooler, the temperatures dropped to around -5 °C at idle throttle and increased 30°C at %100 throttle. (Figure 3-50), resulting in a temperature decrease of approximately 50 °C at idle throttle, and 110 °C at %100 throttle phase in the LP intercooler (Figure 3-51). The air entering the HP compressor at was compressed, causing the temperatures to rise to around 50 °C at idle throttle and 105 °C at %100 throttle. (Figure 3-52). In the HP intercooler, these temperatures were reduced to around -2 °C for idle throttle and 12 °C for %100 throttle (Figure 3-53). The approximate temperature decrease in the HP intercooler was 50°C for idle and 90 °C for %100 throttle (Figure 3-54).

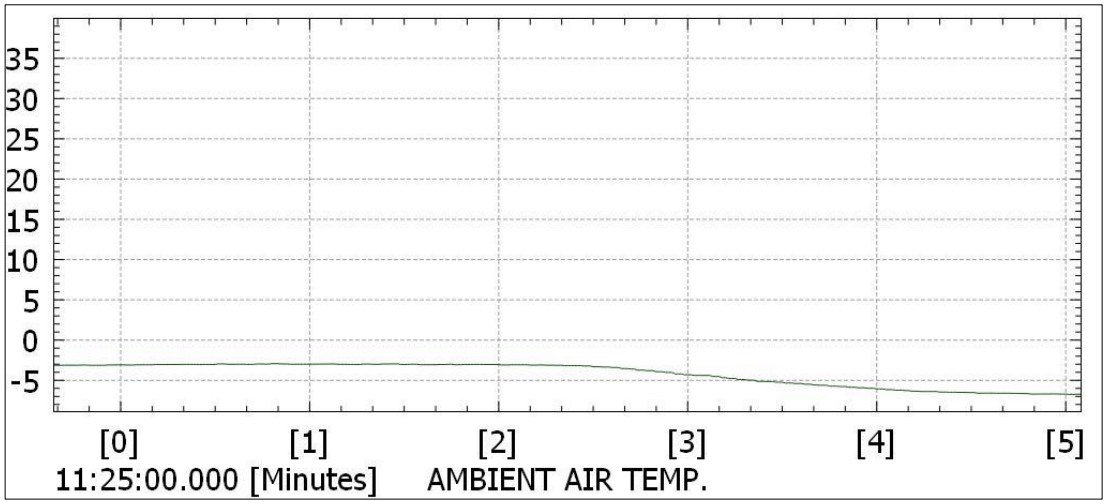

Figure 3.47 : Old Intercooler 20000ft Test 2 - Ambient Air Temperature Graph (°C - min)

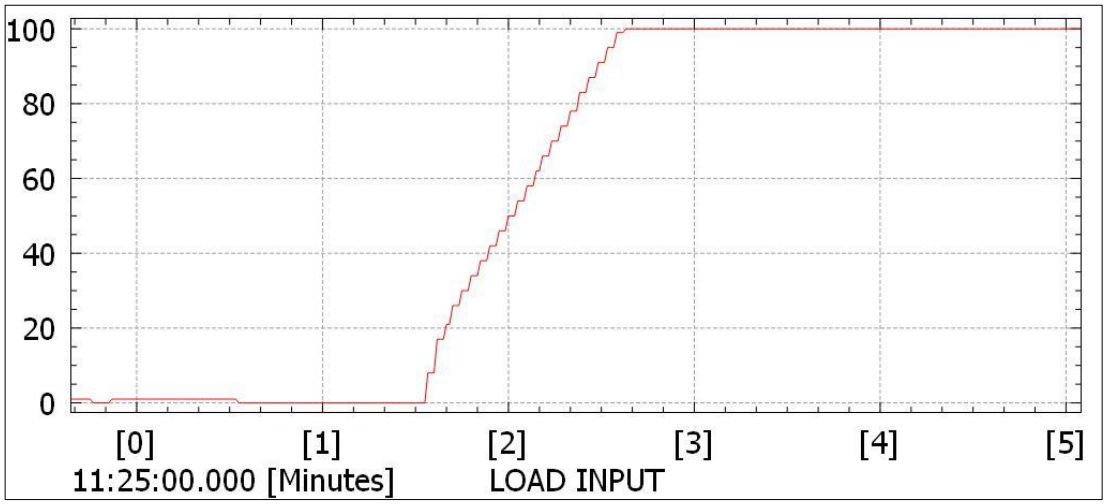

Figure 3.48: Old Intercooler 20000ft Test 2 – Load Input Graph (% - min)

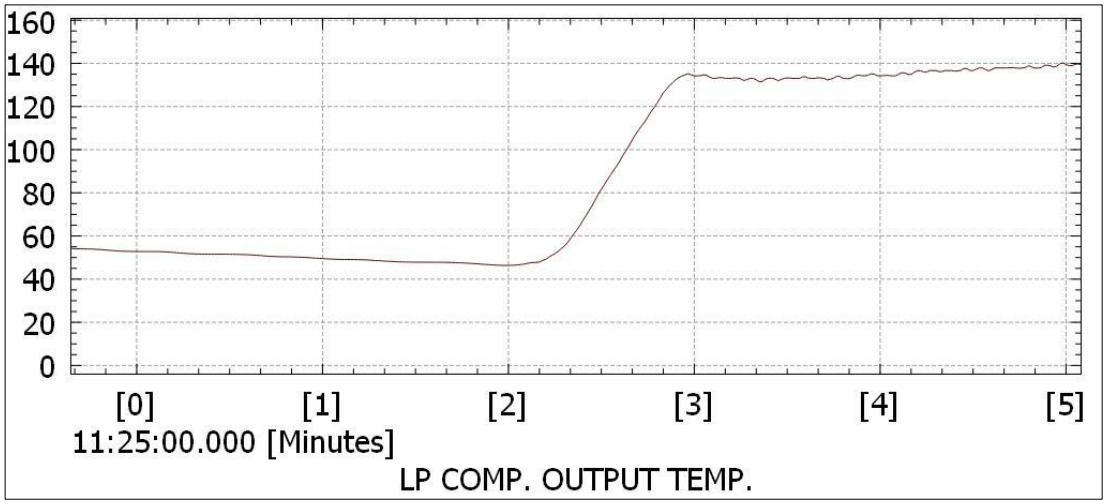

Figure 3.49: Old Intercooler 20000ft Test 2 - LP Turbo Compressor Output Temperature Graph (°C - min)

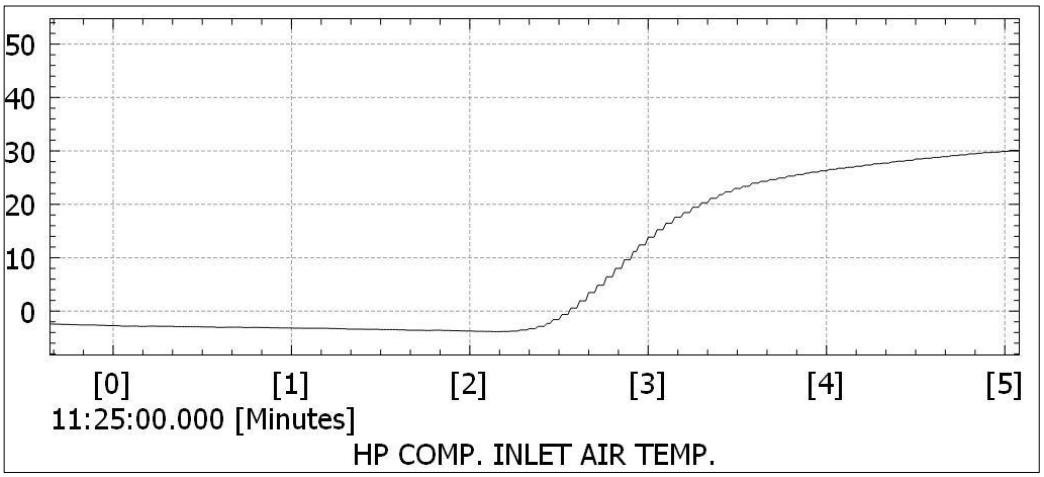

Figure 3.50: Old Intercooler 20000ft Test 2- HP Turbo Compressor Inlet Temperature Graph (°C - min)

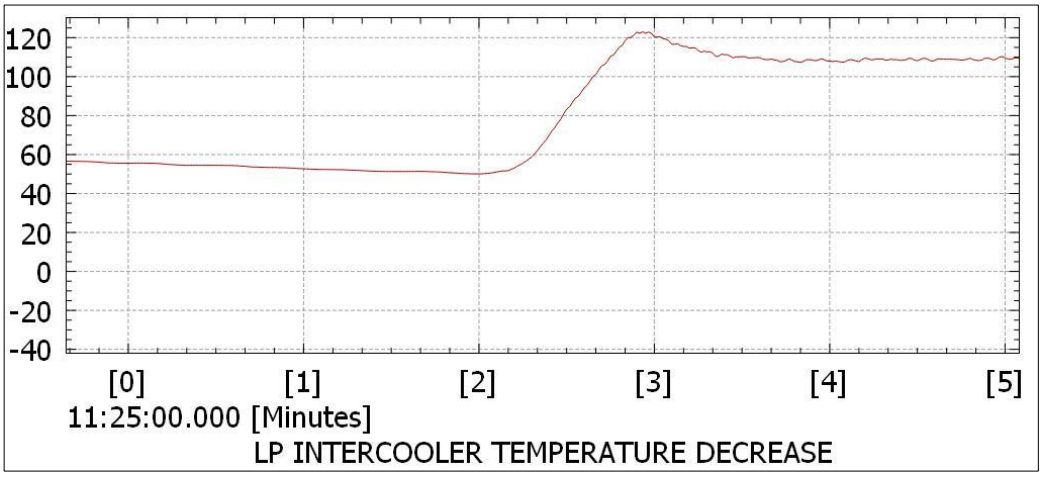

Figure 3.51: Old Intercooler 20000ft Test 2 – LP Intercooler Temperature Decrease Graph (°C - min)

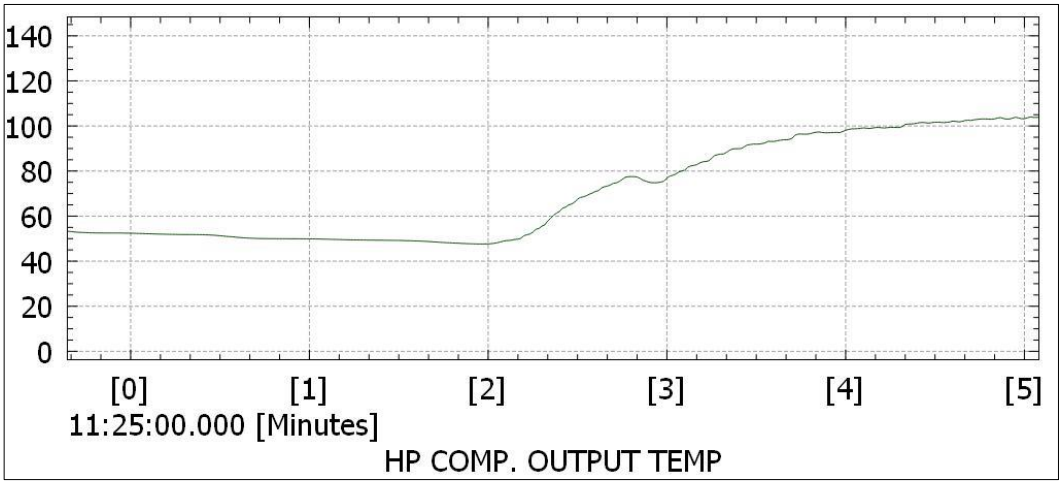

Figure 3.52: Old Intercooler 20000ft Test 2 – HP Turbo Compressor Output Temperature Graph (°C - min)

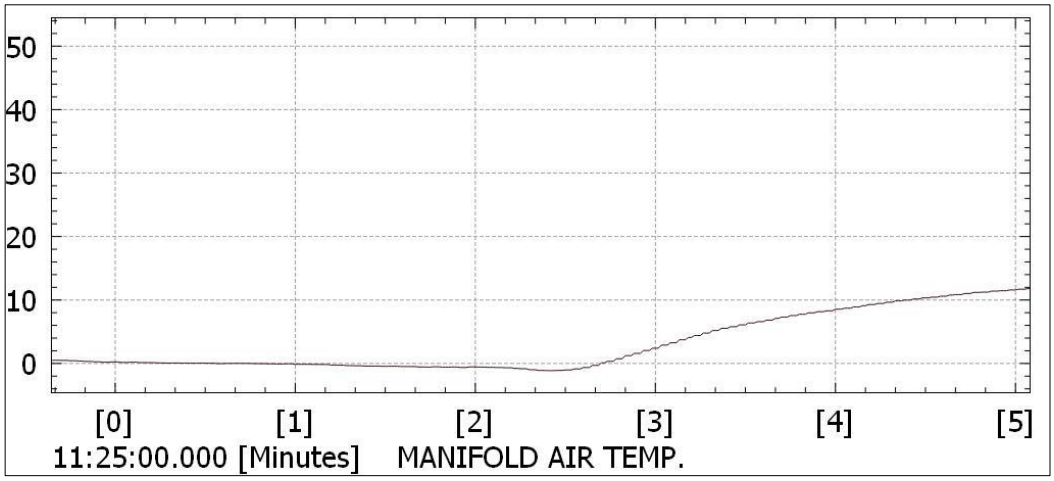

Figure 3.53: Old Intercooler 20000ft Test 2 – Engine Manifold Air Temperature Graph (°C - min)

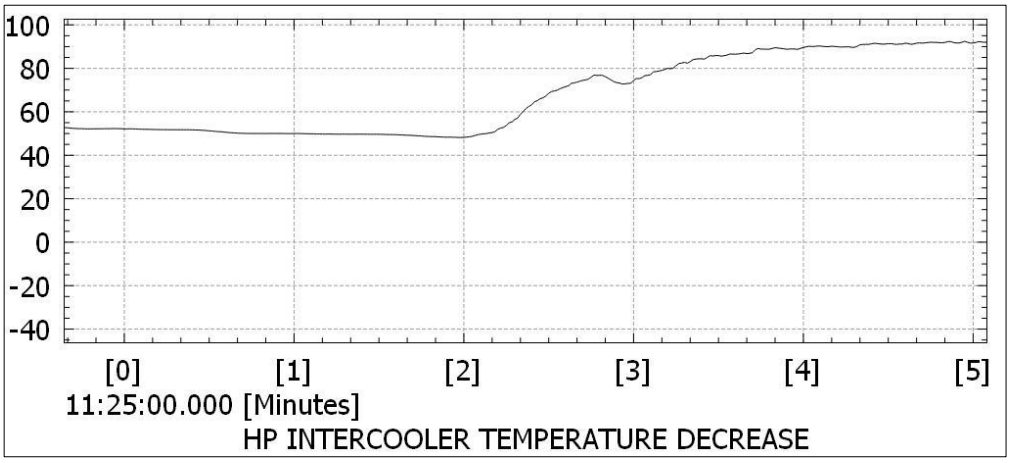

Figure 3.54: Old Intercooler 20000ft Test 2 – HP Intercooler Temperature Decrease Graph (°C - min)

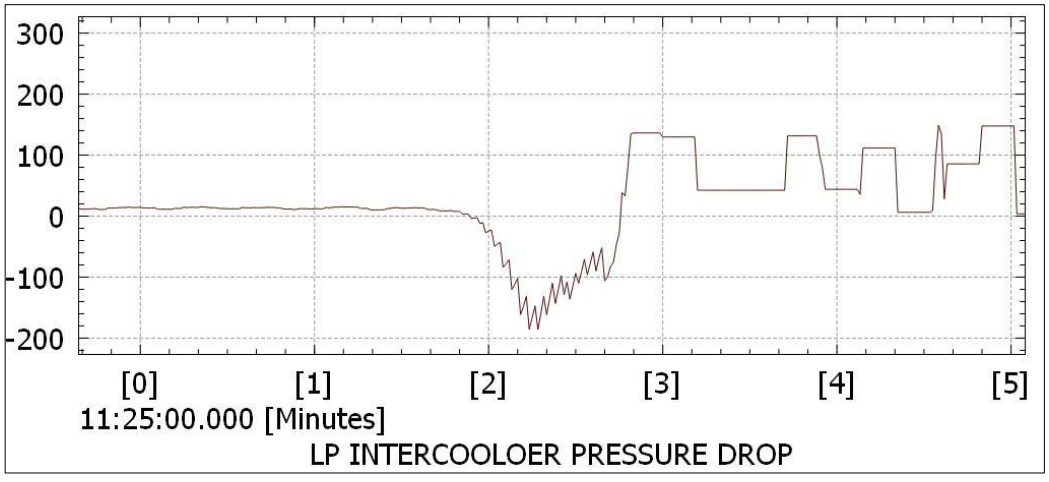

Figure 3.55: Old Intercooler 20000ft Test 2 – LP Intercooler Pressure Drop Graph (mbar - min)

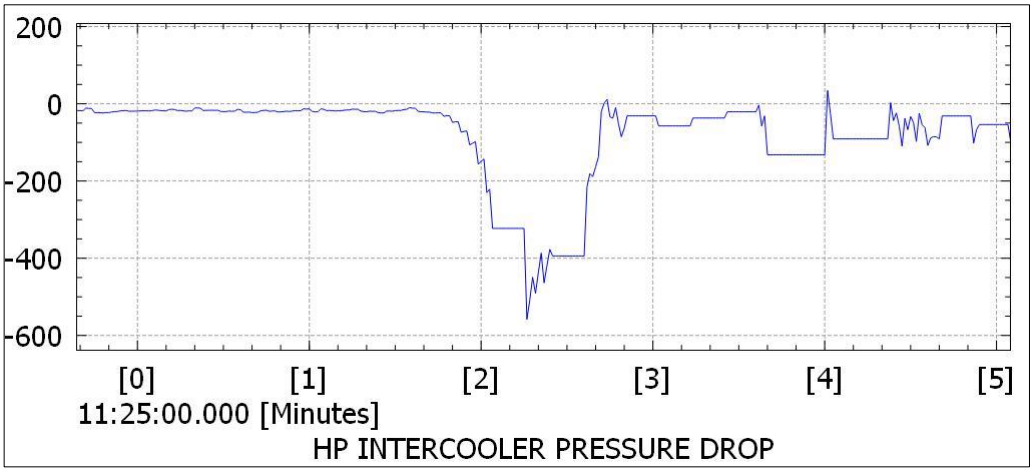

Figure 3.56: Old Intercooler 20000ft Test 2 – HP Intercooler Pressure Drop Graph (mbar - min)

3.3. By Pass System Integration

3.3.1. By Pass System Descriptions

The intercooler bypass system is a critical component in turbocharged piston engines, particularly for applications in unmanned Medium Altitude Long Endurance (MALE) aircraft. This system is designed to regulate the temperature of the engine's inlet air, ensuring optimal performance across a wide range of operating conditions, from ground level to high altitudes.

An efficiently designed intercooler bypass system enhances engine performance and longevity by maintaining optimal inlet air temperatures. This leads to improved fuel efficiency, reduced emissions, and lower risks of engine knock or component wear. In unmanned MALE aircraft, where long-duration flights at varying altitudes are common, the intercooler bypass system is particularly beneficial, ensuring consistent engine performance and reliability throughout the mission profile.

Turbochargers increase the pressure of the inlet air, which in turn raises its temperature. While intercoolers are used to cool this compressed air before it enters the engine, maintaining an optimal air temperature is vital. If the air is too hot, it can lead to performance losses and damage engine components. Conversely, overcooling the air can cause irregular combustion and the formation of undesirable chemicals in the combustion chamber.

The intercooler bypass system addresses the challenges of both overheating and overcooling by providing a means to control the airflow through the intercooler. At lower altitudes and during high-power operations such as takeoff, the intercooler is fully utilized to manage the high thermal loads. However, at higher altitudes, where the ambient air is significantly cooler, the need for extensive intercooling diminishes.

The intercooler bypass system operates by diverting a portion of the compressed air around the intercooler, allowing it to bypass the cooling process when necessary. This is achieved through a network of valves and sensors that monitor the temperature and pressure of the air. When the system detects that the air temperature is below a certain threshold, it activates the bypass valve, reducing the amount of air passing through the intercooler. This prevents overcooling and ensures that the engine receives air at an optimal temperature for combustion.

Designing an effective intercooler bypass system involves several key considerations, high-precision sensors are essential for accurately monitoring air temperature and pressure, ensuring timely and appropriate adjustments by the bypass system.

The bypass valves must operate swiftly and reliably to respond to rapid changes in operating conditions, particularly during transitions between different flight phases.

3.3.2. By Pass System Layout & Design

The By Pass system has been placed in front of the HP intercooler to have a more immediate effect on the engine inlet manifold air temperature. It is connected before the HP intercooler via a T-Pipe. The By Pass system valve is controlled by the engine's FADEC and operates either fully open or fully closed. It opens and closes based on a software logic that monitors the pressure and temperature sensors at the engine air intake manifold.

When closed, all the air from the HP compressor passes through the HP intercooler. When open, the air from the HP compressor flows both through the HP intercooler and the By Pass line, merging before the engine air intake via a Y-Yipe and entering the air intake manifold. By reducing the amount of air passing through the HP intercooler and sending hot air through the BY Pass line to the engine intake, the system prevents excessive cooling of the engine inlet air, thus increasing the MAT.

Operating Principle;

Normally closed and only opens at altitude when the temperature drops.

By Pass valve opens when MAT < 0 degrees Celsius

By Pass valve closes when MAT > 45 degrees Celsius

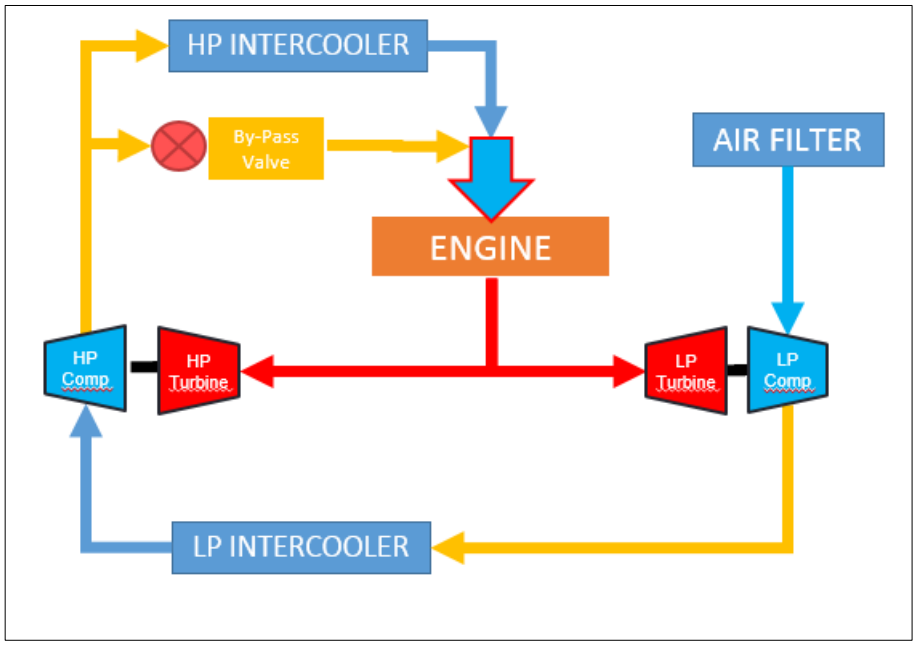

Figure 3.57: Air Cooling System Layout with By Pass System

3.3.3. Flight Test Results

In these two tests, Test 3 and Test 4, it was intended to check whether the By Pass system was mechanically operating correctly and to control the response time of the manifold inlet temperature according to the operating algorithm. During these tests, the operating temperature limits in the By Pass algorithm were adjusted as follows to stay within the safe zone.

By Pass valve opens when MAT < 10 degrees Celsius

By Pass valve closes when MAT > 40 degrees Celsius

Based on these test results, Tests 5 and 6 were performed with the final operating temperature ranges specified in the section 3.3.2.

3.3.3.1. Test Flight-3 with Old Intercoolers and By Pass System

Flight Test 3 was performed under ISA +27 weather conditions. During the test, throttle sweep tests were performed. The purpose of this test was to check by pass opening and closing conditions.

Full Load Take-off Section Test Datas:

The data regarding the Take-off phase of Test 3 performed with the old intercoolers and by pass system is presented below. The take-off occurred when the outside air temperature was 36 °C (Figure 3-58). Climbing was performed at full throttle (100% throttle) (Figure 3-59). The exit air temperatures at the LP turbo compressor increased to approximately 95 °C. (Figure 3-60). After passing through the LP intercooler, the temperatures dropped to around 50 °C (Figure 3-61), resulting in a temperature decrease of approximately 45 °C in the LP intercooler (Figure 3-62). The air entering the HP compressor at 45 °C was compressed, causing the temperatures to rise to around 125 °C. (Figure 3-8). In the HP intercooler, these temperatures were reduced to around 48 °C (Figure 3-9). The approximate temperature decrease in the HP intercooler was 77 °C (Figure 3-10). The pressure drop measurement was taken from both HP and LP intercooler, for LP Intercooler it was approximately 90 mbar (Figure 3-67), and for HP Intercooler it was nearly 125 mbar (Figure 3-66).

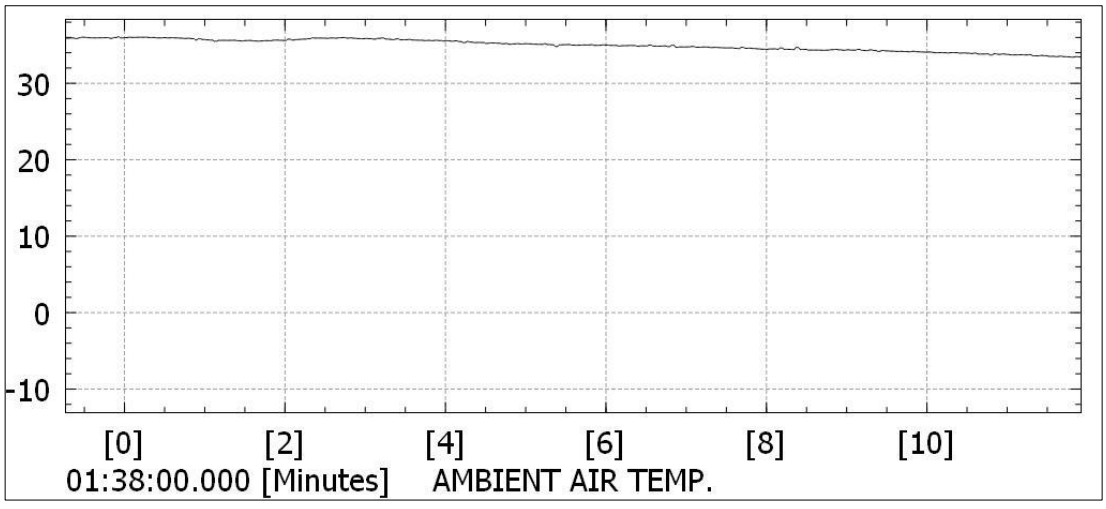

Figure 3.58 : Test -3, Take Off – Ambient Air Temperature Graph (°C - min)

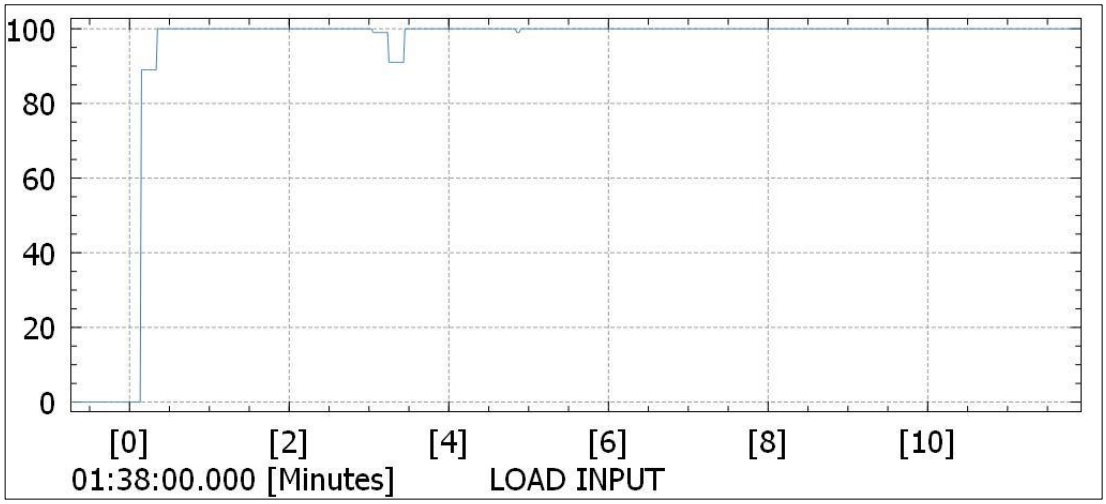

Figure 3.59 : Test -3, Take Off – Load Input Graph (% - min)

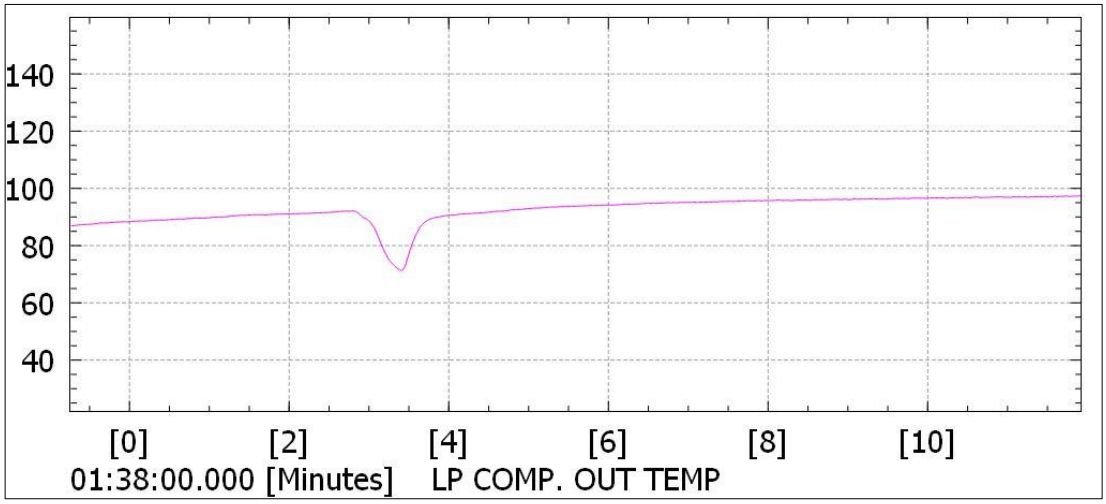

Figure 3.60: Test -3, Take Off - LP Turbo Compressor Output Temperature Graph (°C - min)

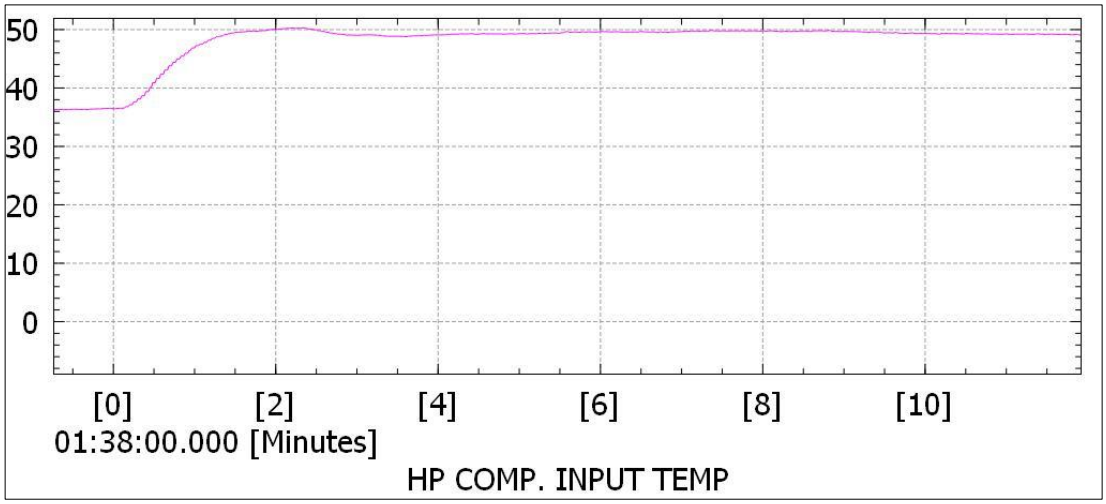

Figure 3.61: Test -3, Take Off - HP Turbo Compressor Inlet Temperature Graph (°C - min)

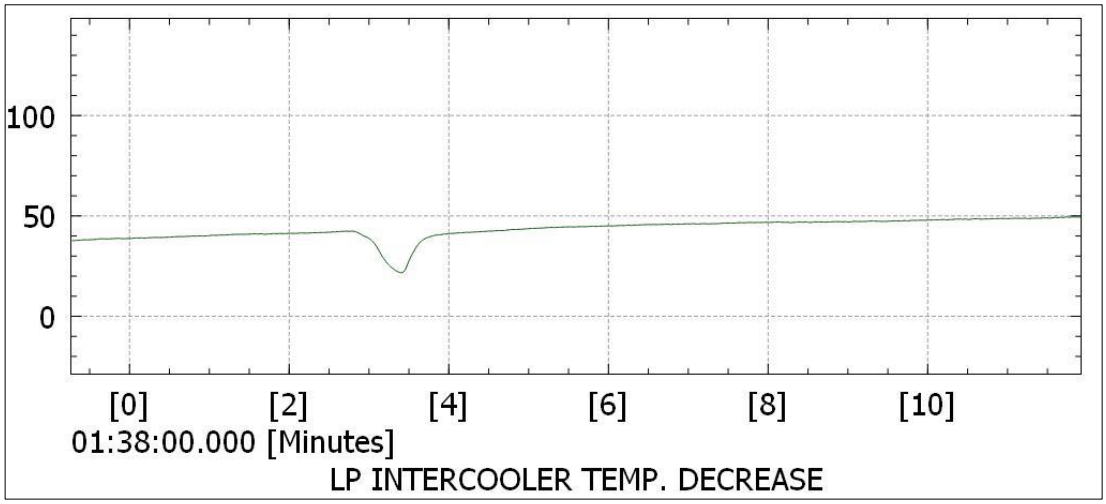

Figure 3.62: Test -3, Take Off – LP Intercooler Temperature Decrease Graph (°C - min)

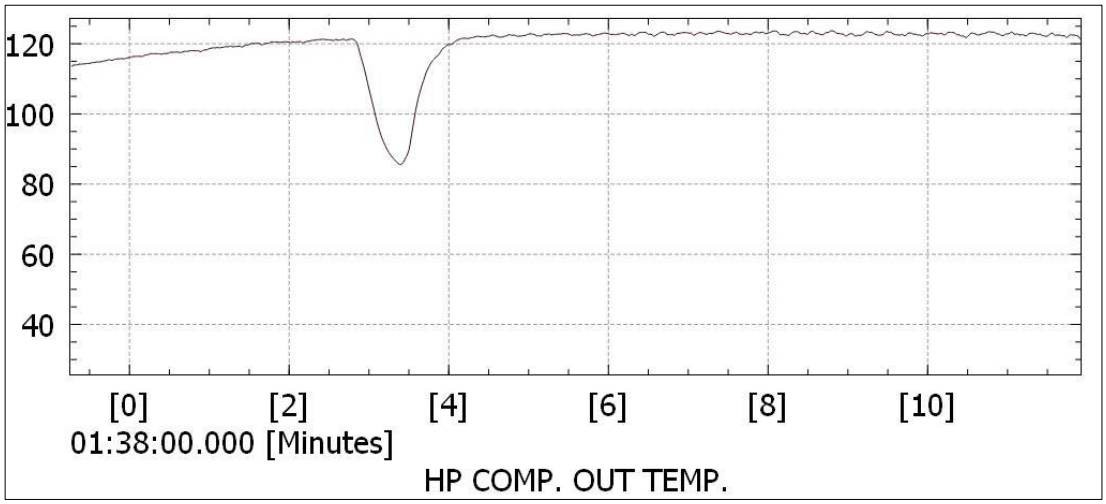

Figure 3.63: Test -3, Take Off – HP Turbo Compressor Output Temperature Graph (°C - min)

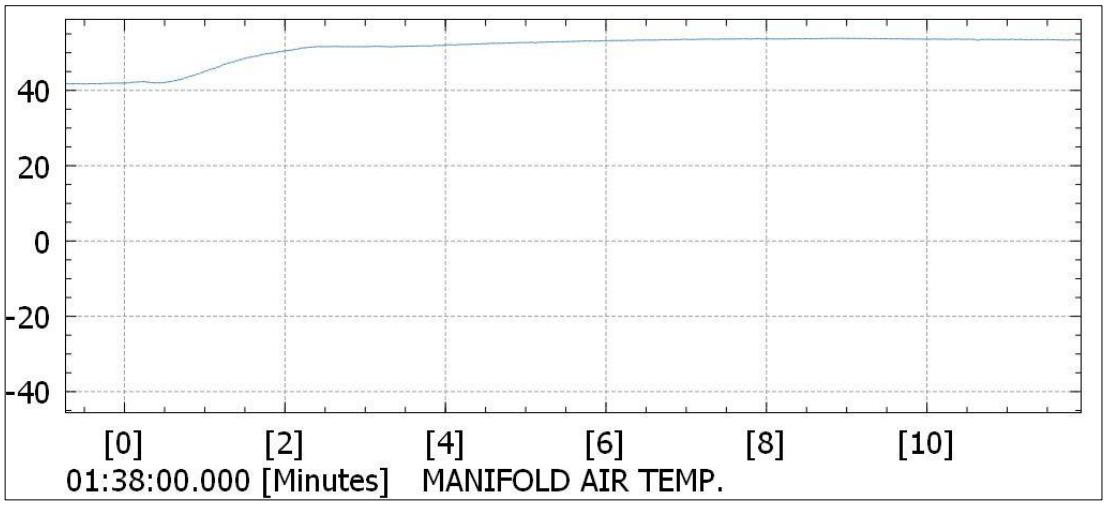

Figure 3.64: Test -3, Take Off – Engine Manifold Air Temperature Graph (°C - min)

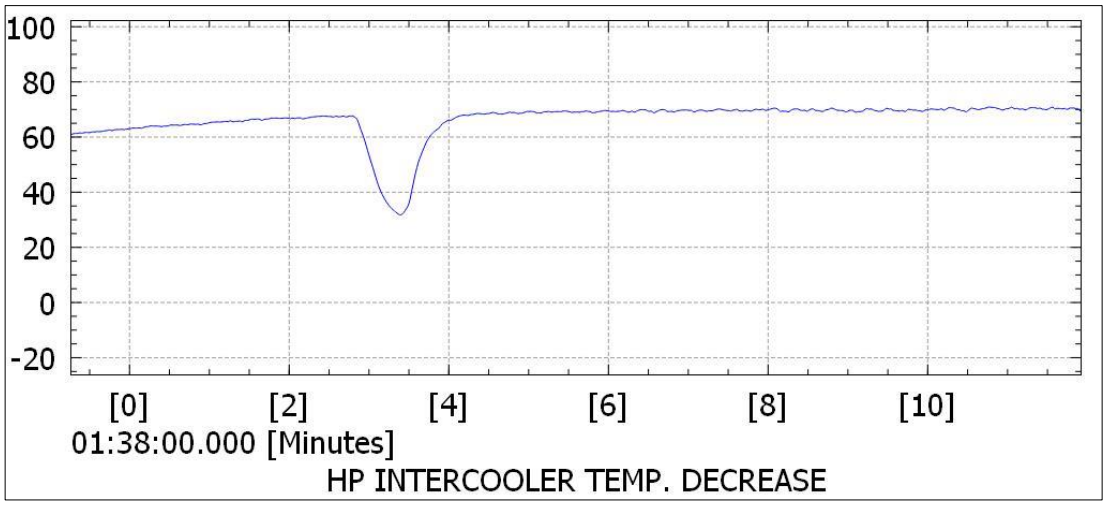

Figure 3.65: Test -3, Take Off – HP Intercooler Temperature Decrease Graph (°C-min)

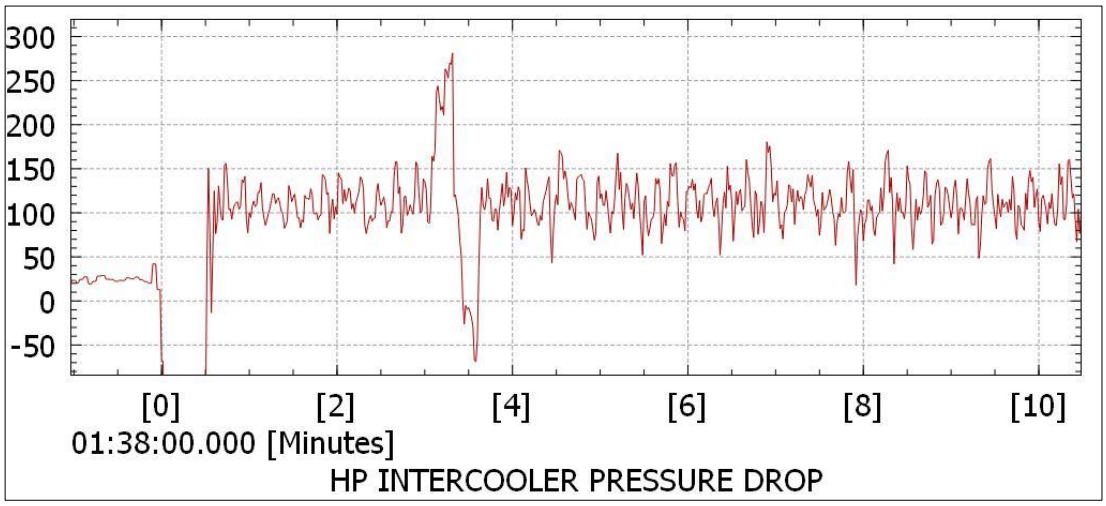

Figure 3.66: Test -3, Take Off – HP Intercooler Pressure Drop Graph (bar - min)

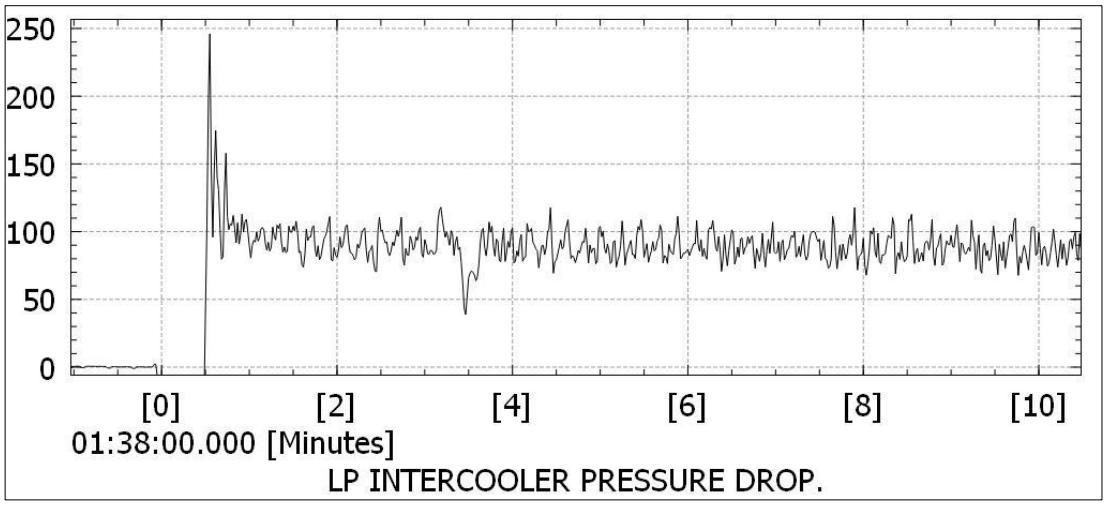

Figure 3.67: Test -3, Take Off - LP Intercooler Pressure Drop Graph (bar - min)

By Pass Opening Section Test Datas:

The data regarding the By Pass Opening Section of Test 3 performed with the old intercoolers and by pass system is presented below. This section performed when the outside air temperature was -2 °C (Figure 3-68). UAV flights at cruise mode with %55-%60 throttle. (Figure 3-69). The exit air temperatures at the LP turbo compressor increased to approximately 150 °C. (Figure 3-70). After passing through the LP intercooler, the temperatures dropped to around 10 °C (Figure 3-71), resulting in a temperature decrease of approximately 140 °C in the LP intercooler (Figure 3-72). The air entering the HP compressor at 10 °C was compressed, causing the temperatures to rise to around 110 °C. (Figure 3-74). In the HP intercooler, these temperatures were reduced to 10 °C then by pass valve opened, Manifold air temperature is increased to 46 °C in seconds (Figure 3-73). The temperature decrease in the HP intercooler before by pass opening was 95 °C after by pass opening HP Intercooler Temperature decrease was 60 °C (Figure 3-75). The pressure drop measurement was taken from both HP and LP intercooler, values are not reliable because of the sensor but decrease trend on HP Intercooler pressure drop value could be shown in (Figure 3-76).

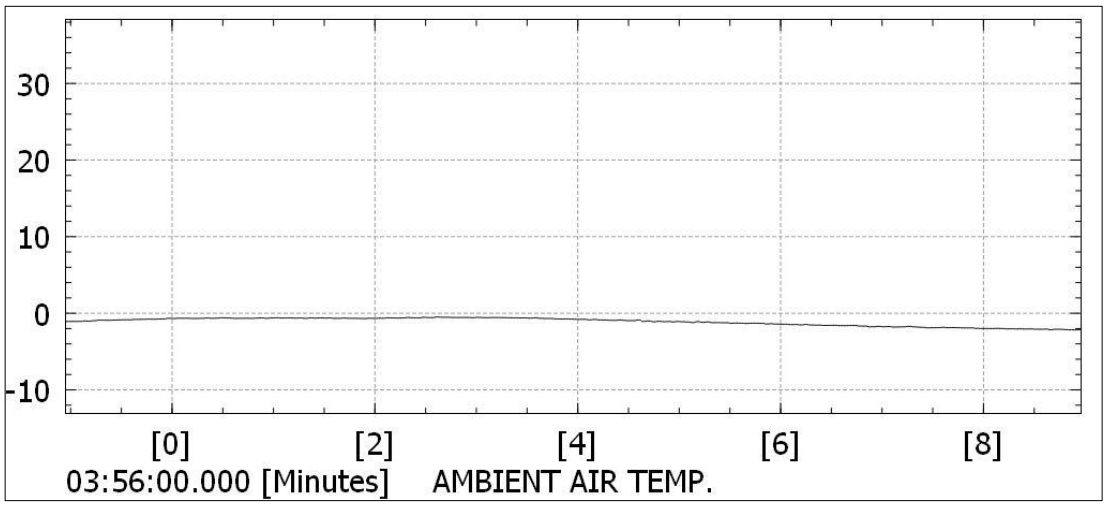

Figure 3.68 : Test -3, By Pass Opening – Ambient Air Temperature Graph (°C - min)

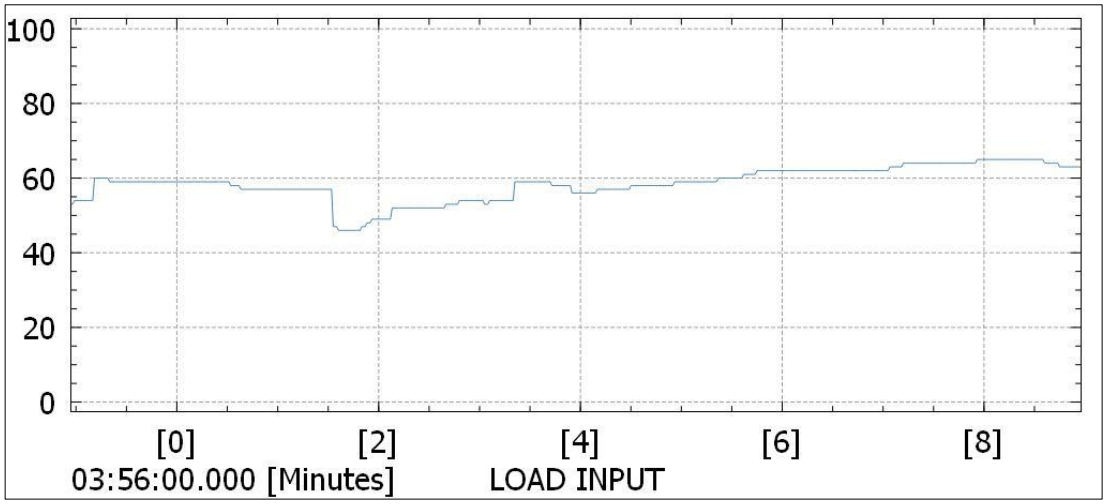

Figure 3.69 : Test -3, By Pass Opening – Load Input Graph (% - min)

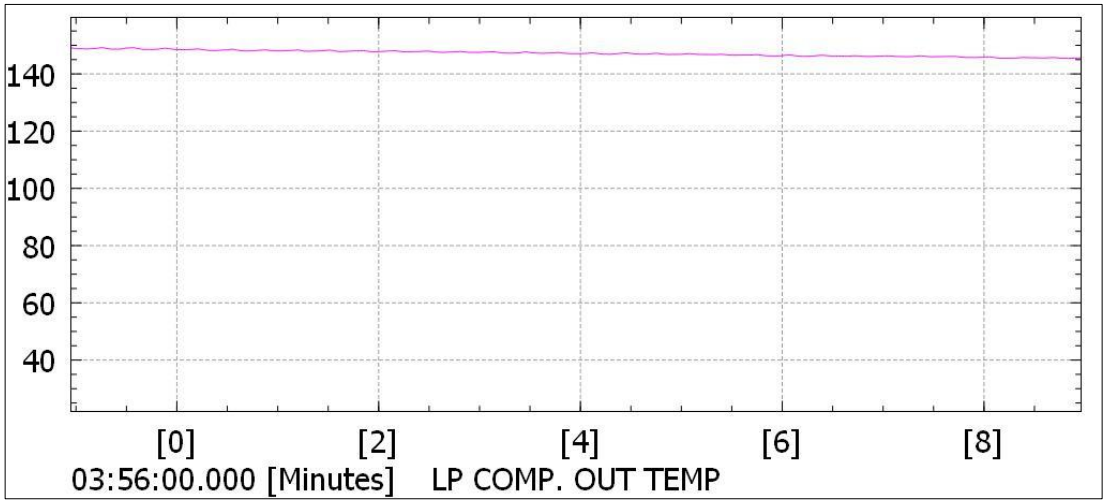

Figure 3.70: Test -3, By Pass Opening – LP Turbo Compressor Output Temperature Graph (°C - min)

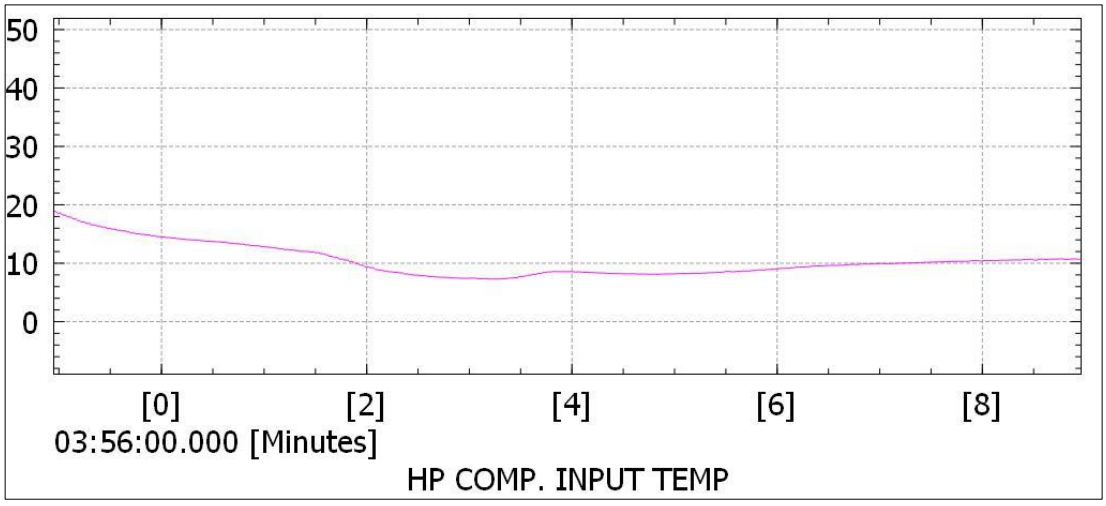

Figure 3.71: Test -3, By Pass Opening – HP Turbo Compressor Inlet Temperature Graph (°C - min)

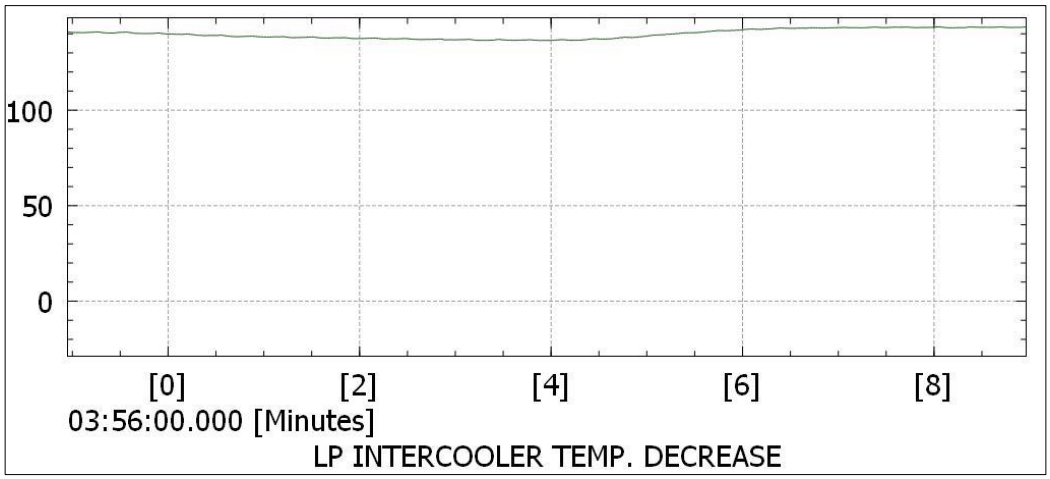

Figure 3.72: Test -3, By Pass Opening – LP Intercooler Temperature Decrease Graph (°C - min)

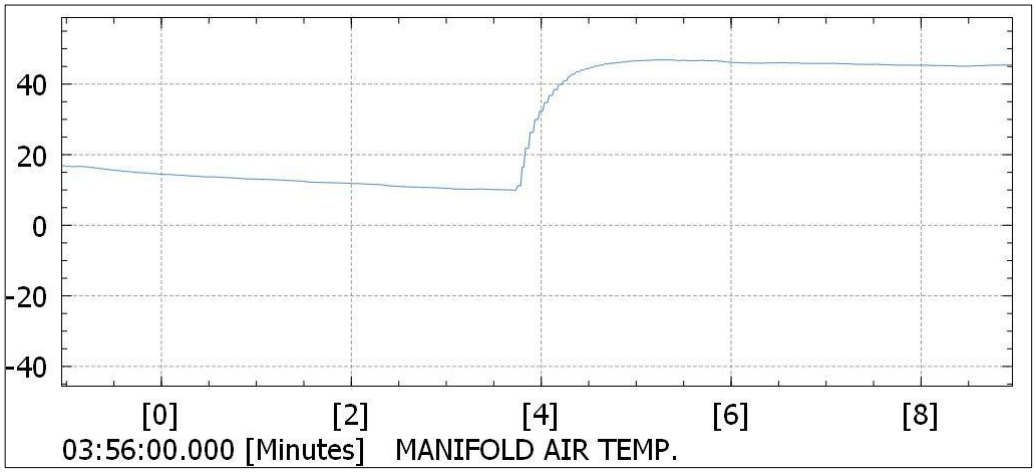

Figure 3.73: Test -3, By Pass Opening – Engine Manifold Air Temperature Graph (°C - min)

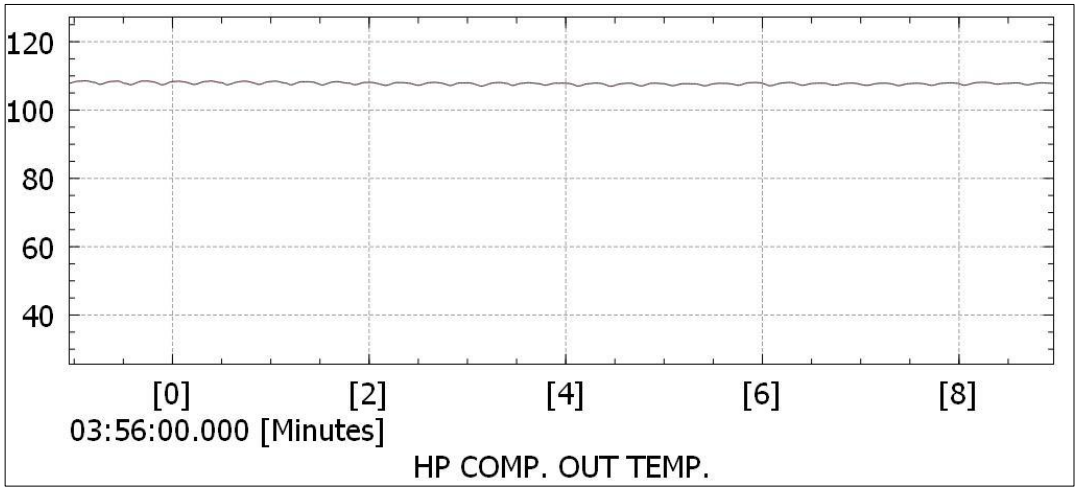

Figure 3.74: Test -3, By Pass Opening – HP Turbo Compressor Output Temperature Graph (°C - min)

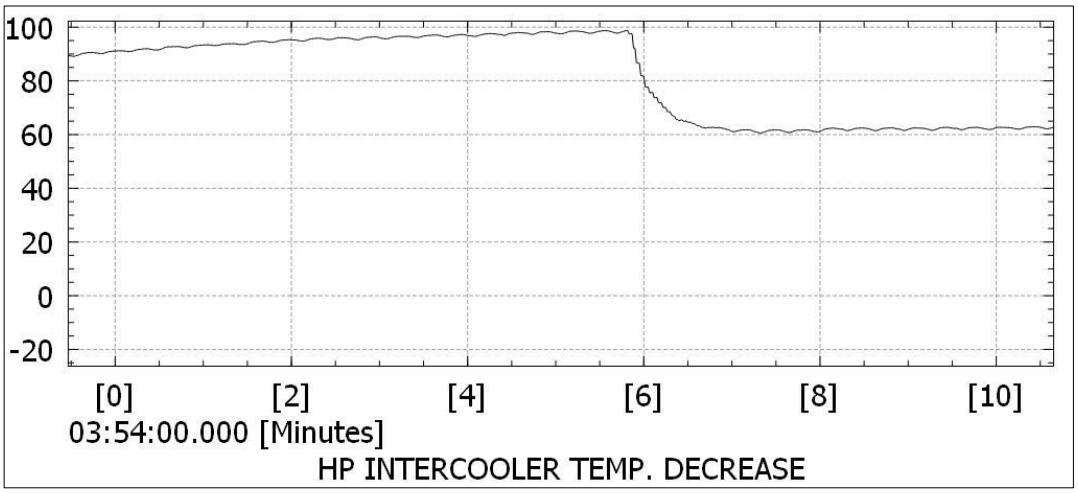

Figure 3.75: Test -3, By Pass Opening – HP Intercooler Temperature Decrease Graph (°C - min)

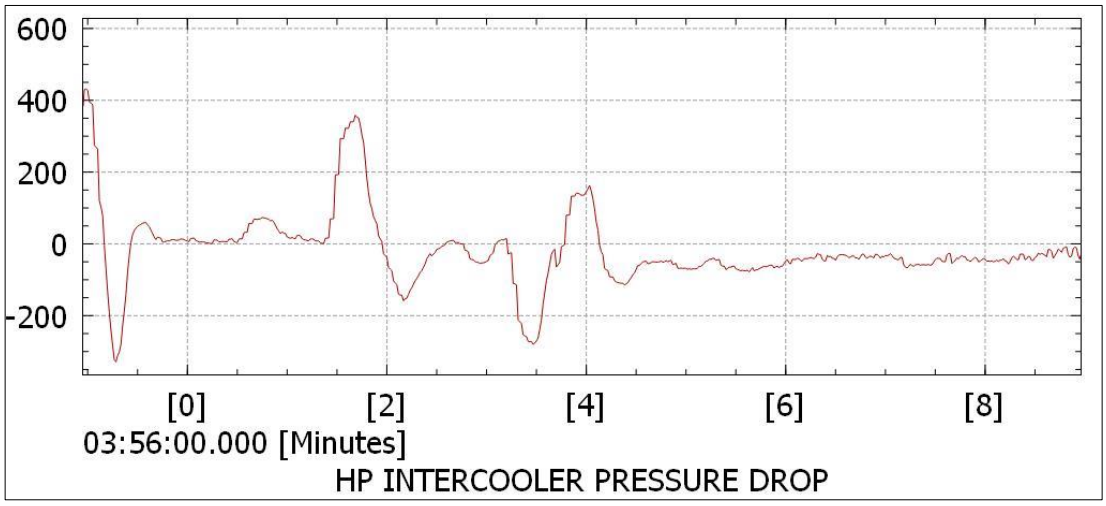

Figure 3.76: Test -3, By Pass Opening – HP Intercooler Pressure Drop (mbar-min)

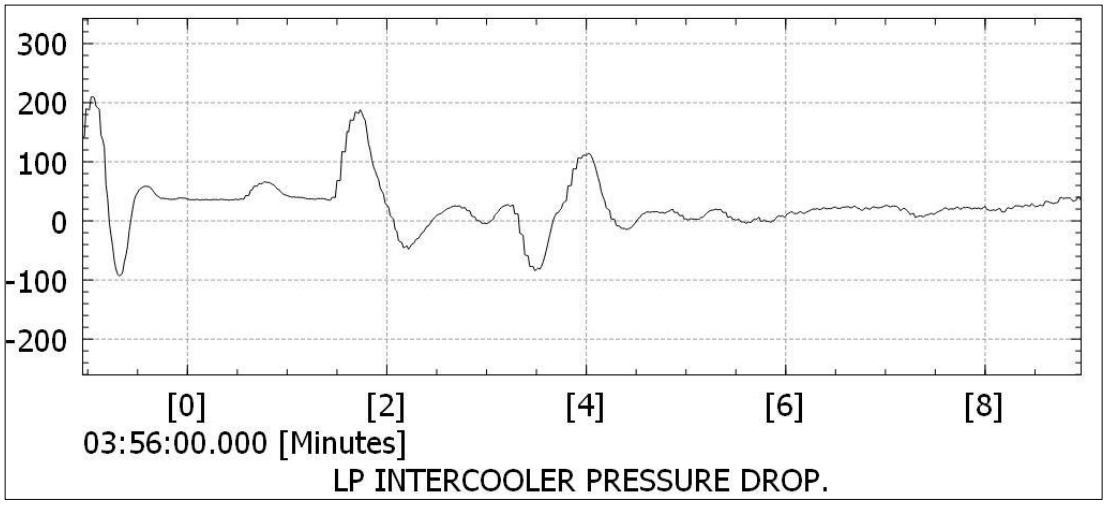

Figure 3.77: Test -3, By Pass Opening – LP Intercooler Pressure Drop (mbar-min)

3.3.3.2. Test Flight-4

Flight Test 4 was performed under ISA +21 weather conditions. During the test, throttle sweep tests were performed. The purpose of this test was to check by pass opening and closing conditions. Only Engine Inlet Manifold Air temperatures are checked during this flight.

Full Load Take-off Section Test Datas:

The data regarding the Take-off phase of Test 4 performed with the old intercoolers and by pass system is presented below. The take-off occurred when the outside air temperature was 31 °C (Figure 3-78). Climbing was performed at full throttle (100% throttle) (Figure 3-79). Engine Inlet Manifold temperature increased to 54 °C (Figure 3-80).

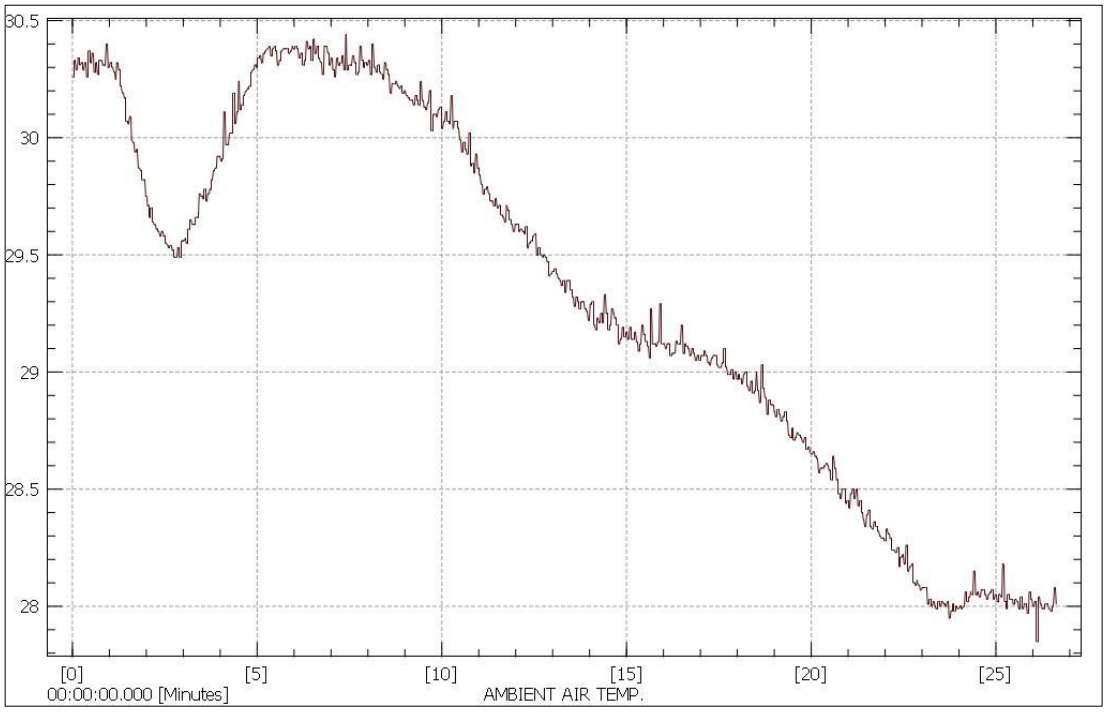

Figure 3.78: Test -4, Take-off – Ambient Air Temperature Graph (°C - min)

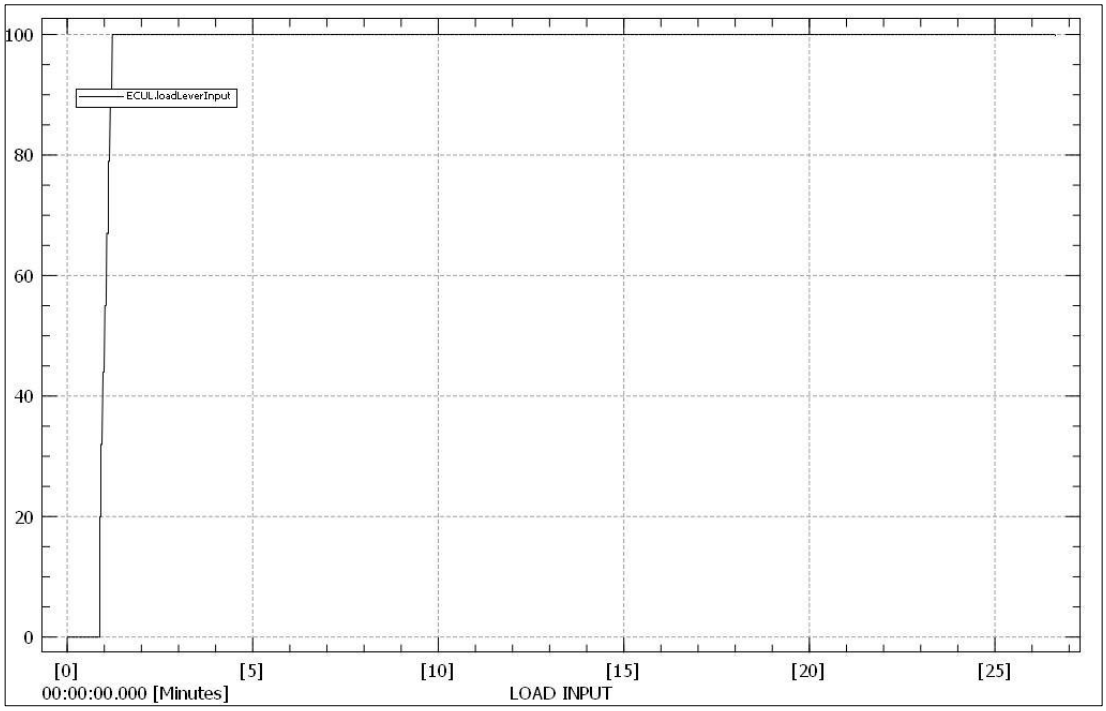

Figure 3.79: Test -4, Take-off – Load Input Graph (%- min)

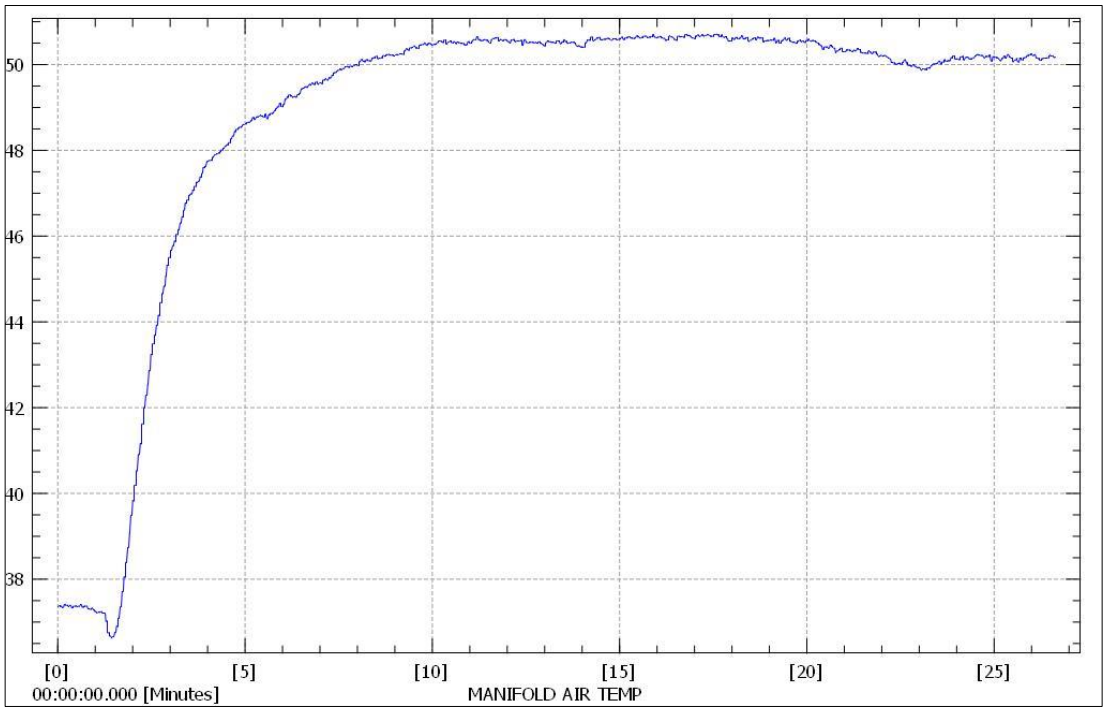

Figure 3.80: Test -4, Take-off – Engine Manifold Air Temperature Graph (°C – min)

By Pass Opening Section Test Datas:

The data regarding the By Pass Opening Section of Test 4 performed with the old intercoolers and by pass system is presented below. This section performed when the

outside air temperature was -11 °C (Figure 3-81). UAV decreases throttle from %100 to cruise mode with %55-%60 throttle. (Figure 3-82). Manifold air temperature was reduced to 10 °C then by pass valve opened, Manifold air temperature is increased to 45 °C in seconds (Figure 3-83).

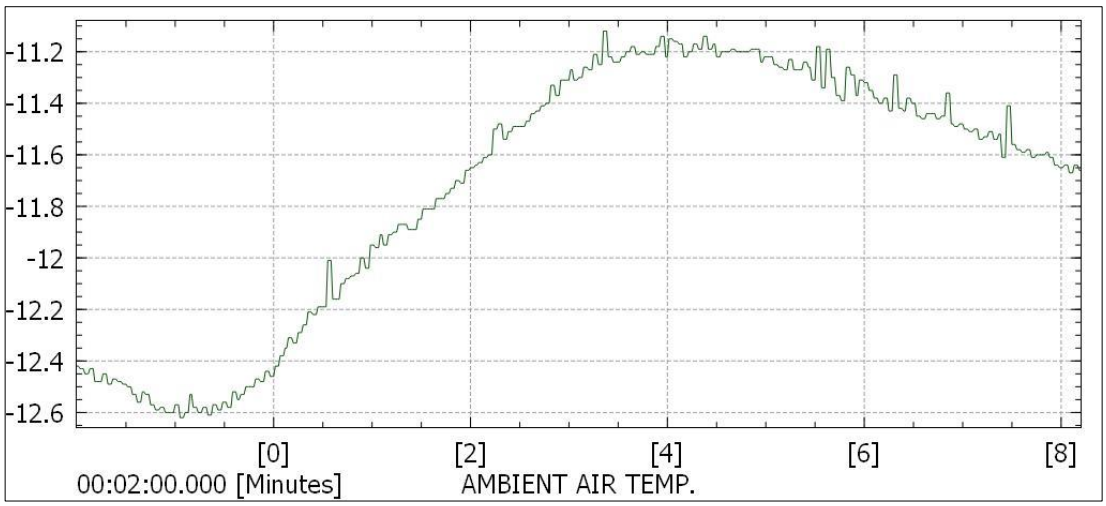

Figure 3.81: Test -4, By Pass Opening – Ambient Air Temperature Graph (°C - min)

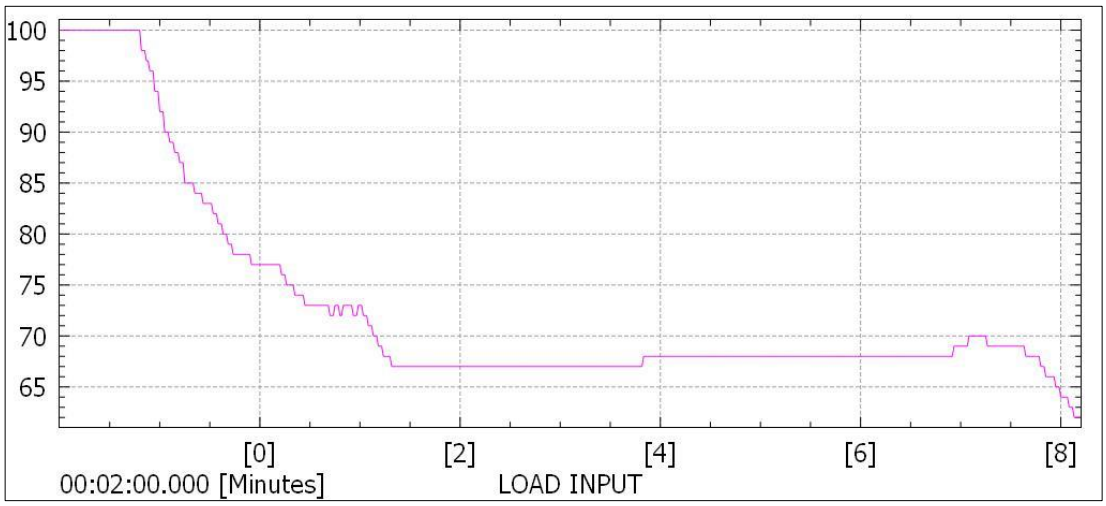

Figure 3.82 : Test -4, By Pass Opening – Load Input Graph (% - min)

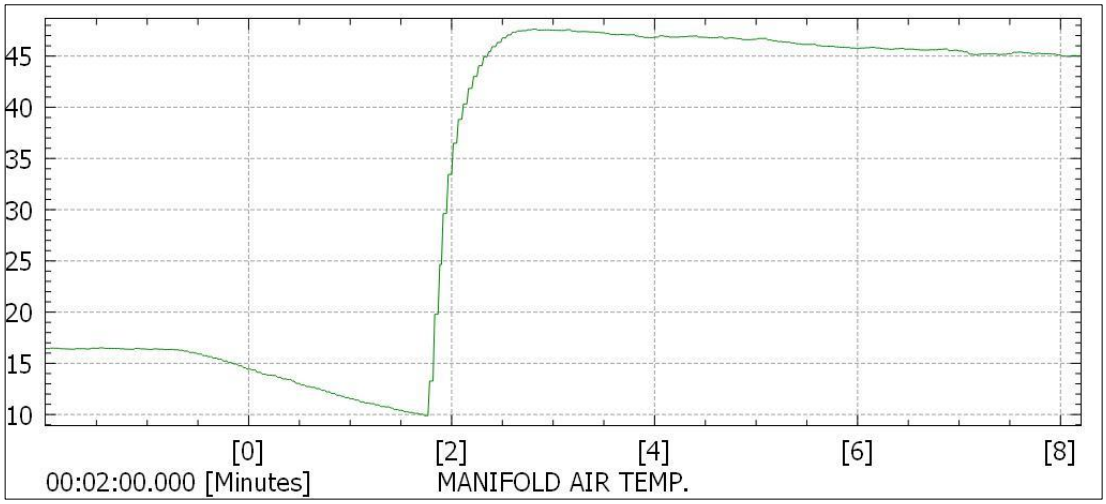

Figure 3.83: Test -4, By Pass Opening – Engine Manifold Air Temperature Graph (°C - min)

3.4. Intercooler Resizing + By-Pass

In the optimization project addressed in this thesis, the goal is to achieve the desired MAT (manifold air temperature) values with minimal modifications on the aircraft. Although a complete redesign could also achieve the target values, the approach taken involves working with the supplier to modify both intercoolers based on take-off test data to increase the MAT by approximately 10 degrees. The aim is to complete this work without making any changes on the intercooler placement or air intake ducts on the aircraft. Calculations indicate that shortening each intercooler by 100 mm as per our requirements would achieve the desired temperature and pressure drop values. Consequently, a new set of intercoolers, detailed below, has been implemented and was validated in flight tests.

3.4.1. New HP Intercooler Specifications

Table 3.8: New HP Intercooler Technical Specifications

Nomenclature	Value
Core Length	385 mm
Core Height	150 mm
Core Depth	80 mm
Tube Dimensions	80x10 mm
Number Of Tube	7
Fin Type	Straight Fin
Flow Type	I Flow

Table 3.9: New HP Intercooler Supplier Analysis

Nomenclature	Value	Units
Total Heat Transfer Rate	14,7	kW
Warm Fluid		
Flow Rate	0,1833	kg/s
Temperature In	160	°C
Temperature Out	71,8	°C
Inlet Pressure (abs.)	3	bar
Pressure Drop	74,25	mbar
Cold Fluid		
Flow Rate	0,6288	kg/s
Temperature In	43	°C
Temperature Out	68,2	°C
Inlet Pressure	1013,25	mbar
Pressure Drop	11	mbar

3.4.2. New LP Intercooler Specifications

Table 3.10: New LP Intercooler Technical Specifications

Nomenclature	Value
Core Length	385 mm
Core Height	130 mm
Core Depth	80 mm
Tube Dimensions	80x10 mm
Number Of Tube	6
Fin Type	Straight Fin
Flow Type	I Flow

Table 3.11: New LP Intercooler Supplier Analysis

Nomenclature	Value	Units
Total Heat Transfer Rate	13,2	kW
Warm Fluid		
Flow	0,1833	kg/s
Temperature In	155	°C
Temperature Out	74,5	°C
Inlet Pressure (abs.)	2	bar
Pressure Drop	140,5	mbar
Cold Fluid		
Flow Rate	0,55	kg/s
Temperature In	43	°C
Temperature Out	68,5	°C
Inlet Pressure	1013,25	mbar
Pressure Drop	11	mbar

3.4.3. Test Results

3.4.3.1. Test Flight-5 With New Intercoolers and By Pass System

Flight Test 5 was performed under ISA -2 weather conditions. During the test, throttle sweep tests were performed at 20,000, 25,000, and 30,000 feet. The purpose of this test was to observe the minimum Manifold Air Temperature achieved at high altitude with the new intercoolers and by pass system.

Bypass Valve opening temperature limits are finalized before this test,

By Pass valve opens when MAT < 0 degrees Celsius

By Pass valve closes when MAT > 45 degrees Celsius

Full Load Take-off Section Test Datas:

The data regarding the Take-off phase of Test 5 performed with the new intercoolers + by pass system is presented below. The take-off occurred when the outside air temperature was 8 °C (Figure 3-84). Climbing was performed at full throttle (100% throttle) (Figure 3-85). The exit air temperatures at the LP turbo compressor increased to approximately 80 °C. (Figure 3-86). After passing through the LP intercooler, the temperatures dropped to around 25 °C (Figure 3-87), resulting in a temperature decrease of approximately 55 °C in the LP intercooler (Figure 3-88). The air entering the HP compressor at 55 °C was compressed, causing the temperatures to rise to around 118 °C. (Figure 3-89). In the HP intercooler, these temperatures were reduced to around 33 °C (Figure 3-90). The approximate temperature decrease in the HP intercooler was 85 °C (Figure 3-91). The pressure drop measurement was taken from both LP and HP intercoolers. LP Intercooler Pressure Drop was around 150mbar (Figure 3-92). And HP Intercooler Pressure Drop was around 125mbar (Figure 3-93).

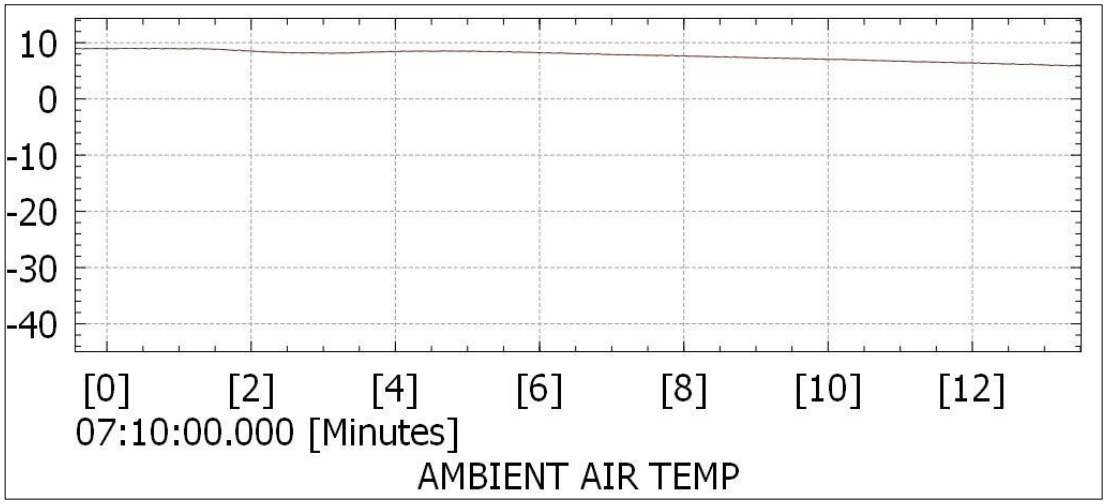

Figure 3.84 : Test -5, Take Off – Ambient Air Temperature Graph (°C - min)

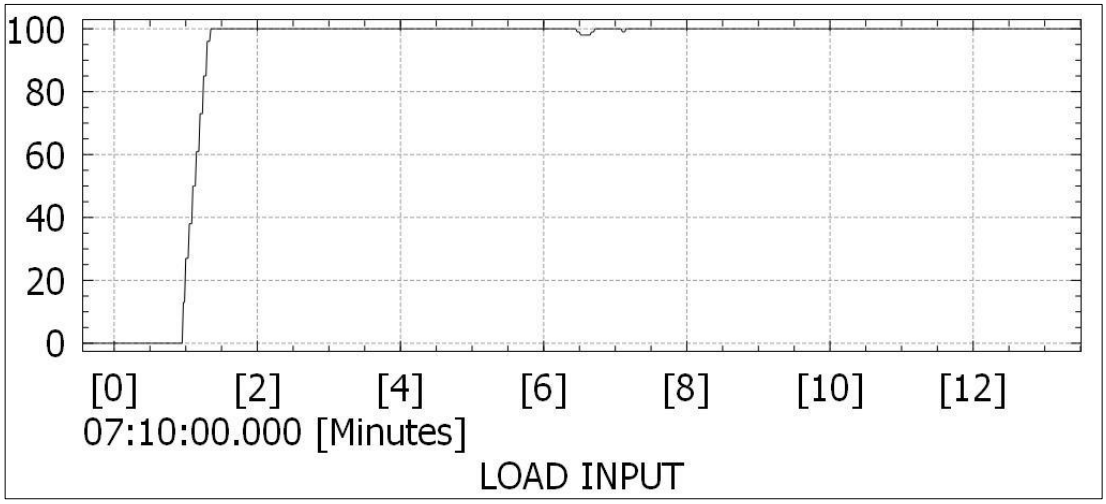

Figure 3.85: Test -5, Take Off – Load Input Graph (% - min)

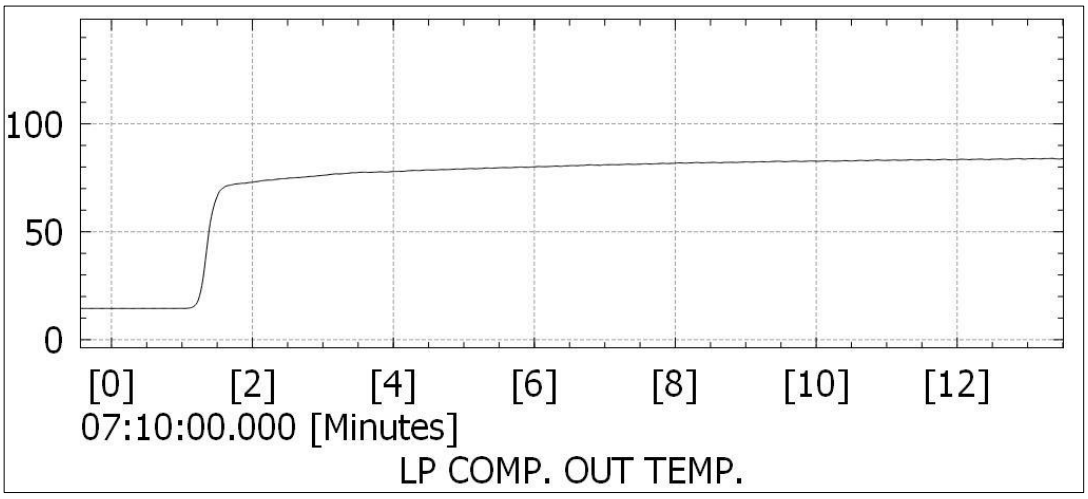

Figure 3.86: Test -5, Take Off – LP Turbo Compressor Output Temperature Graph (°C - min)

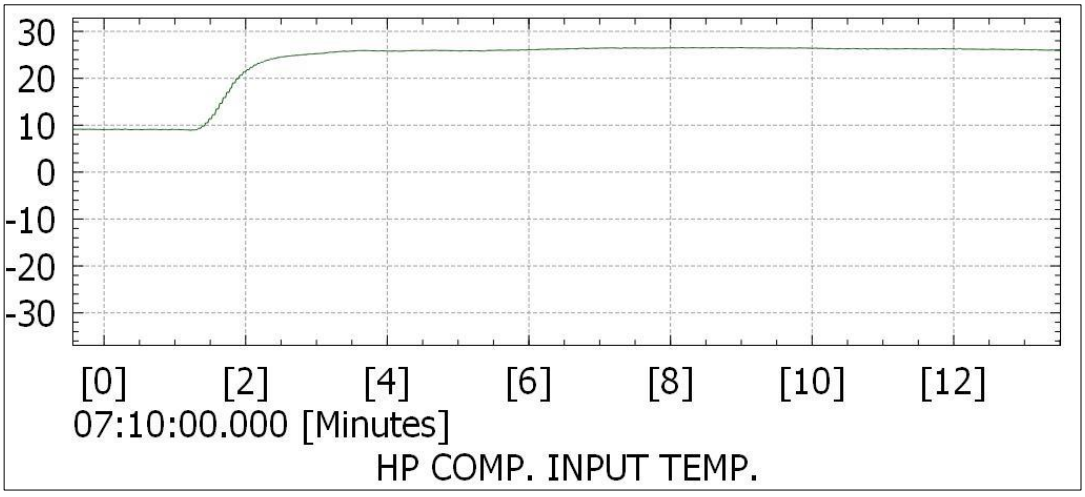

Figure 3.87 : Test -5, Take Off – HP Turbo Compressor Inlet Temperature Graph (°C - min)

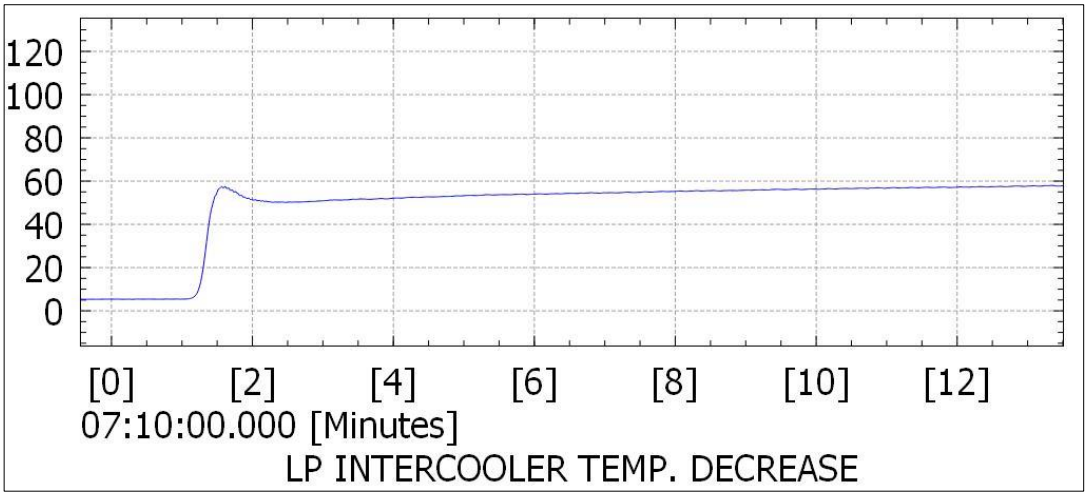

Figure 3.88 : Test -5, Take Off – LP Intercooler Temperature Decrease Graph (°C - min)

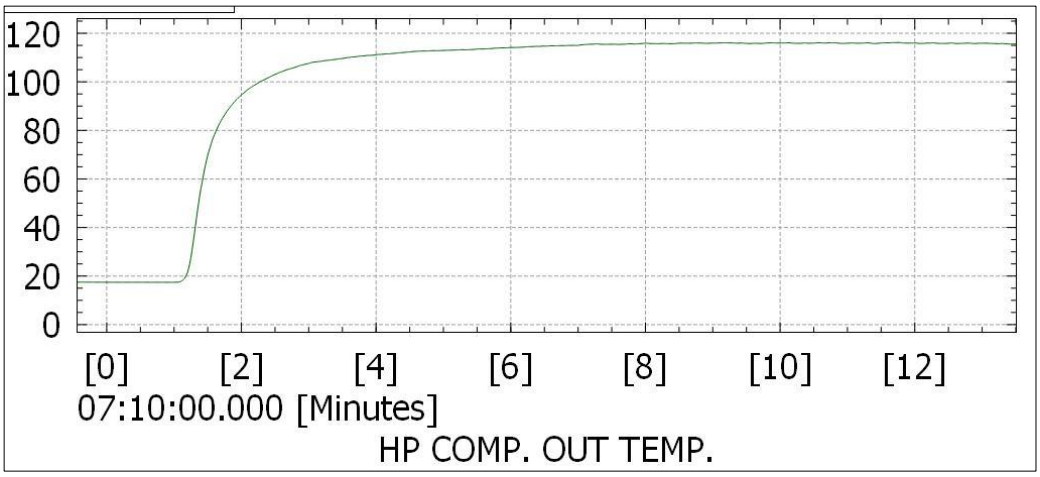

Figure 3.89 : Test -5, Take Off – HP Turbo Compressor Output Temperature Graph (°C - min)

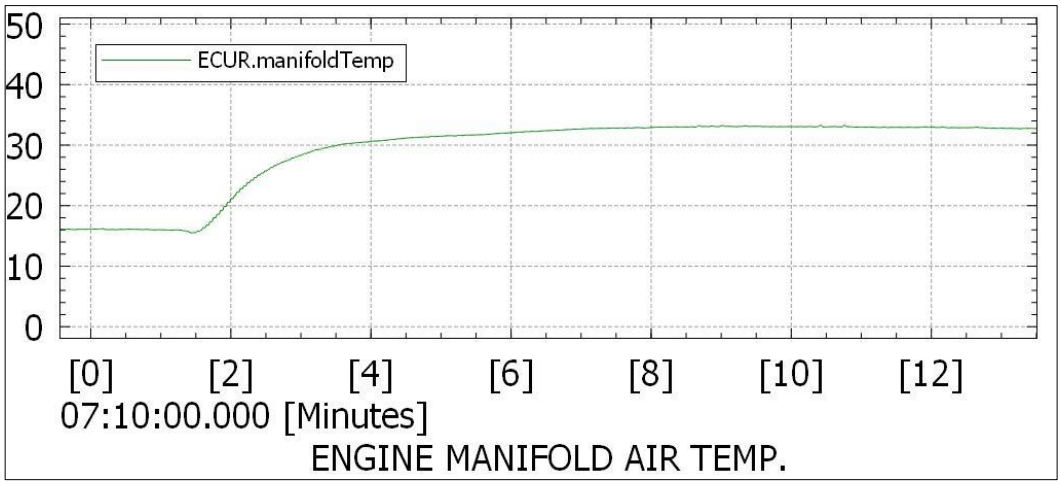

Figure 3.90 : Test -5, Take Off – Engine Manifold Air Temperature Graph (°C - min)

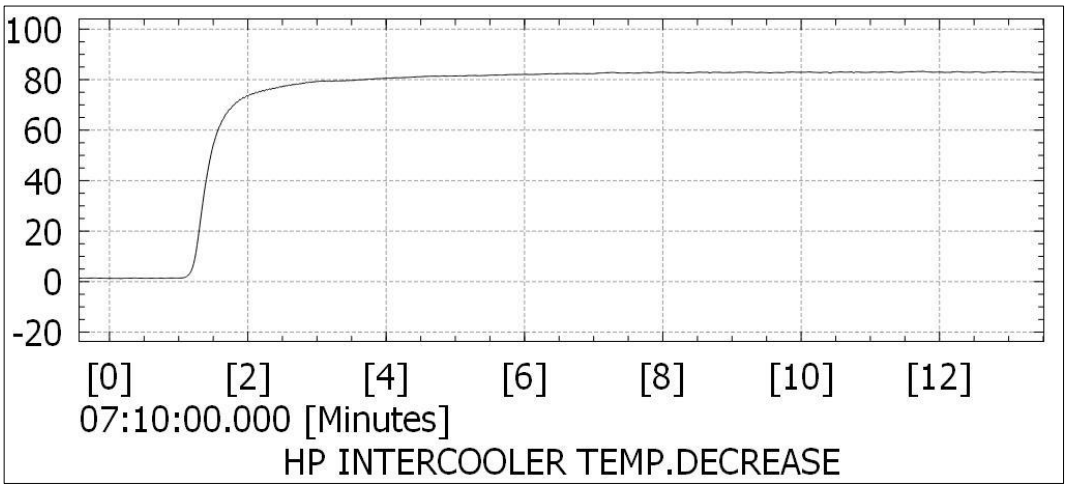

Figure 3.91: Test -5, Take Off – HP Intercooler Temperature Decrease Graph (°C - min)

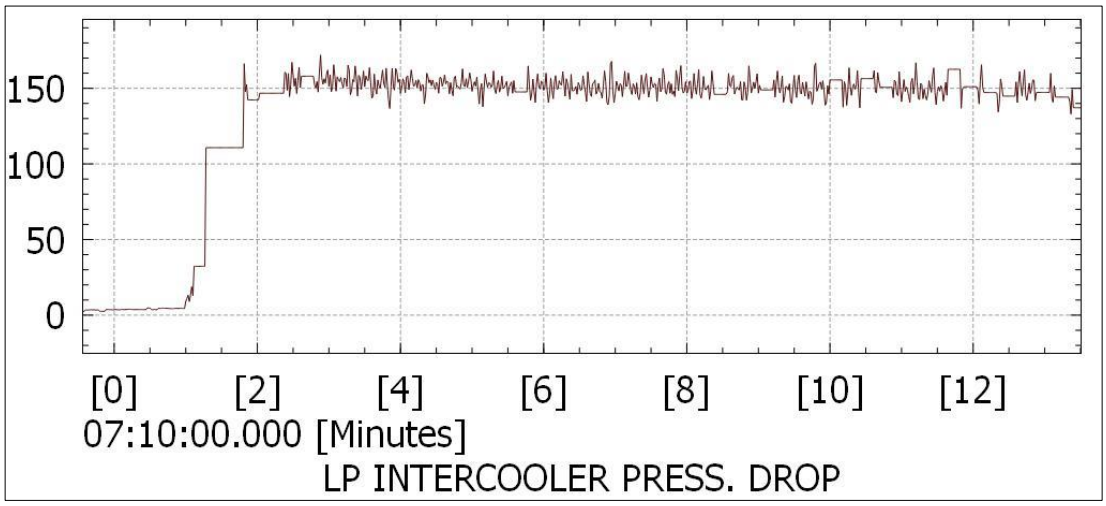

Figure 3.92: Test -5, Take Off – LP Intercooler Pressure Drop (mbar-min)

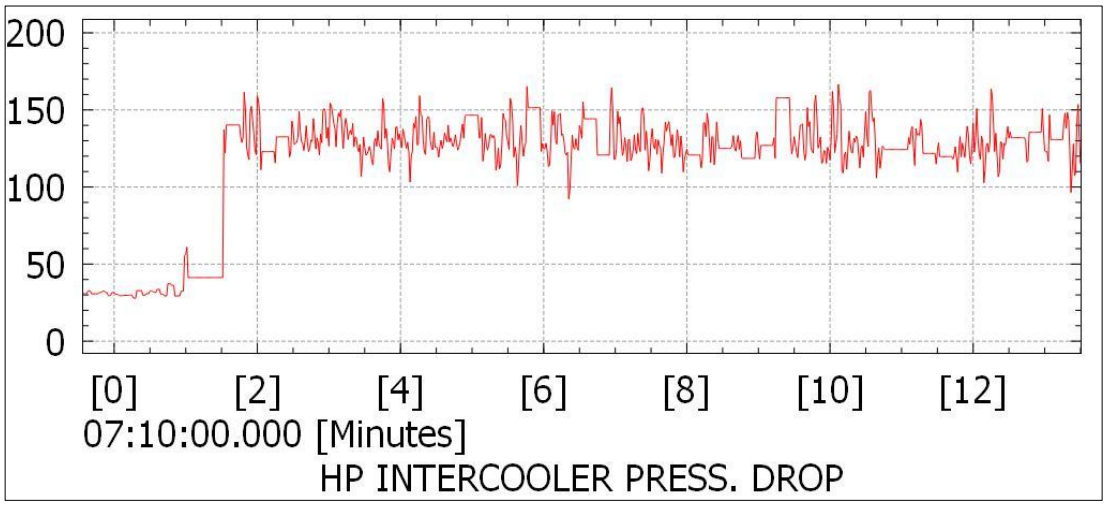

Figure 3.93: Test -5, Take Off – HP Intercooler Pressure Drop (mbar-min)

By Pass Opening Section Test Datas:

The data regarding the By Pass Opening Section of Test 5 performed with the new intercoolers and by pass system is presented below. This section performed when the outside air temperature was -38 °C (Figure 3-94). UAV flights at %100 throttle and decreased throttle to %65 throttle. (Figure 3-95). The exit air temperatures at the LP turbo compressor increased to approximately 130 °C. (Figure 3-96). After passing through the LP intercooler, the temperatures dropped to around 8 °C (Figure 3-97), resulting in a temperature decrease of approximately 123 °C in the LP intercooler (Figure 3-98). The air entering the HP compressor at 8 °C was compressed, causing the temperatures to rise to around 90 °C. (Figure 3-99). In the HP intercooler, these temperatures were reduced to 0 °C then by pass valve opened, Manifold air temperature is increased to 26 °C in seconds (Figure 3-100). The temperature decrease in the HP intercooler before by pass opening was 100 °C after by pass opening HP Intercooler Temperature decrease was 62 °C (Figure 3-101). The pressure drop measurement was taken from both HP and LP intercooler. LP Intercooler Pressure Drop was around 100-120mbar (Figure 3-102). And HP Intercooler Pressure Drop was around 80mbar before by pass opening, after bypass opening Hp Intercooler pressure drop decreases to nearly 10mbar, because By pass line's pressure drop is dramatically smaller than the hp intercooler core (Figure 3-103).

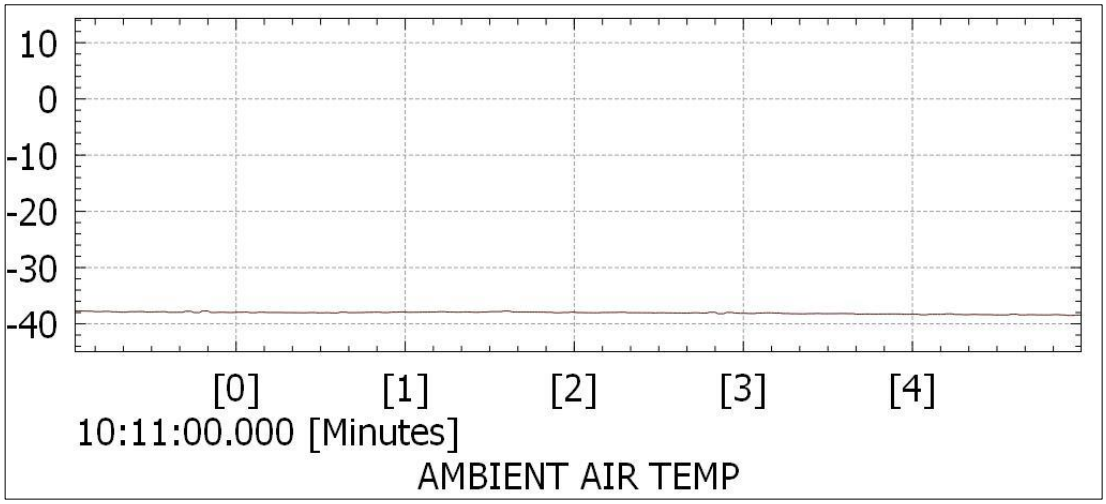

Figure 3.94 : Test -5, By Pass Opening – Ambient Air Temperature Graph (°C -min)

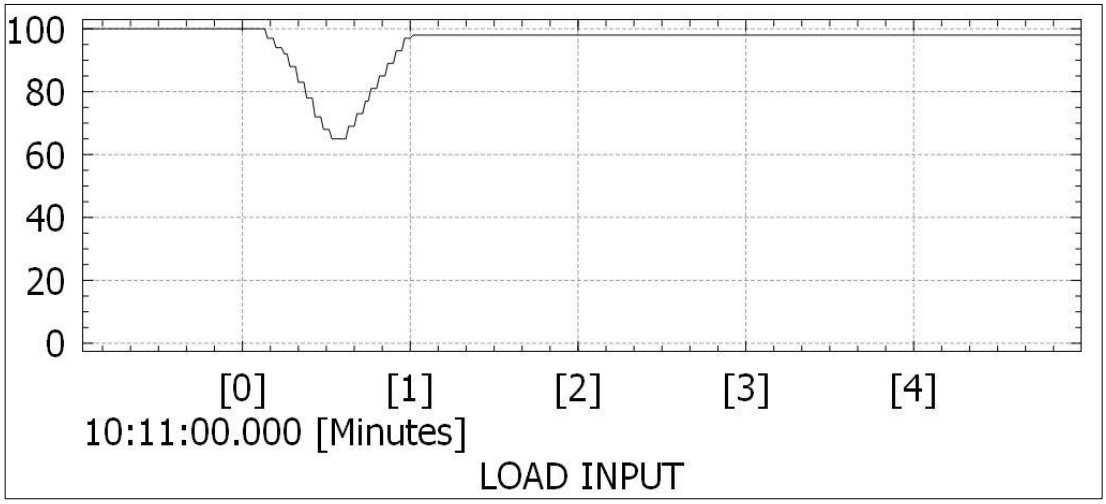

Figure 3.95 : Test -5, By Pass Opening – Load Input Graph (% - min)

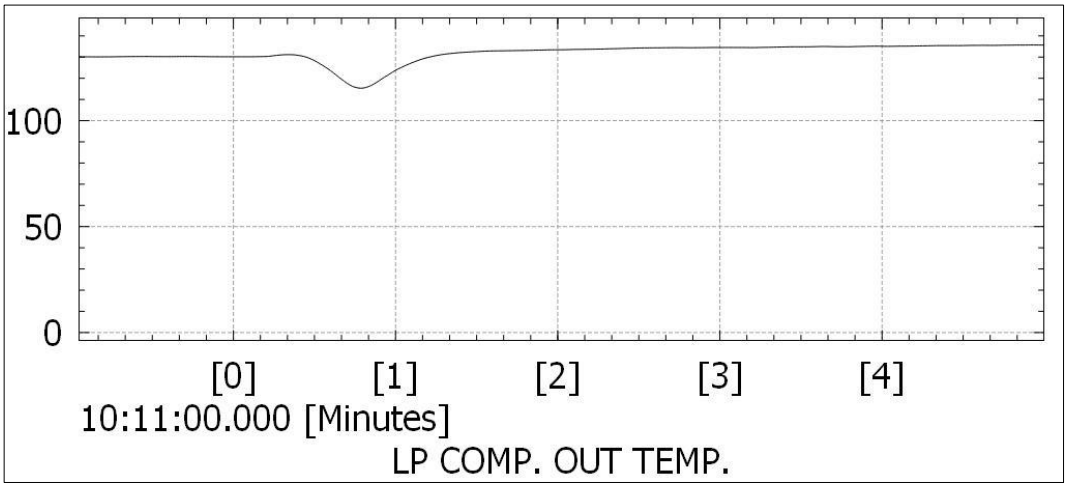

Figure 3.96: Test -5, By Pass Opening – LP Turbo Compressor Output Temperature Graph (°C – min)

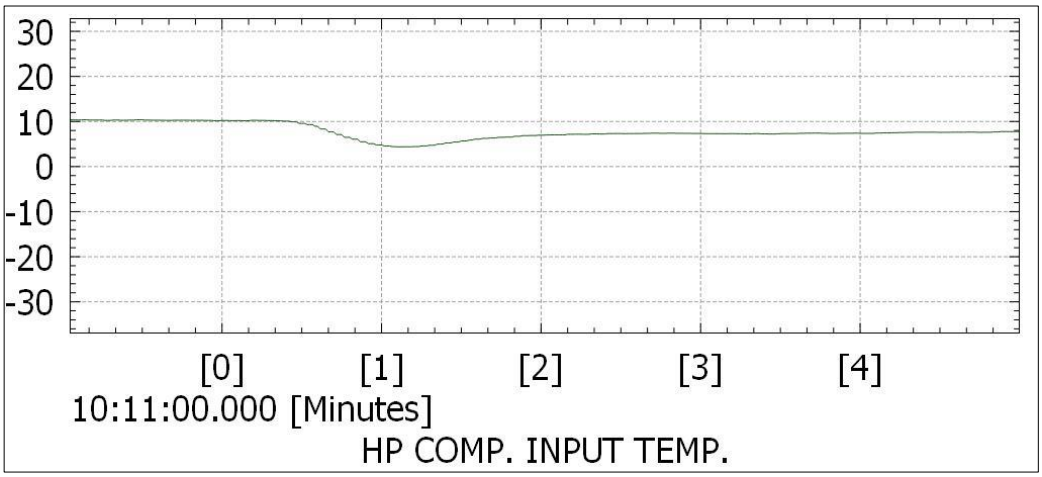

Figure 3.97: Test -5, By Pass Opening – HP Turbo Compressor Inlet Temperature Graph (°C - min)

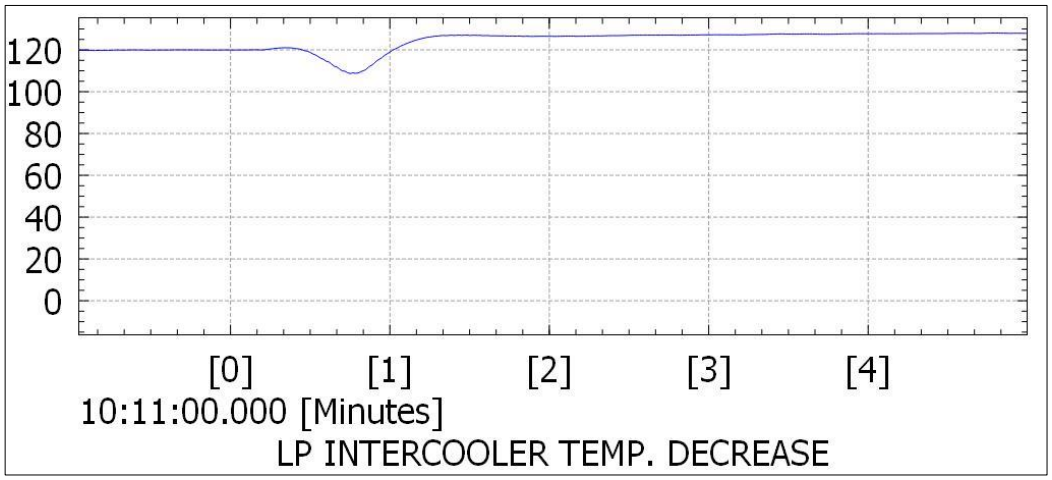

Figure 3.98: Test -5, By Pass Opening – LP Intercooler Temperature Decrease Graph (°C - min)

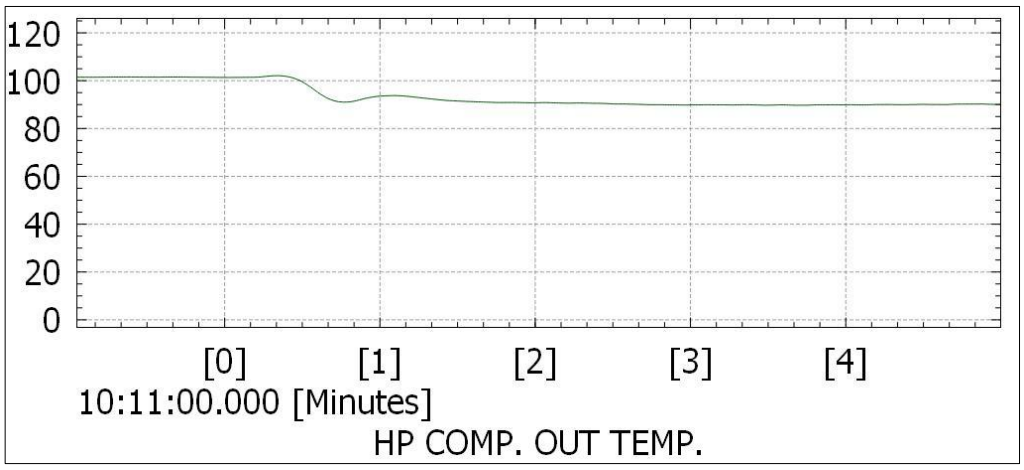

Figure 3.99: Test -5, By Pass Opening – HP Turbo Compressor Output Temperature Graph (°C – min)

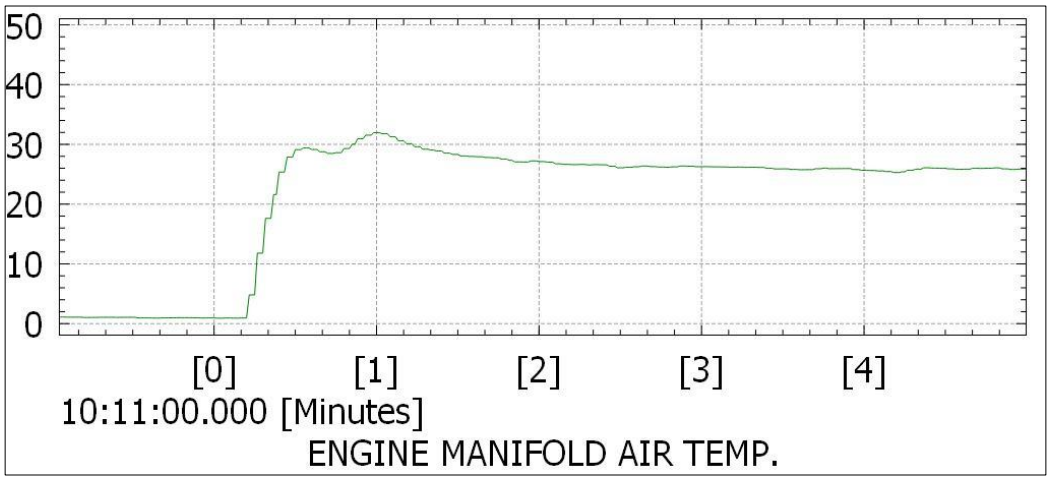

Figure 3.100: Test -5, By Pass Opening – Engine Manifold Air Temperature Graph (°C - min)

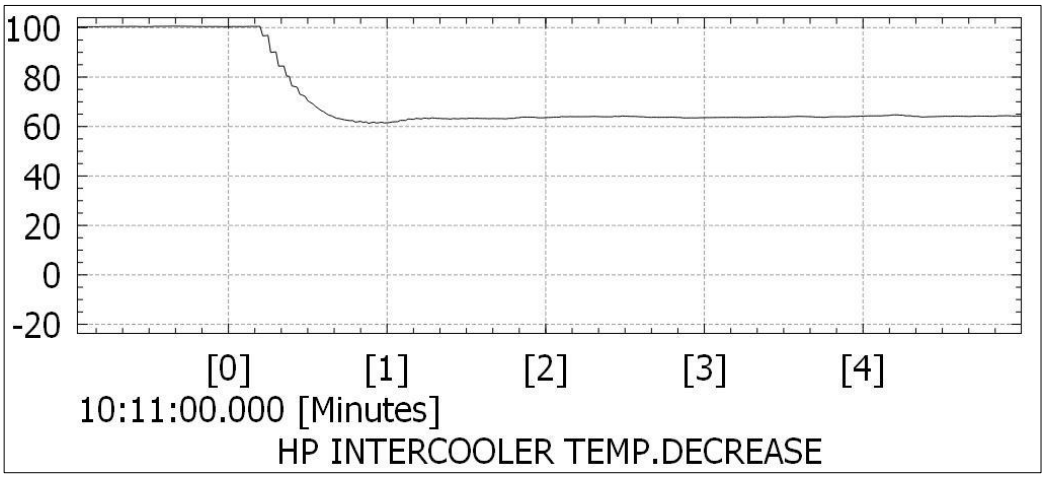

Figure 3.101: Test -5, By Pass Opening – HP Intercooler Temperature Decrease Graph (°C - min)

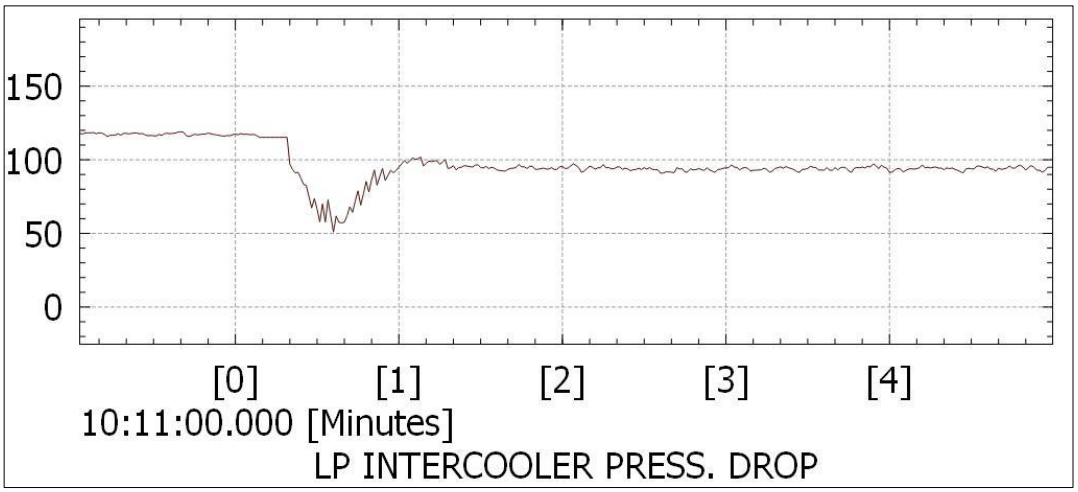

Figure 3.102: Test -5, By Pass Opening – LP Intercooler Pressure Drop (mbar-min)

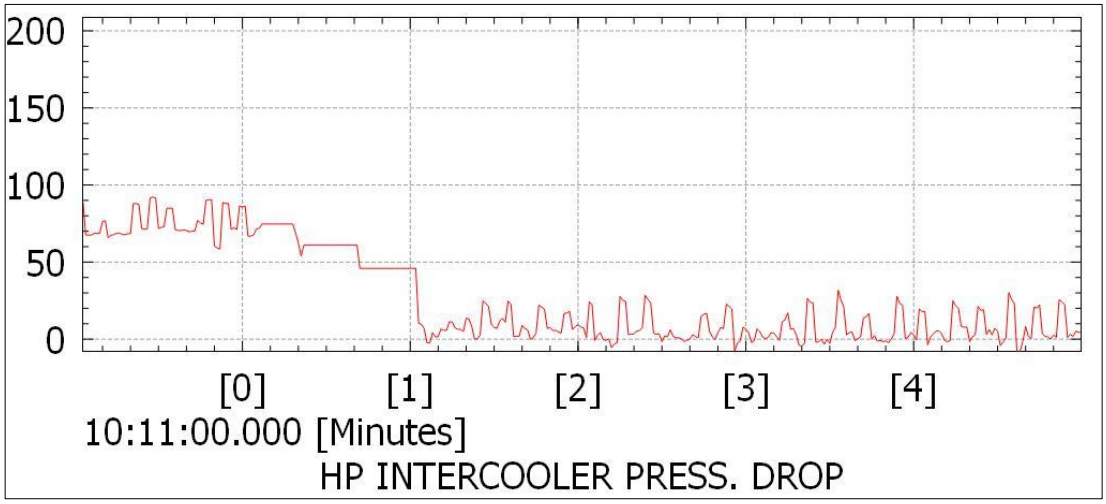

Figure 3.103: Test -5, By Pass Opening – HP Intercooler Pressure Drop (mbar-min)

30000ft Test Section with %0 Load Input:

The data regarding the 30000 ft phase of Test 5 conducted with the new intercoolers and bypass system is presented below. The outside air temperature was around -42 °C (Figure 3-104). 30000ft test was performed at idle (0% throttle) (Figure 3-105). The exit air temperatures at the LP turbo compressor increased to approximately 30 °C at idle throttle. (Figure 3-106). After passing through the LP intercooler, the temperatures dropped to around -34 °C at idle throttle (Figure 3-107), resulting in a temperature decrease of approximately 64°C in the LP intercooler (Figure 3-108). The air entering the HP compressor at was compressed, causing the temperatures to rise to around 30 °C. (Figure 3-109). After HP intercooler and by pass system, these temperatures were reduced to around 0,2 °C, because by pass valve is opened (Figure 3-110). The approximate temperature decrease in the HP intercooler was only 30 °C (Figure 3-111). The pressure drop measurement was taken from both HP and LP intercooler. LP Intercooler Pressure Drop was around 20mbar (Figure 3-112). And HP Intercooler Pressure Drop was around 25mbar while by pass was opened (Figure 3-113).

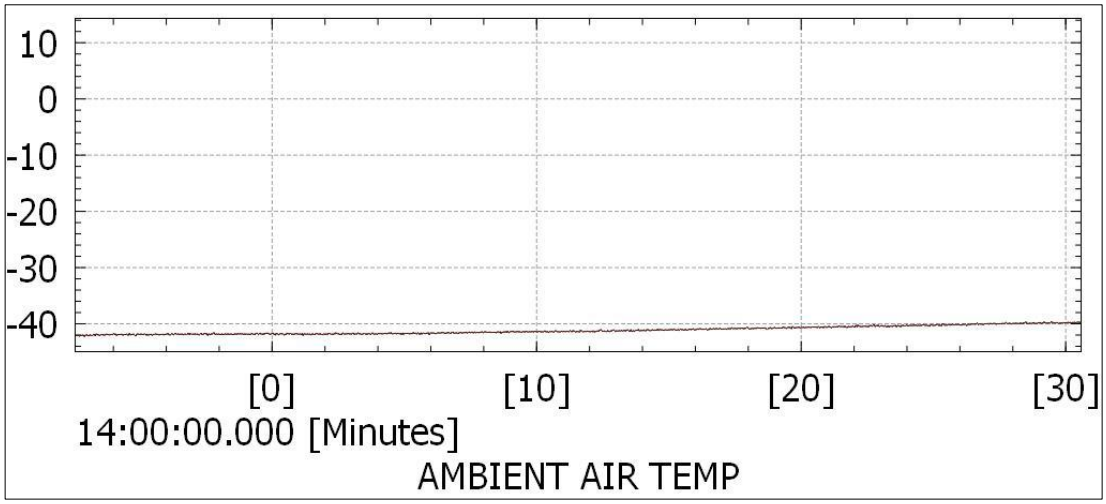

Figure 3.104: Test -5, 30kft Idle – Ambient Air Temperature Graph (°C - min)

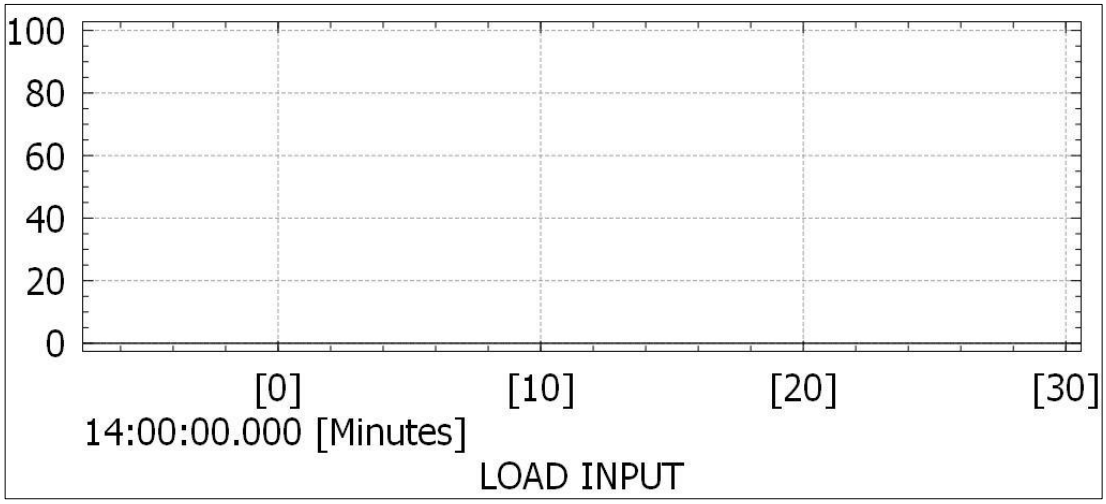

Figure 3.105 : Test -5, 30kft Idle – Load Input Graph (% - min)

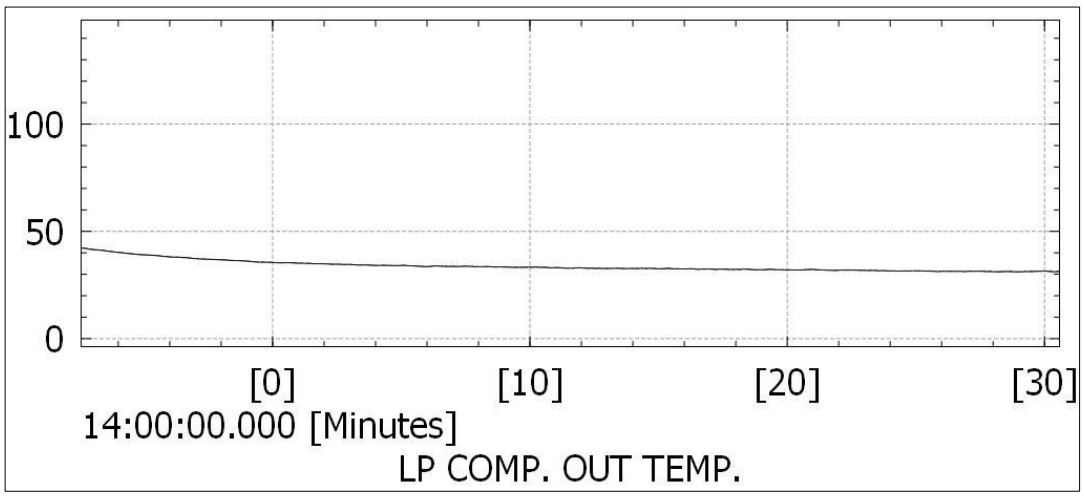

Figure 3.106: Test -5, 30kft Idle – LP Turbo Compressor Output Temperature Graph (°C - min)

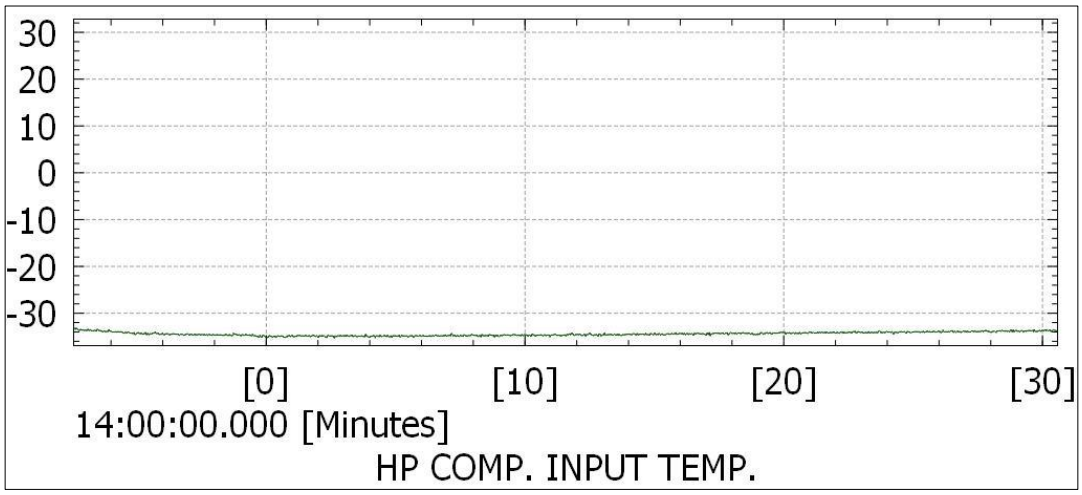

Figure 3.107: Test -5, 30kft Idle – HP Turbo Compressor Inlet Temperature Graph (°C - min)

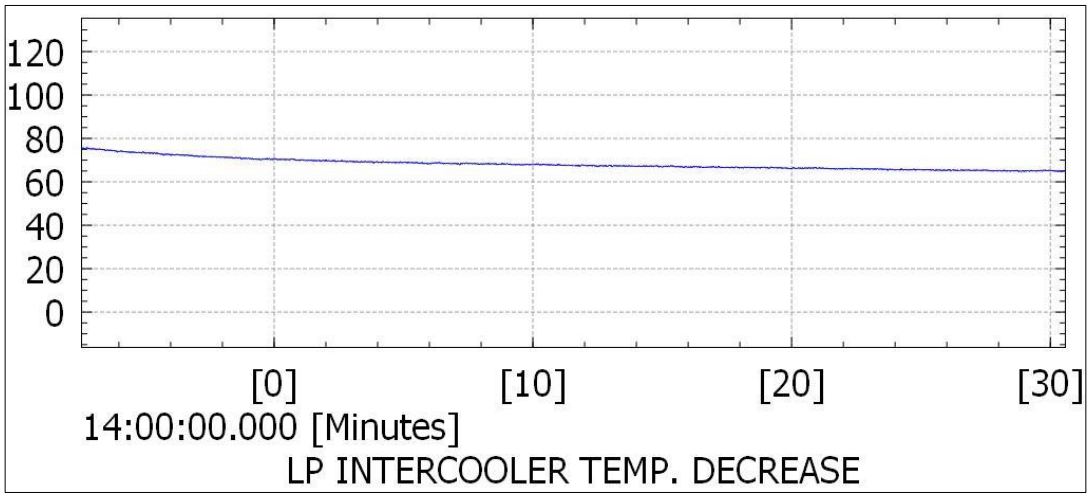

Figure 3.108: Test -5, 30kft Idle – LP Intercooler Temperature Decrease Graph (°C - min)

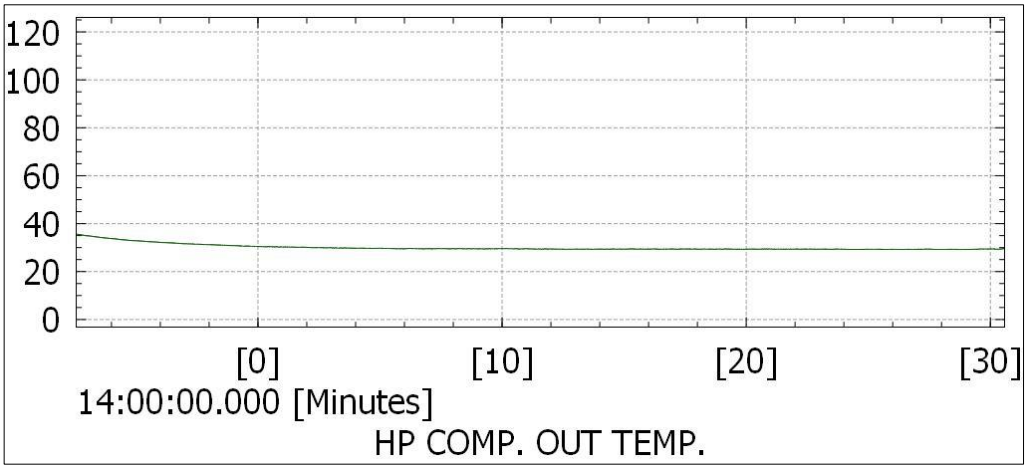

Figure 3.109: Test -5, 30kft Idle – HP Turbo Compressor Output Temperature Graph (°C - min)

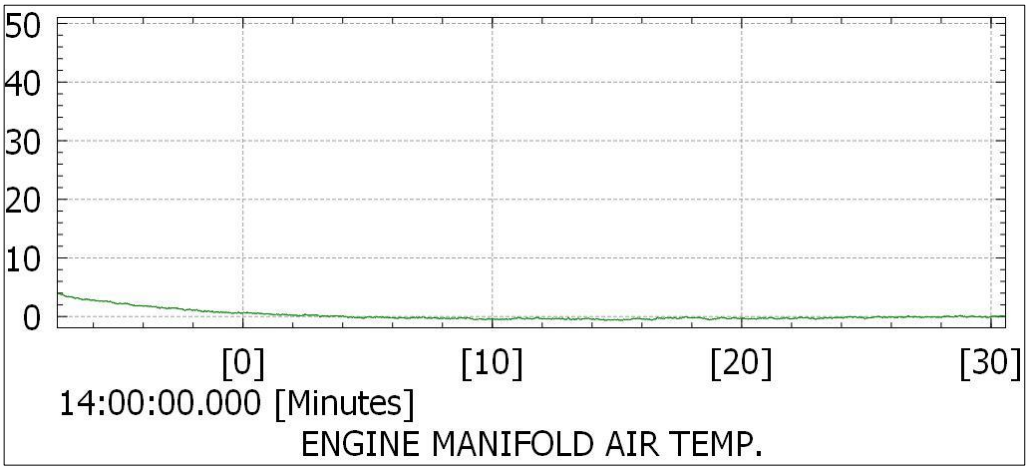

Figure 3.110: Test -5, 30kft Idle – Engine Manifold Air Temperature Graph (°C - min)

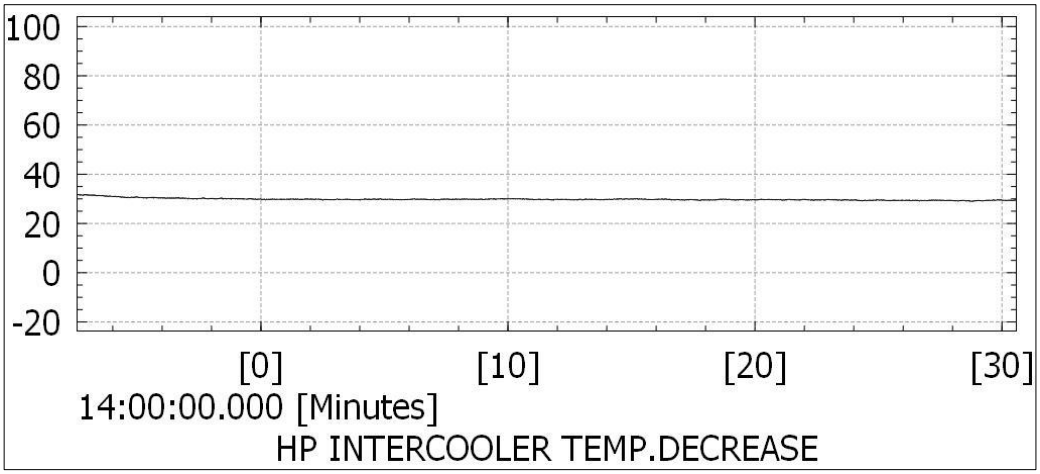

Figure 3.111: Test -5, 30kft Idle – HP Intercooler Temperature Decrease Graph (°C - min)

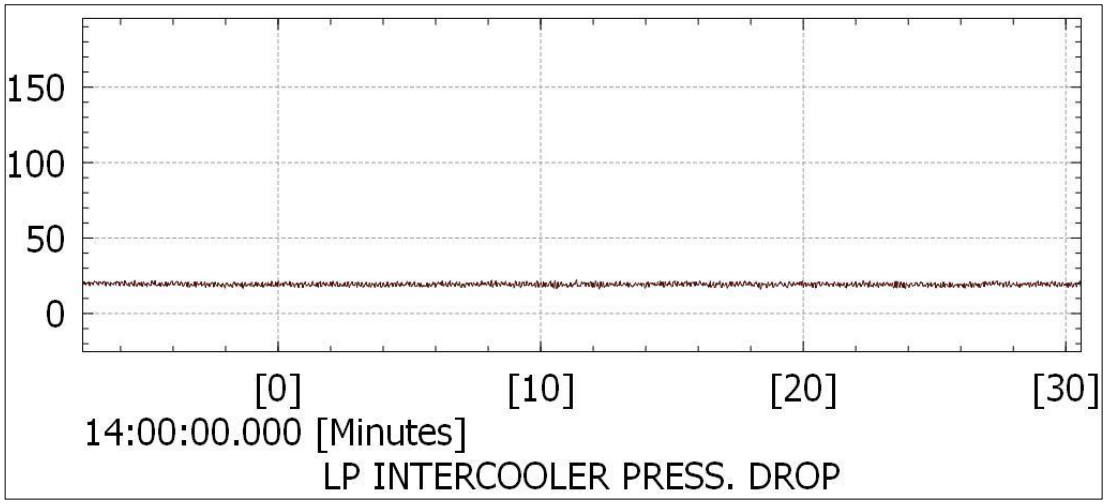

Figure 3.112: Test -5, 30kft Idle – LP Intercooler Pressure Drop (mbar-min)

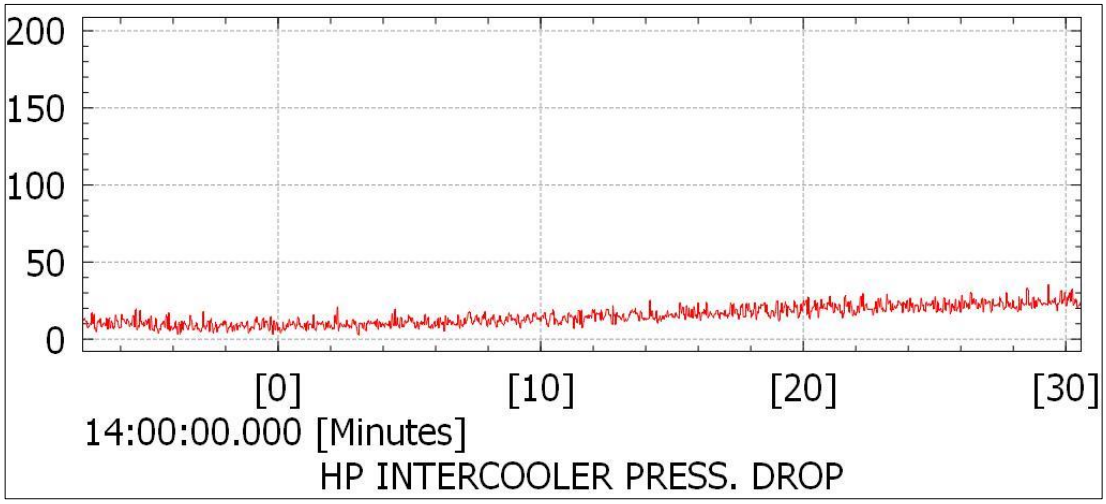

Figure 3.113: Test -5, 30kft Idle – HP Intercooler Pressure Drop (mbar-min)

25000ft Test Section Datas with %0 Load Input:

The data regarding the 25000 ft phase of Test 5 conducted with the new intercoolers and bypass system is presented below. The outside air temperature was around -33 °C (Figure 3-114). 30000ft test was performed at idle (0% throttle) (Figure 3-115). The exit air temperatures at the LP turbo compressor increased to approximately 35 °C at idle throttle. (Figure 3-116). After passing through the LP intercooler, the temperatures dropped to around -28 °C at idle throttle (Figure 3-117), resulting in a temperature decrease of approximately 63°C in the LP intercooler (Figure 3-118). The air entering the HP compressor was compressed, causing the temperatures to rise to around 31 °C. (Figure 3-119). After HP intercooler and bypass system, these temperatures were reduced to around 4 °C, because by pass valve is opened (Figure 3-

120). The approximate temperature decrease in the HP intercooler was only 27 °C (Figure 3-121). The pressure drop measurement was taken from both HP and LP intercooler. LP Intercooler Pressure Drop was around 20mbar (Figure 3-122). And HP Intercooler Pressure Drop was around 35mbar while by pass was opened (Figure 3-123).

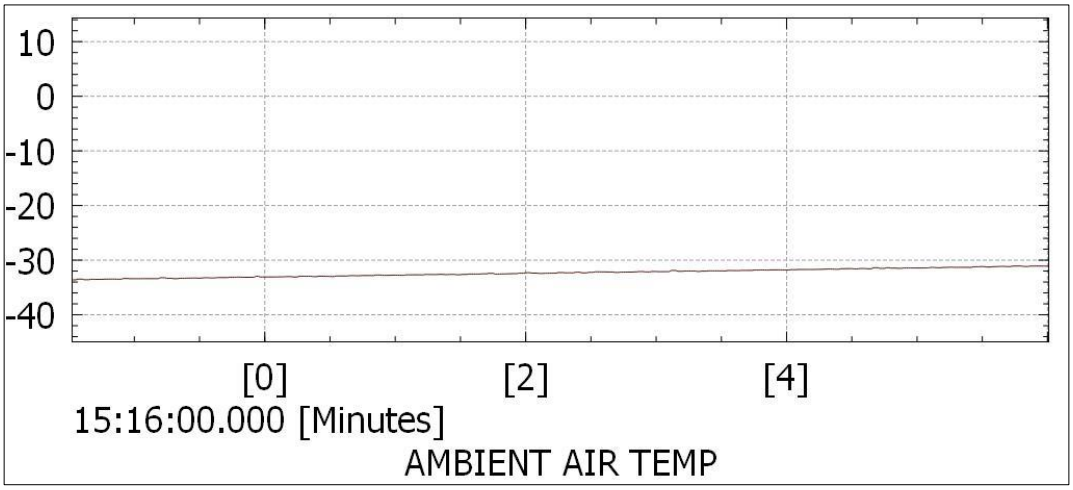

Figure 3.114: Test -5, 25kft Idle – Ambient Air Temperature Graph (°C - min)

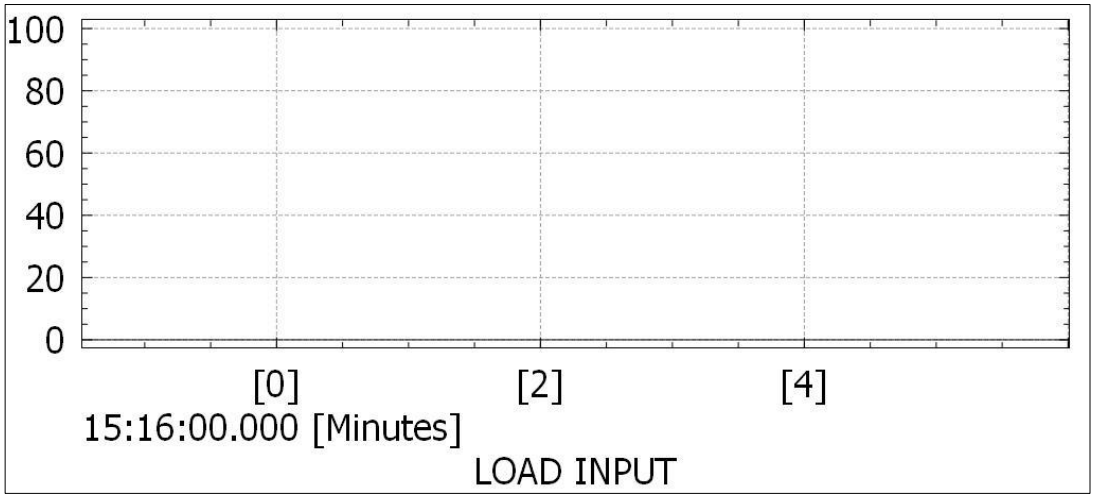

Figure 3.115: Test -5, 25kft Idle – Load Input Graph (% - min)

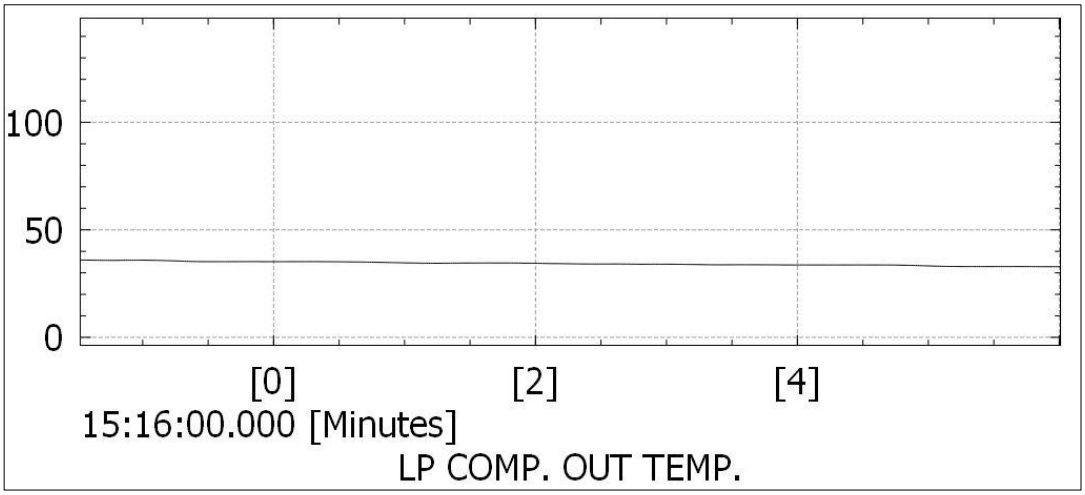

Figure 3.116: Test -5, 25kft Idle – LP Turbo Compressor Output Temperature Graph (°C - min)

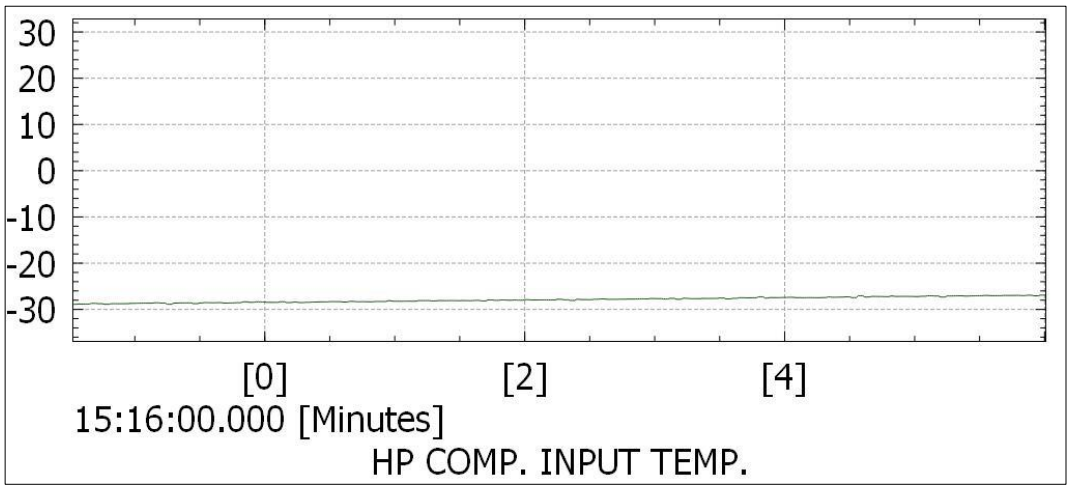

Figure 3.117: Test -5, 25kft Idle – HP Turbo Compressor Inlet Temperature Graph (°C - min)

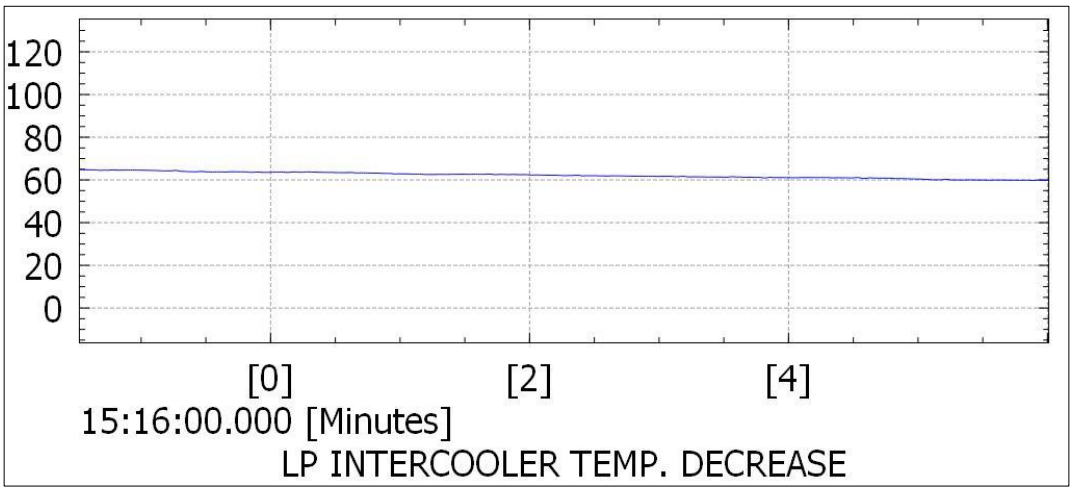

Figure 3.118: Test -5, 25kft Idle – LP Intercooler Temperature Decrease Graph (°C - min)

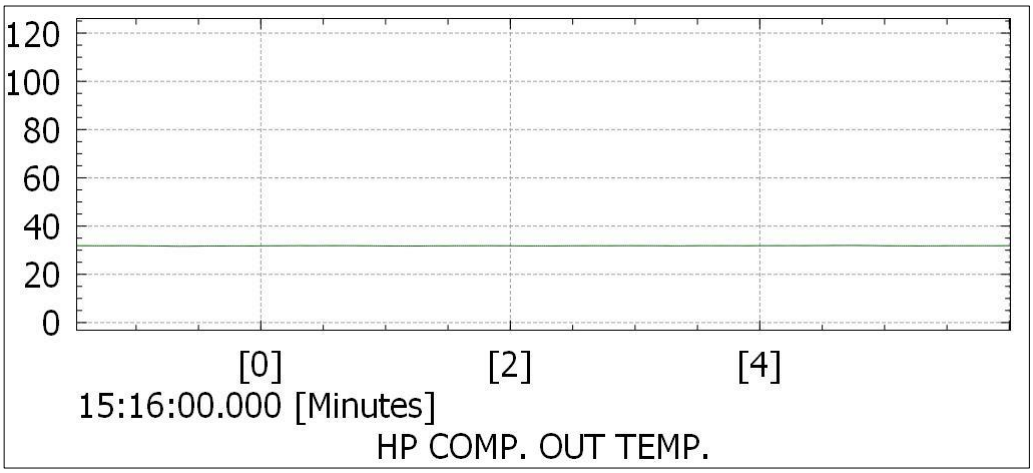

Figure 3.119: Test -5, 25kft Idle – HP Turbo Compressor Output Temperature Graph (°C - min)

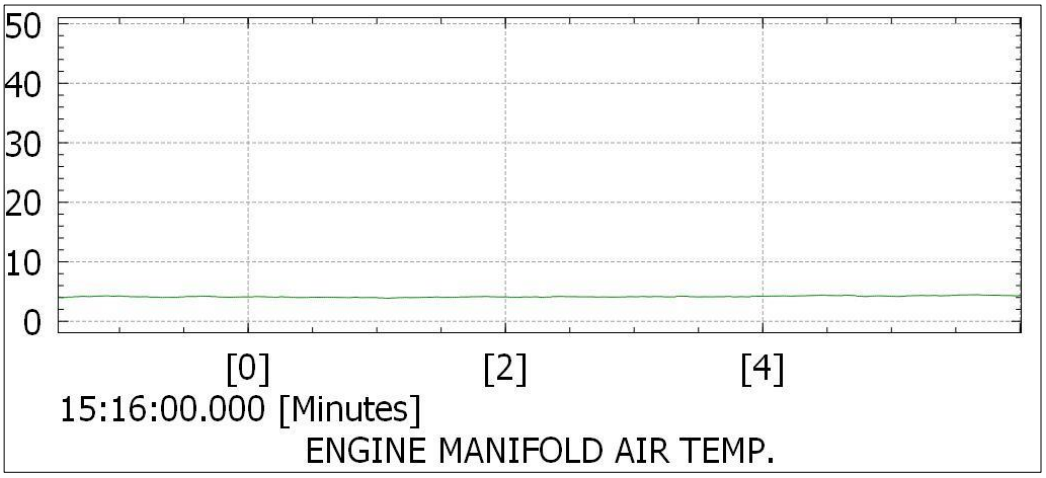

Figure 3.120: Test -5, 25kft Idle – Engine Manifold Air Temperature Graph (°C - min)

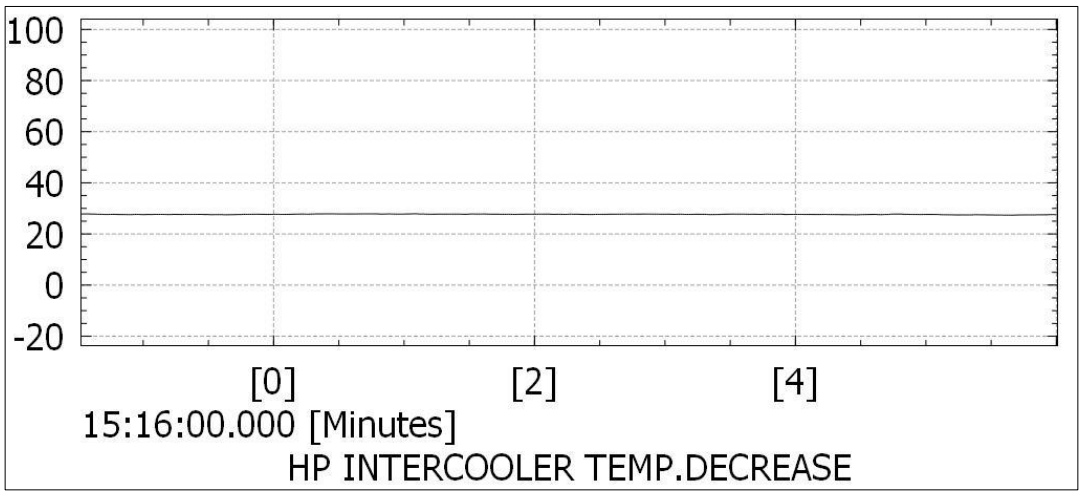

Figure 3.121: Test -5, 25kft Idle – HP Intercooler Temperature Decrease Graph (°C - min)

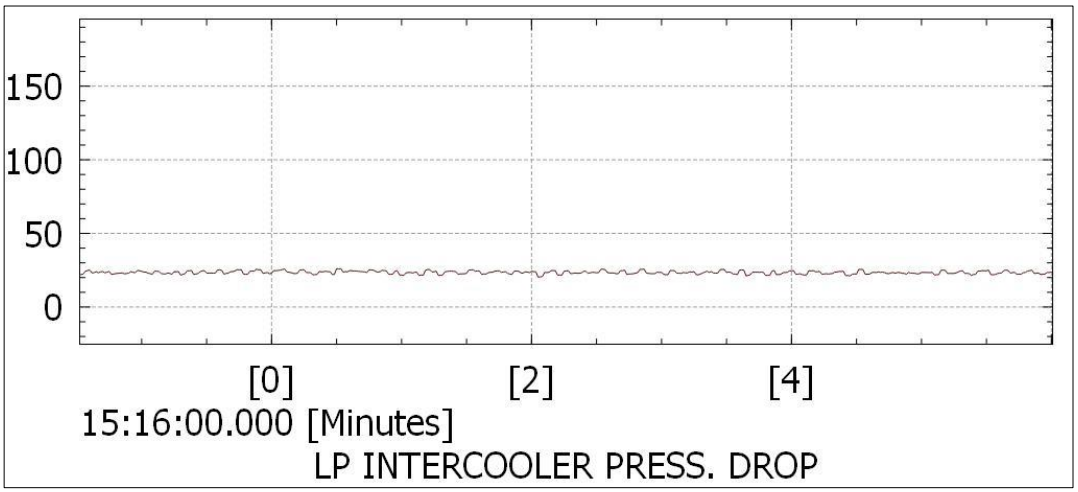

Figure 3.122: Test -5, 25kft Idle – LP Intercooler Pressure Drop (mbar-min)

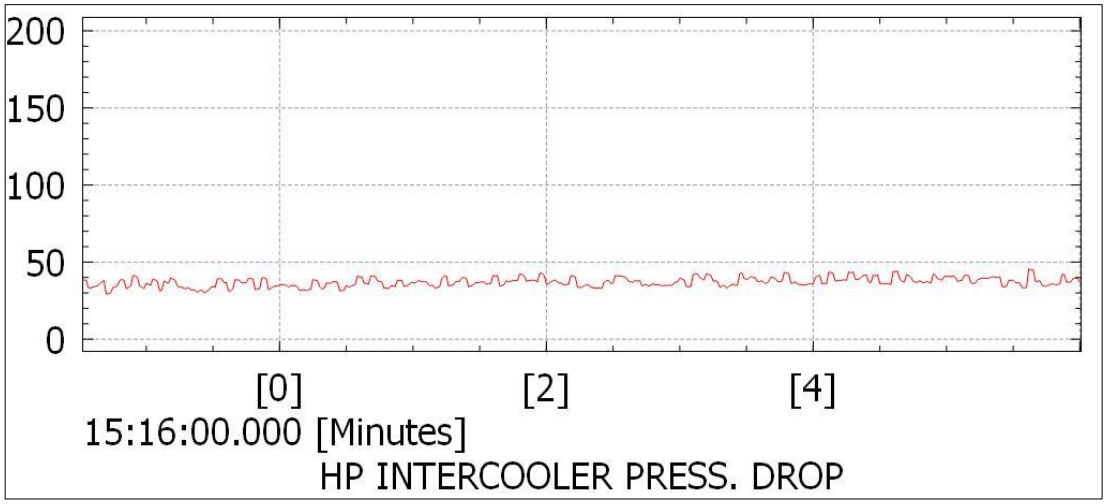

Figure 3.123: Test -5, 25kft Idle – HP Intercooler Pressure Drop (mbar-min)

20000ft Test Section Datas with %100 and %0 Load Input:

The data regarding the 20000 ft phase of Test 5 conducted with the new intercoolers and bypass system is presented below. The outside air temperature was around -24 °C (Figure 3-124). 20000ft test was performed at idle (0% throttle) (Figure 3-125). The exit air temperatures at the LP turbo compressor increased to approximately 28 °C at idle throttle. (Figure 3-126). After passing through the LP intercooler, the temperatures dropped to around -21 °C at idle throttle (Figure 3-127), resulting in a temperature decrease of approximately 49°C in the LP intercooler (Figure 3-128). The air entering the HP compressor was compressed, causing the temperatures to rise to around 32 °C. (Figure 3-129). After HP intercooler and bypass system, these

temperatures were reduced to around 8 °C, because by pass valve is opened (Figure 3-130). The approximate temperature decrease in the HP intercooler was only 24 °C (Figure 3-131). The pressure drop measurement was taken from both HP and LP intercooler. LP Intercooler Pressure Drop was around 25mbar (Figure 3-132). And HP Intercooler Pressure Drop was around 40mbar while by pass was opened (Figure 3-133).

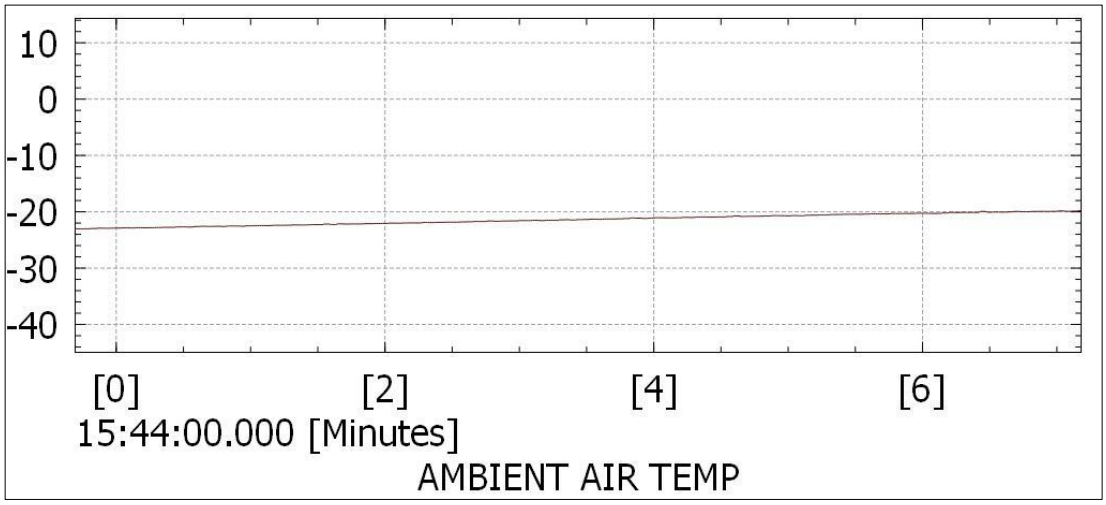

Figure 3.124: Test -5, 20kft Idle – Ambient Air Temperature Graph (°C - min)

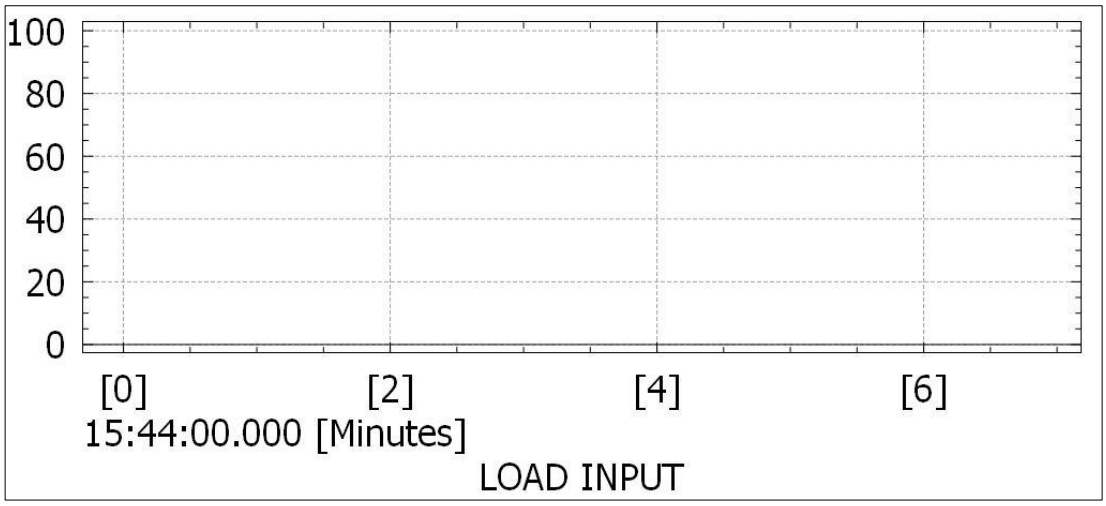

Figure 3.125: Test -5, 20kft Idle – Load Input Graph (% - min)

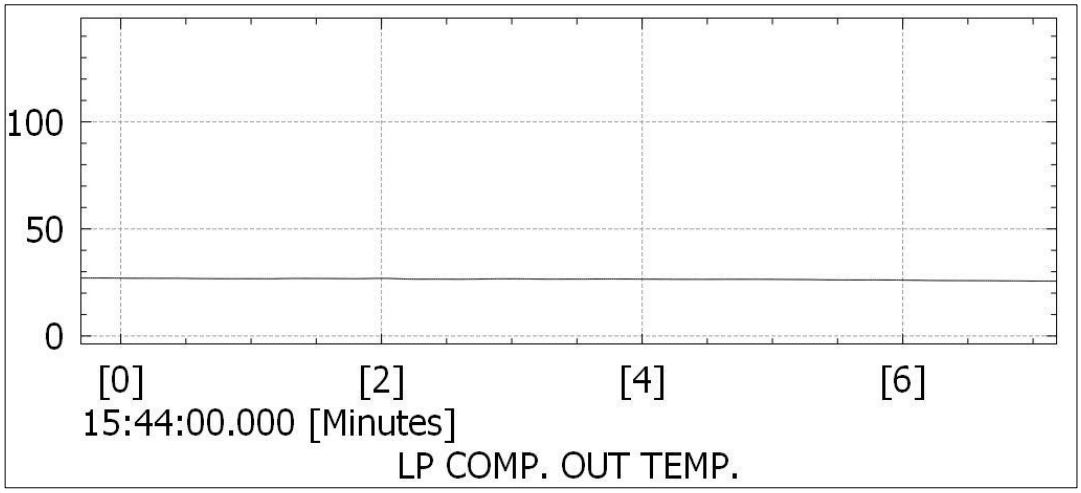

Figure 3.126: Test -5, 20kft Idle – LP Turbo Compressor Output Temperature Graph (°C - min)

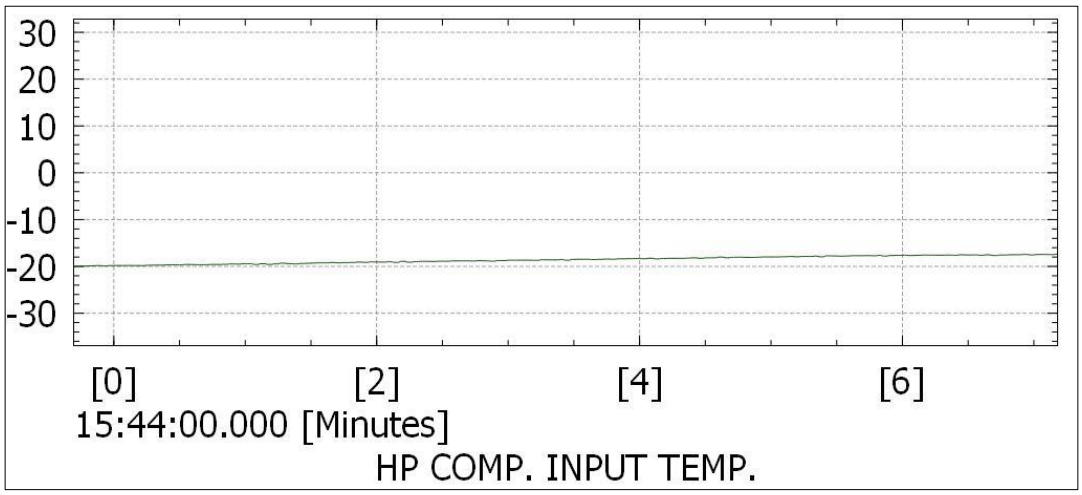

Figure 3.127: Test -5, 20kft Idle – HP Turbo Compressor Inlet Temperature Graph (°C - min)

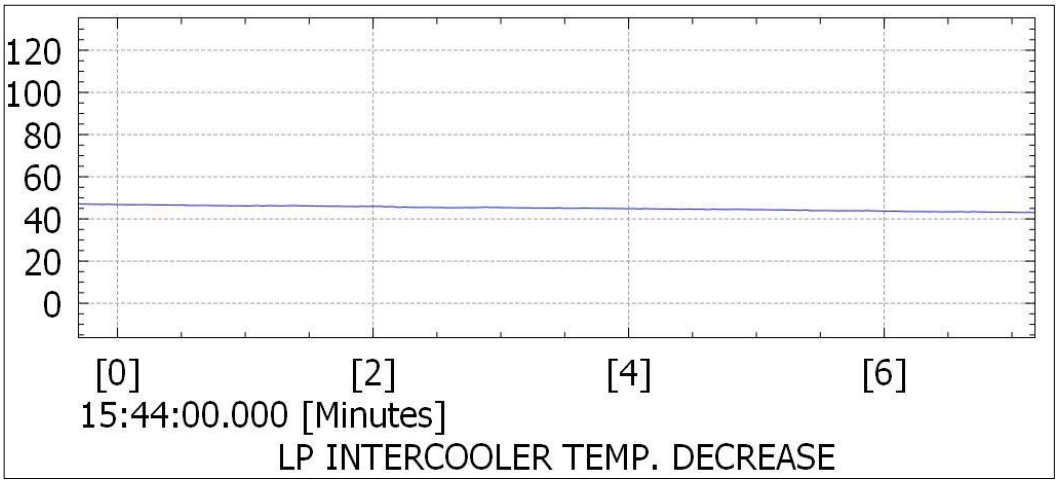

Figure 3.128: Test -5, 20kft Idle – LP Intercooler Temperature Decrease Graph (°C - min)

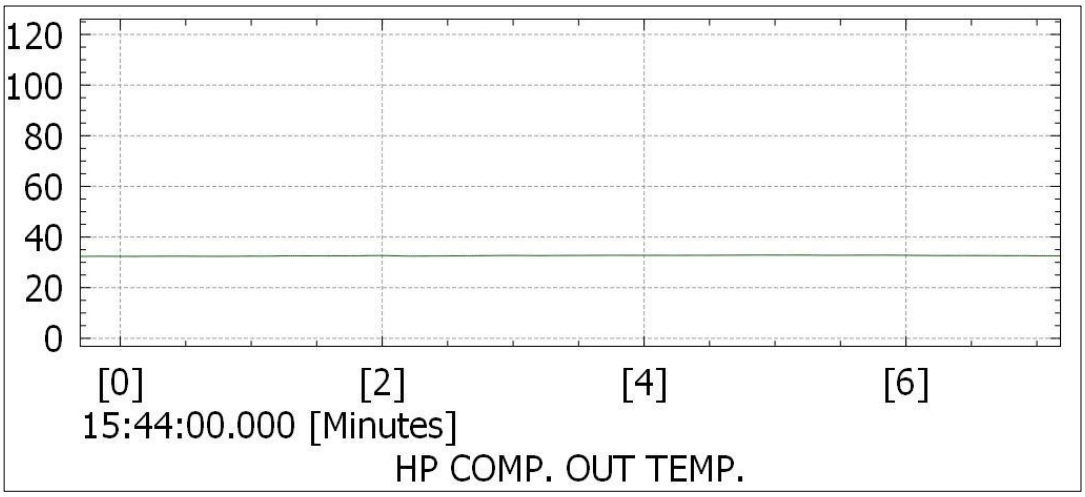

Figure 3.129: Test -5, 20kft Idle – HP Turbo Compressor Output Temperature Graph (°C - min)

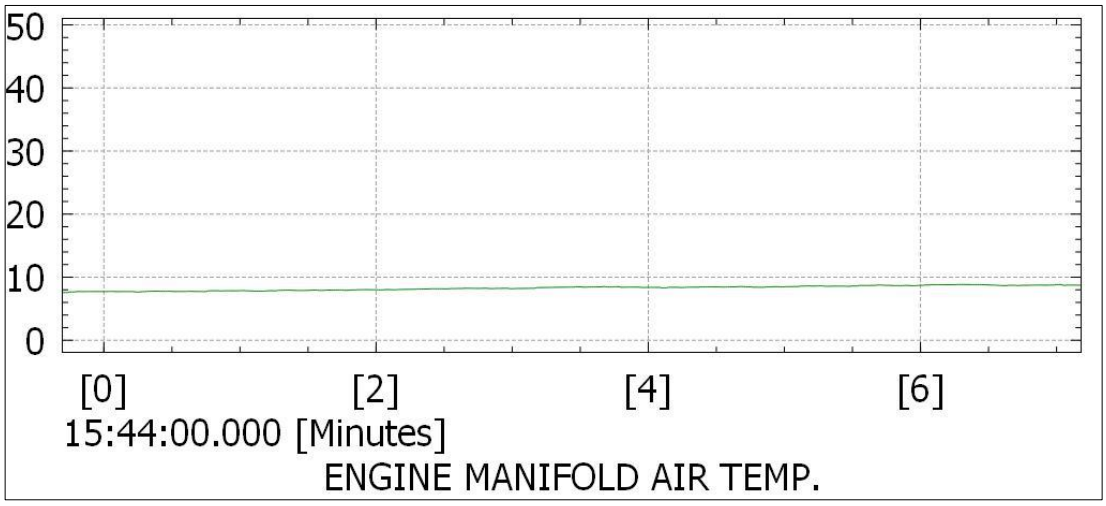

Figure 3.130: Test -5, 20kft Idle – Engine Manifold Air Temperature Graph (°C - min)

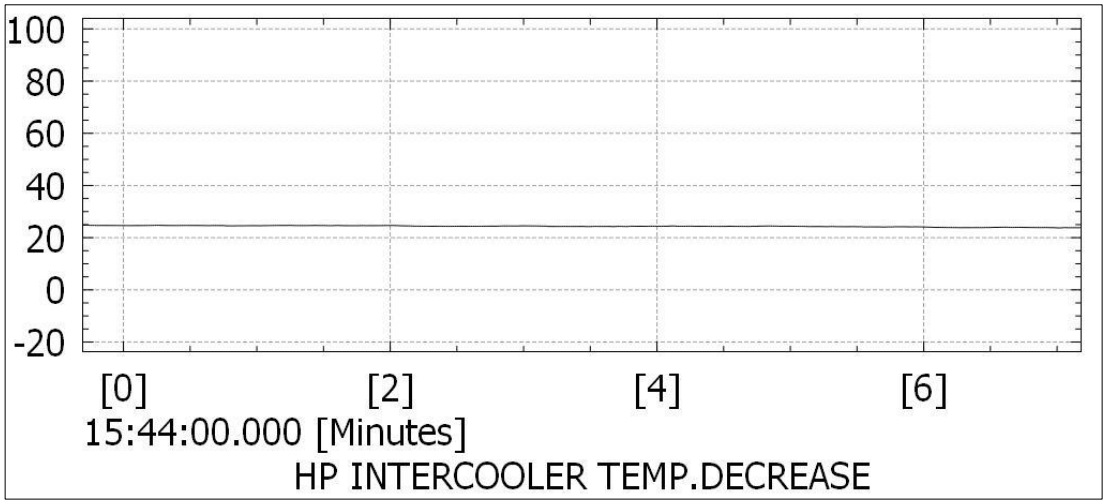

Figure 3.131: Test -5, 20kft Idle – HP Intercooler Temperature Decrease Graph (°C - min)

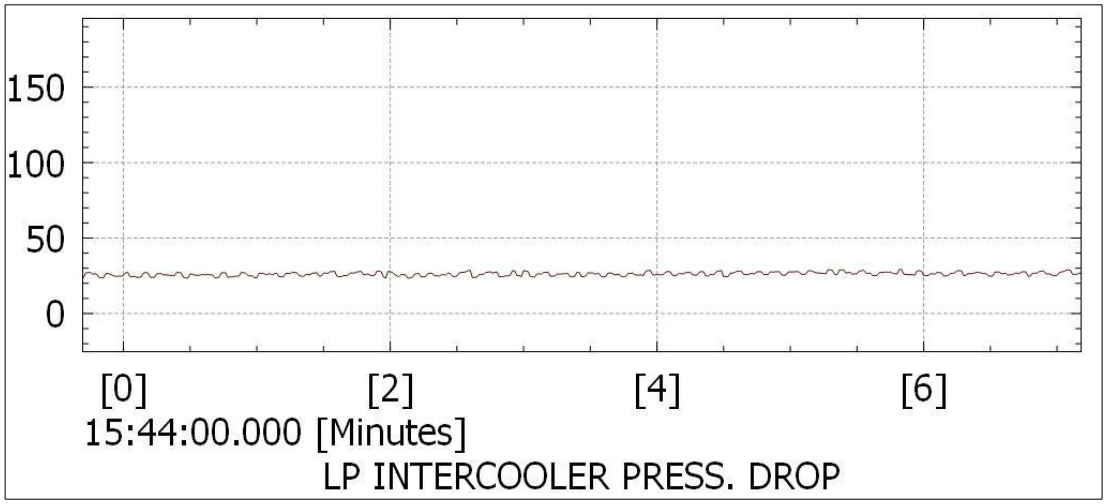

Figure 3.132: Test -5, 20kft Idle – LP Intercooler Pressure Drop (mbar-min)

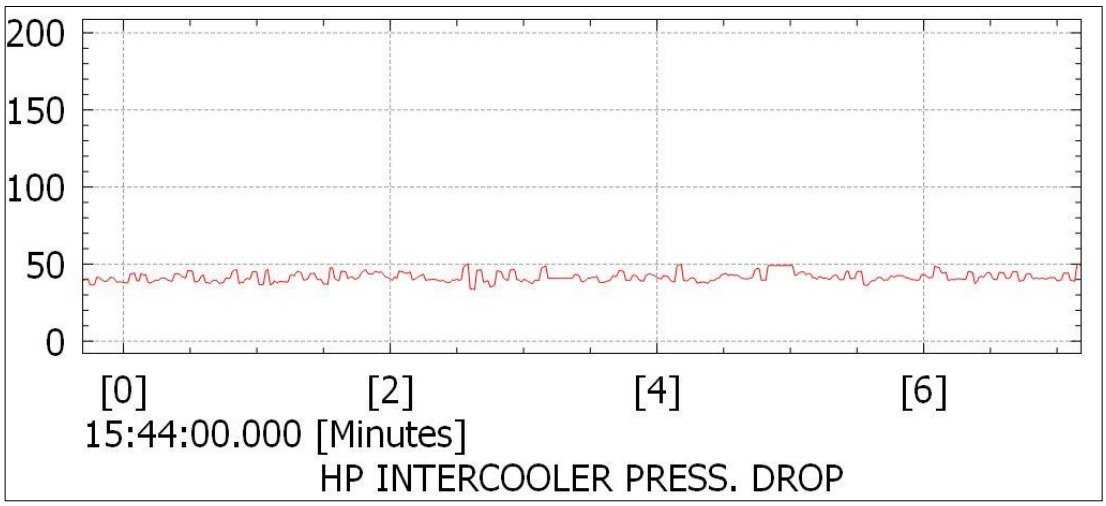

Figure 3.133 : Test -5, 20kft Idle – HP Intercooler Pressure Drop (mbar-min)

4. RESULTS

In the final case, LP and HP intercoolers have been shortened so as not to exceed the maximum manifold air temperature during hot weather takeoffs, and a by pass system has been designed to prevent the manifold air temperature from falling below the minimum allowable temperature value during low throttle flights at high altitude and low ambient temperature. The data obtained from the Take-off, 30k, 25k and 20k tests, as well as the data of the old design air cooling system and the new design air cooling system, are presented in comparative graphics.

After Intercoolers are shortened take-off test under hot weather conditions performed, despite the ambient temperature being 2 °C lower, the manifold air temperature (MAT) with the new intercoolers showed an increase of approximately 10 °C. With the old intercoolers, the MAT observed was 53 °C, which increased to 63 °C with the new intercoolers. During the intercooler design change phase, the target for the MAT was set to a maximum of 70 °C at an ambient temperature of 43 °C. Based on the tests performed, 63 °C MAT was observed at an ambient temperature of 36 °C, indicating that the target values are expected to be achieved at an ambient temperature of 43 °C (Figure 4.1, Figure 4.2).

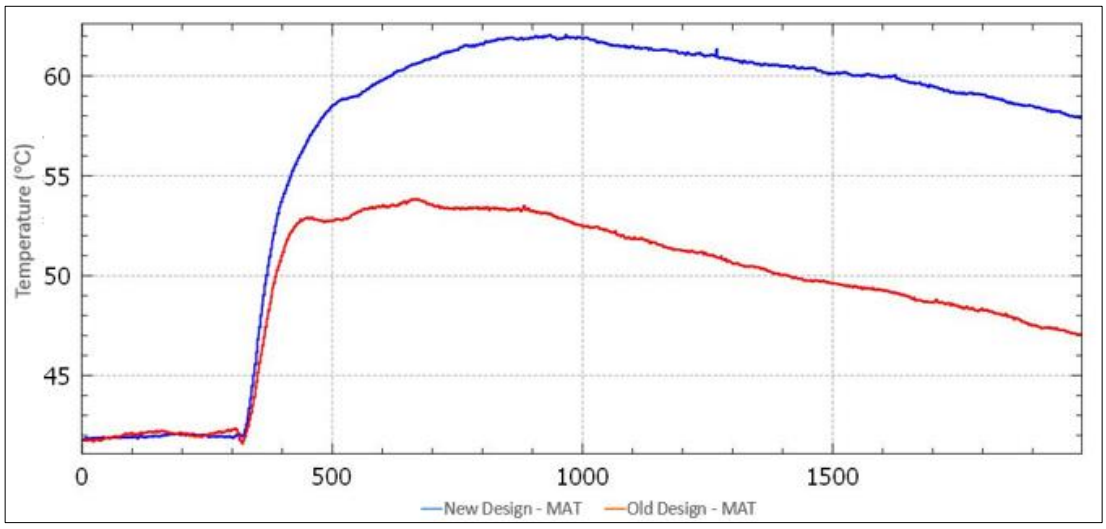

Figure 4.1: Take-Off Manifold Air Temp Comparison Btw Old & New Air Cooling Systems

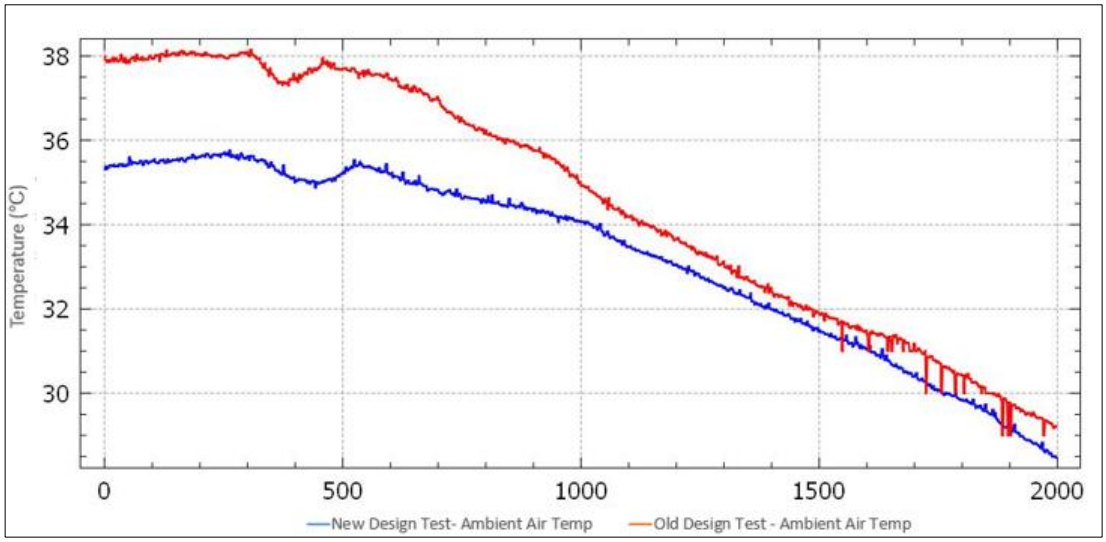

Figure 4.2: Take Off- Ambient Air Temp Comparison Btw Old & New Air Cooling System

In the 30kft tests performed after the intercooler design modification and the addition of the bypass system, it was observed that with the new design, the MAT (manifold air temperature) decreased to a minimum of 0.5 °C. In tests with the old design under ambient air temperature 8 °C warmer, the MAT was observed to drop to -24 °C. With the bypass system and new intercoolers, the MAT at 30kft increased by approximately 24 °C, preventing the formation of undesirable chemicals during combustion in the engine (Figure 4-3, Figure 4-4).

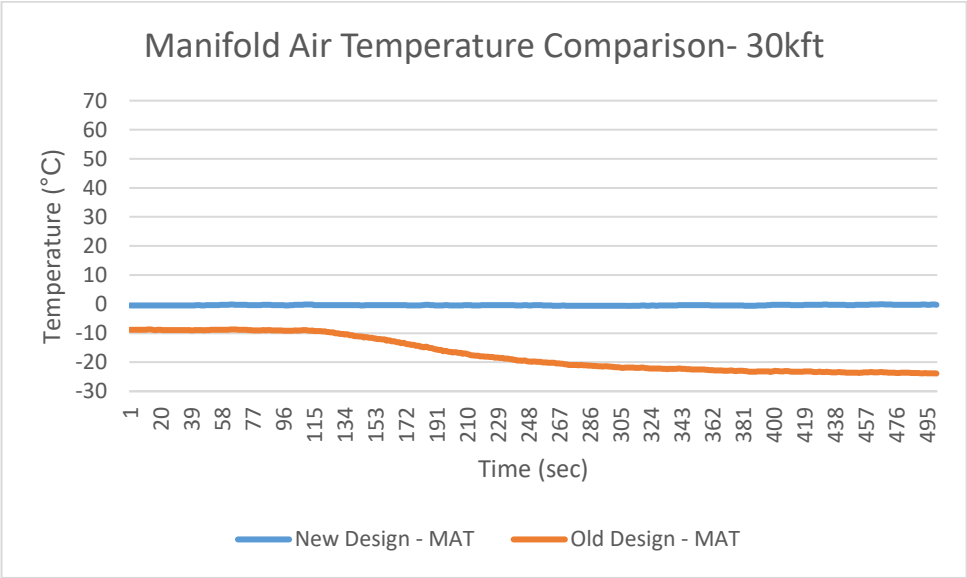

Figure 4.3: - 30kft Manifold Air Temp Comparison Btw Old & New Air Cooling Systems

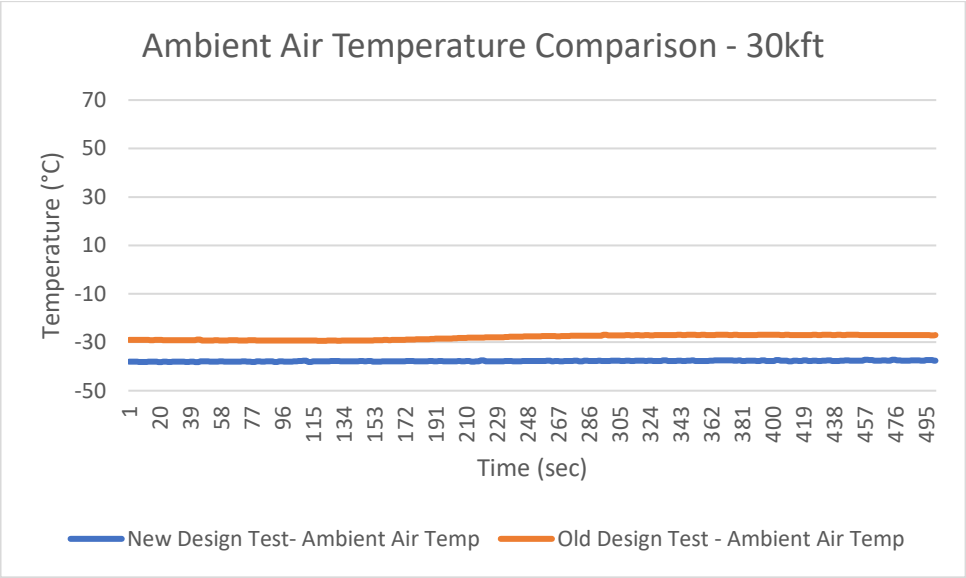

Figure 4.4: - 30kft Ambient Air Temp Comparison Btw Old & New Air Cooling Systems

In the 25kft and 20kft tests, it was observed that with the new design, the MAT (manifold air temperature) is warmer with the new design intercoolers than old design intercooler MAT values despite the ambient temperature is colder than the old design tests (Figure 4-5, Figure 4-6, Figure 4-7, Figure 4-8).

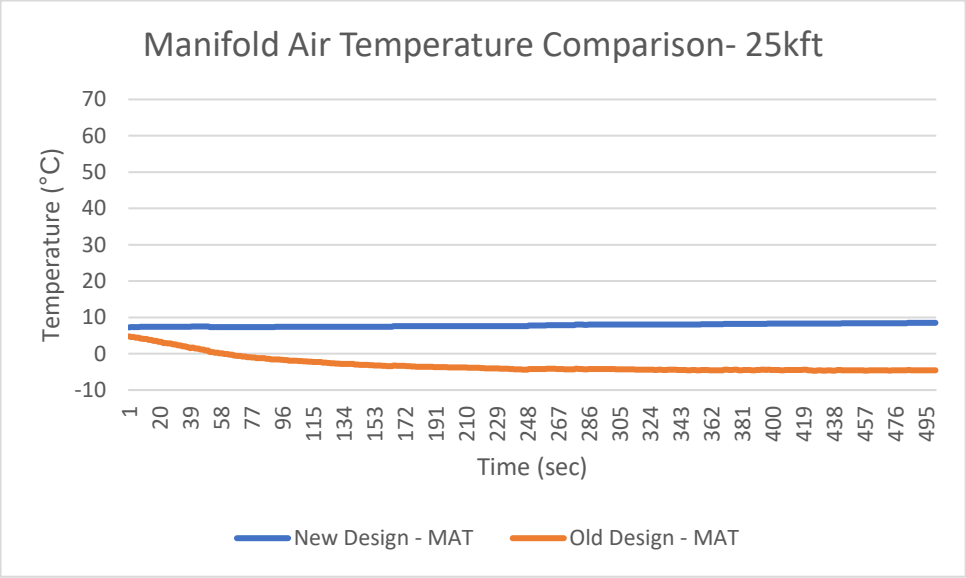

Figure 4.5: 25kft Manifold Air Temp Comparison Btw Old & New Air Cooling Systems

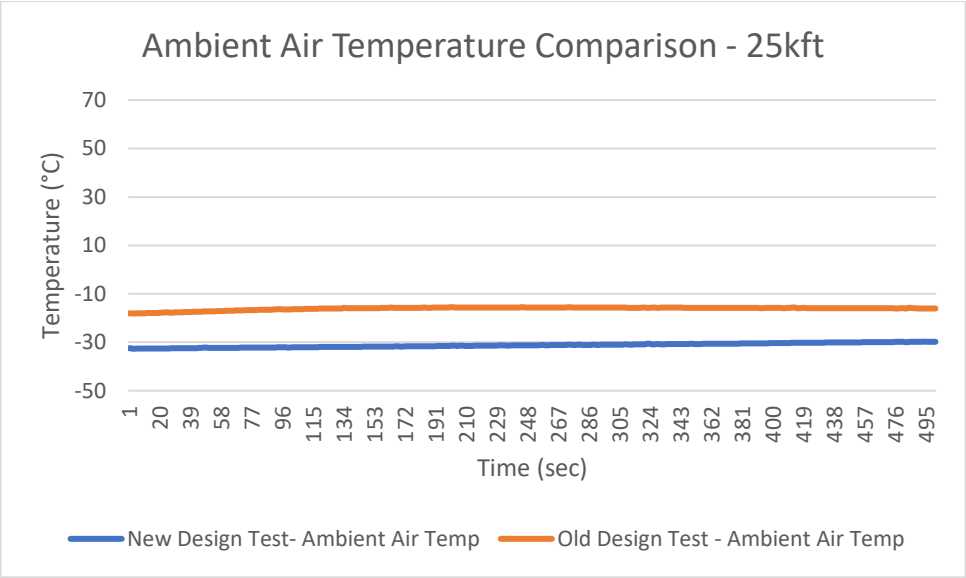

Figure 4.6: 25kft Ambient Air Temp Comparison Btw Old & New Air Cooling Systems

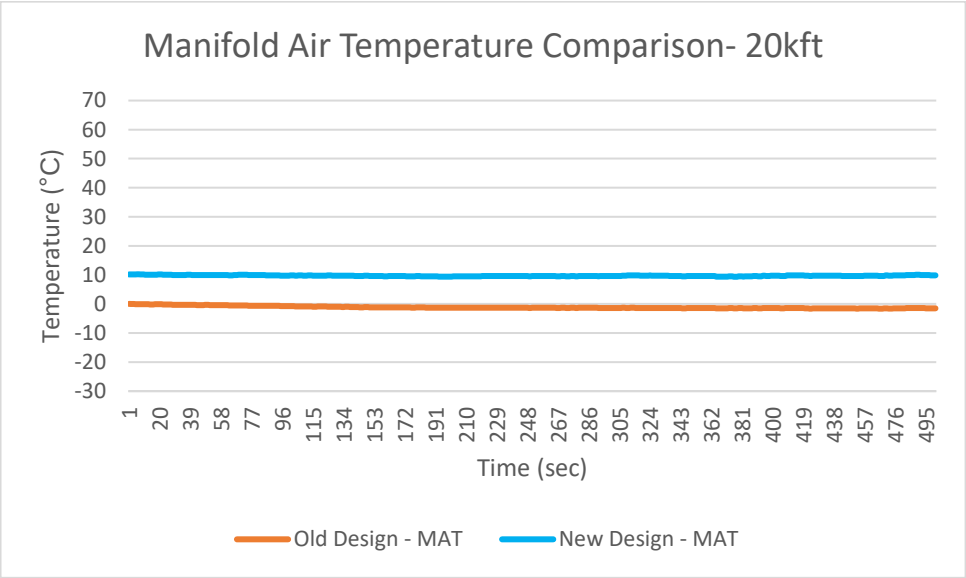

Figure 4.7: 20kft Manifold Air Temp Comparison Btw Old & New Air Cooling Systems

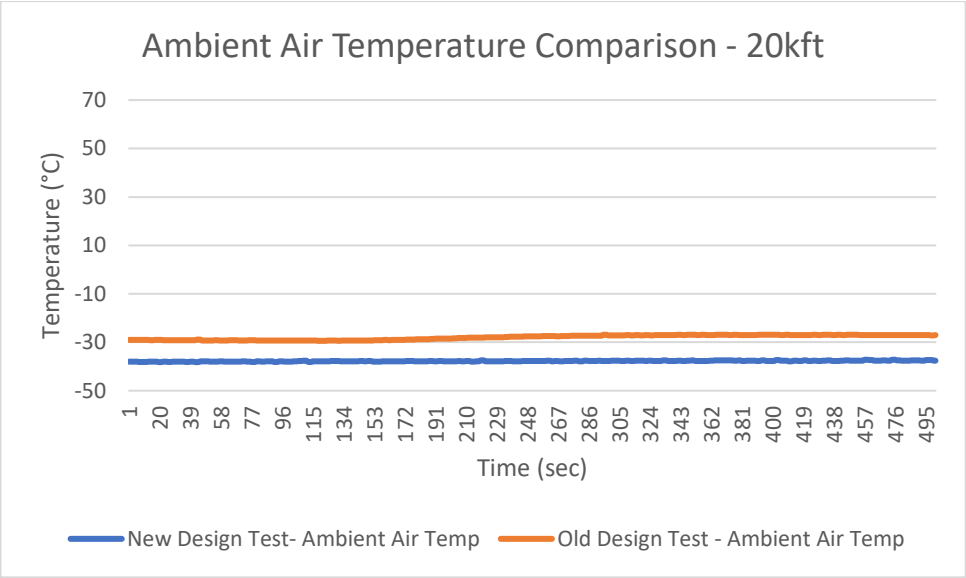

Figure 4.8: - 20kft Ambient Air Temp Comparison Btw Old & New Air Cooling Systems

When designing or optimising the air cooling system for unmanned aerial vehicles equipped with a two-stage turbocharged HFE engine, it is essential to consider the placement and weight impacts. The intercoolers should be sized to ensure they do not exceed the maximum MAT (manifold air temperature) permitted by the engine during the hottest take-off conditions, while remaining as small as possible. However, at high altitudes, even with small intercoolers, the two-stage cooling will inevitably cause the MAT to fall below zero in low throttle flights, especially in cold weather conditions. To prevent the MAT from dropping into negative temperatures, one practical solution is to add a bypass system in front of the intercooler, close to the engine air intake. This system allows the warm air from the bypass line to mix with the cooled air from the intercooler at the engine intake, preventing the intake air temperature from becoming negative. To minimize the weight impact of the bypass system, it would be sensible to design a mechanically integrated bypass system with the intercooler.

REFERENCES

Bents D. J., Harp J. L., King J. F., Schmitz P. C., (1998), "Propulsion system for very high altitude subsonic unmanned aircraft", NASA Lewis Research Center.

Bents D. J., Mockler T., Maldonado J., Harp J. L., King J. F., Schmitz P. C., (1988), "Propulsion system for very high altitude subsonic unmanned aircraft", NASA Technical Memorandum 206636.

Canli E., (2010), "Supercharging and Intercooling Systems in Internal Combustion Engines", Selcuk University Natural and Applied Sciences Institute, Konya.

Elafi F. M., Naas A. M., Farhat S., (2020), "Improving the performance of CI engine by using turbo-charger with an inter-cooler", The International Journal of Engineering and Information Technology (IJEIT), 6(2), 811-891.

Farias M. S., Schlosser J. F., Negri G. M., Casali L., Bertollo G. M., Da Rosa L. S., (2021), "Performance of an agricultural engine using turbocharger and intercooler", Engenharia Agrícola, 29(1), 100-106.

Honeywell, "Turbocharger Guide", 5th, Garrett by Honeywell.

Kang Y. S., Lim B. J., Cha B. J., (2017), "Multi-stage turbocharger system analysis method for high altitude UAV engine", Journal of Mechanical Science and Technology, 31(6), 2803-2811.

Kapse R., Arakerimath R. R., (2017), "Study and comparison of charge air cooling techniques & their effects on efficiency of automobile engine", International Journal of Engineering Research & Technology (IJERT), 6(7), 196-201.

Lee Y. J., Rhee D. H., Kang Y. S., Lim B. J., (2017), "Intercooler for multi-stage turbocharger design and analysis of the hydrogen reciprocating engine for HALE UAV", KSFM Journal of Fluid Machinery, 20(2).

Liu Z., Liu J., (2021), "Effect of altitude conditions on combustion and performance of a turbocharged direct-injection diesel engine", Proceedings of the Institution of Mechanical Engineers, Part D: Journal of Automobile Engineering, 235(1), 1-12.

Liu R., Yang C., Zhang Z., Jiao Y., Zhou G., (2019), "Experimental study on thermal balance of regulated two-stage turbocharged diesel engine at variable altitudes", Journal of Thermal Science, 28(4), 682-694.

Loth J. L., Morris G. J., Metlapalli P. B., (1997), "Staged turbocharging for high altitude IC engines" AIAA, 1997-3970.

Manglik R. M., Bergles A. E., (1995), "Heat transfer and pressure drop correlations for the rectangular offset strip fin compact heat exchanger", Experimental Thermal and Fluid Science, 10(2), 171-180.

Metlapalli P. B., (1996), “Three-staged turbocharger modeling with passive control system” , Doctoral Dissertation, West Virginia University.

Mifdal M. Y. A., Nuraida M. H., Norzalina O., Shamil A. H., (2015), “Turbo intercooler cooling system”, International Journal of Engineering Science Invention, 4(1), 49-56.

Motahari S., Chitsaz I., (2019), “Effects of altitude and temperature on the performance and efficiency of turbocharged direct injection gasoline engine”, Journal of Applied Fluid Mechanics, 12(6), 1825-1836.

Murcela T. R., (2017), “Condensation within a charge air cooler”, Instituto Superior Técnico, Universidade de Lisboa.

Oun M. S., Farhat S. A., Al-Rabeei M. A., (2017), “The effect of turbocharger pressure and intercooler temperature on engine performance”, Journal of Engineering Research (University of Tripoli, Libya), (23), 103-116.

Shah R. K., Sekulic D. P., (2003), “Fundamentals of heat exchanger design”, John Wiley & Sons.

Shan P., Zhou Y., Zhu D., (2014), “Mathematical model of two-stage turbocharging gasoline engine propeller propulsion system and analysis of its flying characteristic”, Journal of Engineering for Gas Turbines and Power, 137(5), 051201.

Web 1, (2024), https://www.tusas.com/urunler/iha/yuksek-faydali-yuk-kapasitesi/aksungur , (Date of Access: 17/06/2024).

Web 2, (2024), https://www.tusas.com/urunler/iha/operatif-stratejik-iha-sistemleri/anka , (Date of Access: 17/06/2024).

Web 3, (2024), https://www.tusas.com/urunler/iha/operatif-stratejik-iha-sistemleri/anka-III, (Date of Access: 17/06/2024).

Web 4, (2024), https://www.airbus.com/en/products-services/defence/uas/vsr700 , (Date of Access: 17/06/2024).

Web 5, (2024), https://umsskeldar.aero/unmanned-vtol-system-v-200-skeldar/ , (Date of Access: 17/06/2024).

Web 6, (2024), https://flyingbasket.com/fb3-order , (Date of Access: 17/06/2024).

Web 7, (2024), https://www.bellflight.com/products/bell-v-247 , (Date of Access: 17/06/2024).

Web 8, (2024), https://www.naval-technology.com/projects/vector-hawk-small-unmanned-aircraft-system-suas/ , (Date of Access: 17/06/2024).

Web 9, (2024), https://quantum-systems.com/wp-content/uploads/2023/01/QS_TrinityF90_Overview_220912.pdf , (Date of Access: 17/06/2024).

Web 10, (2024), https://www.geaerospace.com/sites/default/files/datasheet-TF34_1.pdf , (Date of Access: 17/06/2024).

Web 11, (2024), https://airandspace.si.edu/collection-objects/pratt--whitney-j58-jt11d-20-turbojet-engine/nasm_A19920006000 , (Date of Access: 17/06/2024).

Web 12, (2024), https://www.geaerospace.com/commercial/aircraft-engines/h-series , (Date of Access: 17/06/2024).

Web 13, (2024), https://press.siemens.com/global/en/feature/electric-flight , (Date of Access: 17/06/2024).

Web 14, (2024), https://www.dlengine.com/en/rcengine/dle55/ , (Date of Access: 17/06/2024).

Web 15, (2024), https://www.tei.com.tr/urunler/tei-pd170-turbodizel-havacilik-motoru , (Date of Access: 17/06/2024).

Zhao X., Grönstedt T., Kyprianidis K. G., (2013), "Assessment of the performance potential for a two-pass cross flow intercooler for aero engine applications", In Proceedings of the International Symposium on Air Breathing Engines (ISABE-2013-1215). American Institute of Aeronautics and Astronautics.

Zhao X., Grönstedt T., Kyprianidis K. G., (2015), "Aero engine intercooling optimization using a variable flow path", In Proceedings of the International Symposium on Air Breathing Engines (ISABE-2015-20018). American Institute of Aeronautics and Astronautics.

Zhou Y., Shan P., (2016), "Flight characteristic comparison of single and dual stage turbocharging reciprocating engine propeller propulsion system based on mathematical model", Journal of Mechanical Science and Technology, 30(5), 2369-2377.

BIOGRAPHY

The author, Kemal Buğra AVŞAR, commenced his professional journey as a Mechanical Design Engineer in the automotive industry. At present, he holds the position of Design Lead Engineer in the propulsion systems for Unmanned Aerial Vehicles.

PUBLICATIONS AND PRESENTATIONS FROM THE THESIS

Avsar K. B., (2024) "Air Cooling System Design And Optimizations For Two Turbocharger Heavy Fuel Engines Of MALE UAV ", 3rd Bilsel International Ahlat Scientific Researches Congress, 818-822, Bitlis, Türkiye, 08-09 June.